Multiscale Modeling of the Åre 6.2 Thief Zones in the Heidrun Field - Its Potential for Fluid Flow Predictions

M. Adib Sinto Baskoro
Student ID: 4623428

Technische Universiteit Delft

Cover photo source: NOAA photo library

TU Delft Delft University of Technology

Challenge the future

Multiscale Modeling of the Åre 6.2 Thief Zones in the Heidrun Field - Its Potential for Fluid Flow Predictions

By

Muhammad Adib Sinto Baskoro

(4623428)

In partial fulfilment of the requirements for the degree of

Master of Science

In Petroleum Engineering and Geosciences

at Delft University of Technology,

to be defended publicly on Friday, November 16, 2018 at 11.00 AM

Supervisor	: Prof. Dr. A. W. Martinius	TU Delft
Thesis committee	: Dr. K. Nordahl	Equinor
	: Dr. J.E.A. Storms	TU Delft
	: Dr. A. Barnhoorn	TU Delft

Acknowledgements

I would like to take this opportunity to thank the God for the good health and his bless to complete this thesis report, and to thank everyone who supported and helped me in this work. A special gratitude I give to my supervisor, Prof. Allard W. Martinius for the valuable encouragement, guidance, and support that he gave during the whole process of this master thesis. Thanks to Equinor team, especially Kjetil Nordahl and Jan Einar Ringås for allowing me to use the data from Equinor and the Ichron Ltd core descriptions, and their expertise in geological aspect in the Heidrun Field that help me to align this study with previous research. Dr. Joep Stroms and Dr. Auke Barnhoorn for being my thesis committee.

I would also like to thank my scholarship provider, the Indonesian Endowment Fund for Education (LPDP) for giving me a full financial support for my master's degree. It is an honour to have a precious opportunity to study in one of the best universities.

Special thanks to all my classmates in Petroleum Engineering and Geoscience, and Indonesian Student Association (PPI Delft) for their friendship, support, and happiness that they shared during my Journey in the Netherlands. Last but not least, all of this work and effort are dedicated to my beloved parents and family. Thanks for the continuous pray and motivation that you have always given to me.

Abstract

The upper reservoir intervals of the Lower Jurassic Åre Formation in the Heidrun Field (Offshore mid-Norway) are very heterolithic and have the lowest oil recovery factor of the field despite significant amounts of remaining reserves. One of these reservoir zones is the formation Åre 6.2, which is mainly composed of tide-dominated heterolithic channel belt deposits. It contains particular layers that have excellent properties with permeabilities up to 10 Darcy. These layers are predicted to affect the production results as they can act as 'thief zones' within the low permeable heterolithic facies causing large quantities of water to flow through, leading to poor sweep efficiency and early water breakthrough. This study focuses on constructing conceptual depositional models of the Åre 6.2 and building detailed geological models to investigate the effect of the thief zones on overall fluid flow predictions.

Conceptual depositional models were constructed by determining the characteristics of the reservoir and its depositional environment. Seven cored wells were used as the primary data to interpret lithofacies and facies associations. The study showed that Åre 6.2 mainly consisted of structured sandstones and heterolithic lithofacies with features that indicate that tidal process play an important role in the deposition. The influence of tidal process on deposition is further exemplified by the identification of two different types of channel facies associations, which are tidal and distributary channels. The thief zones were found in both facies associations, suggesting that the thief zones were formed during high freshwater discharge into the channels supplying coarse sandy material influx during a phase of high-energy deposition. To make detailed models of the tidal and distributary channels, multiscale modeling techniques were utilized to better represent the reservoir heterogeneities at the lithofacies and facies association scales.

At the lithofacies scale, models were built in SBED™ and the upscaled values of each lithofacies were obtained by applying the Representative Element Volume (REV) concept. The upscaled values were then used as input in the facies association scale models in order to represent the heterogeneities at the lithofacies scale to the next heterogeneity level. This step is essential since heterogeneities at a smaller scale may affect reservoir flow properties. Two different channel models were built in ReservoirStudio™ based on the conceptual depositional model and using outcrop analogue data from the Gule Horn Formation (Neill Klinter Group) in the Albuen area (Greenland). Flow-based upscaling was used to analyze the model uncertainties and determine a proper upscaling grid size. Finally, streamline simulations were performed to identify the effect of the thief zones. The simulation confirms that the thief zones influence fluid flow in the reservoir zone significantly as most flow was concentrated in the thief zones.

Contents

List of Tables

List of Figures

1 Introduction

1.1 Background

Nowadays, the world has been developed into an industrialized economy, and this situation has increased energy demand. The reason for this is that when the economy grows, energy consumption will grow as well, particular in those areas of the world where industrialization has not advanced as much as in first world countries. Fossil fuels are the most important and reliable energy resource and the world still depends on fossil fuels to fulfil the energy needs – now and in the coming decades. Fossil fuels are the leading sources of energy currently contributing eighty percent of the world's primary energy use (Van Roekel, 2008).

In the oil and gas sector, finding new hydrocarbon fields or developing existing fields are the options to maintain the supply. This is crucial because oil and gas fields, at some point, will reach a declining stage of production and hence will need to be replaced. Because exploration costs a lot of money and involves large risks, extending the field life by implementing for example Enhance Oil Recovery (EOR) projects is important. However, this requires a thorough understanding of the field's characteristics at a much higher detail than the initial development stage. These processes involve the static and dynamic characterization and analysis, including static geomodels and dynamic flow model analysis. These will support predictions of short- to long- term behaviour of the geological subsurface and fluids contained in the reservoir. With further developed software and geological modeling techniques, better static and dynamic models can be achieved (Kempka *et al.*, 2017).

The results and associated uncertainty analysis should be as accurate as possible, so choosing the most appropriate geological modelling method at the right hierarchical scale is crucial. The method has to be able to capture important geological features at the scales at which the objects are observed. Focusing on a specific target that is assumed to have a huge influence on the development of the field will be an effective way to improve production levels. The right focus can help the geologist and reservoir engineer to recognize the effect on production and the potential upsides of the development of the reservoir zone or sector that is targeted. Such a strategy is effective as it has shown to be a reliable and proven way forward in many hydrocarbon fields.

This thesis will focus on understanding the distribution and characteristics of thief zones in the Heidrun Field and assessing their potential impact on fluid flow in the reservoir zones they occur. The Heidrun Field is located approximately 190km offshore mid-Norway (Figure 1) and has produced more than 135 MSm^3 of oil (per 2010) since 1985 (Thrana *et al.*, 2014). Nowadays, the production rate of the field is decreasing so the development emphasizes on targeting and extracting the remaining oil reserves. The lowest oil recovery factor of the main producing formations comes from Lower Jurassic Åre Formation although this formation has very significant amounts of remaining reserves. Potential business opportunities are evident, and it is therefore necessary to put serious effort into improving oil recovery from this interval.

One of the reservoir zones with the highest potential in the Åre Formation is the Åre 6.2 reservoir zone. It is composed of tide-dominated and tide-influenced fluvial channel sand bodies, subtidal flats, as well as bay-fill deposits. In some parts, this zone contains layers that have excellent properties with permeabilities up to 10 Darcy. These layers are considered to be thief zones as they act as 'high-ways' during drainage, leaving much producible oil behind in the much less permeable heterolithic surrounding facies.

This thesis project aims to construct a conceptual depositional model for the Åre 6.2 and use this understanding to design a high-resolution geomodelling strategy, and subsequently build detailed geological model to assess key uncertainties in reservoir architecture and connectivity. Challenges come from uncertainties related to the distribution and characteristics of heterolithic facies in the reservoir zone; these need to be modelled at a sufficient degree of detail in order to provide the answers needed to optimize production.

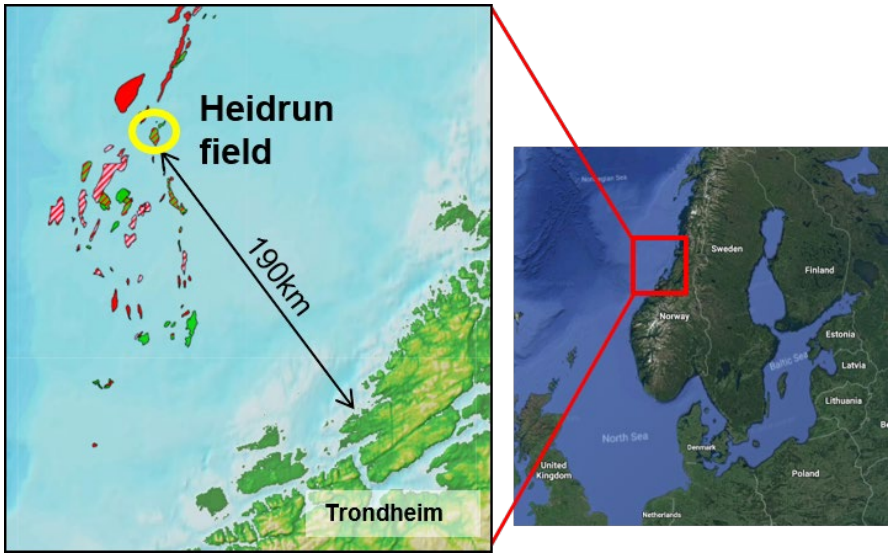

Figure 1. Location of the Heidrun Field (map source: internal Equinor and google maps)

1.2 Objectives of the thesis

This thesis contains three research objectives. The first objective is to make detailed geological models of the tide-influenced channel complex in the Åre 6.2 Zone. Models built at different hierarchical scales need to be integrated in order to obtain better estimations of static and dynamic properties which are going to use in the flow modelling analysis. Therefore, choosing the appropriate modelling method for the targeted zone in a multiple-scale hierarchical approach has been a crucial challenge (Keogh et al., 2014; Ringrose et al., 2008). The models have to include the distribution and characteristic of the thief zones. Secondly, the models have to be validated by evaluating the uncertainties that may exist. Statistic and deterministic approaches should be included to explain the uncertainties in a scientific manner. This is useful for the further implementation of the model. Thirdly, this study aims to evaluate the effects of the thief zones which will highlight the importance of capturing rock heterogeneity in the models. The result of the evaluation is useful to improve the strategy of reservoir modeling and simulation in Heidrun Field or other fields when there is an indication of thief zones in a certain reservoir zone.

1.3 Scope of the study

This study is divided in two parts: reservoir characterization and geomodelling. The characterization part is the first step during which the static characteristics of the reservoir zone (Åre 6.2) were analyzed and the conceptual depositional models were developed. Collecting and assessing relevant data was performed to identify the key characteristics of the Åre 6.2 zone. It includes establishing lithofacies and facies association classification scheme that will be used as building blocks in the modelling part. Therefore, any aspect that potentially has an impact on modelling needs to be recognized and its importance evaluated. This part was carried out by analyzing available core and well log data of the Åre 6.2 reservoir zone.

The second part is the geomodeling part. A modeling strategy was designed based on geological knowledges and specific cases developed in the characterization part. The models should be integrated with conceptual understanding as a guidance when building the models. Outcrop analogue data was also used as input in the modeling process. Outcrops from Gule Horn Formation of the Neill Klinter Group in Albuen Area (Greenland) is considered to be a suitable analogue for the upper Åre Formation due to the depositional environment similarities.

The reservoir zone architecture and the interactions between facies association has to be assessed for building reliable models. Subsequently, detailed geological models were built, and uncertainties in the modeling processes were evaluated by varying the geometries, dimensional properties of the modelling objects, and the internal properties of the models. Upscaling was performed to represent a heterogenous object at a specific heterogeneity scale and represent it by an effective property curve. The constructed models were examined by using simple streamline simulations to identify the effects of the thief zones in the models which can give a better understanding for the further reservoir modeling.

2 Methodology

2.1 Basic of Multiscale Reservoir Modelling and REV

Many different types of geological data can be used as input for geomodeling. They are obtained from a wide range of scales, and these scales form a hierarchical continuum. Each data set at a particular hierarchical scale represents sedimentary and stratigraphic heterogeneities that have an impact on the next hierarchical scale and the associated geomodel and its properties. According to Weber (1986), common sedimentary structures such as lamination, clay drapes, and crossbedding can affect reservoir flow properties in certain cases, and this leads to the necessity to investigate the effect of several scales of reservoir heterogeneity on fluid flow. The result may either be that all scales are important (and need to be incorporated) or that certain hierarchical scales are irrelevant for fluid flow and can be neglected. As this is unknown at the outset of a reservoir characterization study, investigating and applying data from various hierarchical scales to the model in an appropriate way is essential. Multiscale reservoir modeling has been applied for some time, and with recent technology development, multiscale modeling techniques are achievable and produce successful results.

Ringrose (2008) defined multiscale reservoir modelling as any methods that attempts to explicitly represent the rock properties at several scales within a petroleum reservoir. This is because reservoir heterogeneities are present at different scales such as pore, lithofacies, facies association, and full field scale (Nordahl *et al*., 2014) (Figure 2). Each scale consists of its own reservoir heterogeneities and it needs to be described and modelled in order to obtain a better estimation of properties that are populated in each scale. Multiscale modelling allows the model with the assigned properties to be included and upscaled to the next heterogeneity level. Geological concepts and processes are definitely crucial. It acts as guidance to building the models which later can be used for flow simulation, field development planning, and other purposes. Traditionally, common geological modelling approaches such as object-based modelling, only focus on a larger scale and are not honouring heterogeneities at smaller scales. Representing data from different sizes of volume and different physical measurement are the major challenges associated with the previously mentioned modelling methods.

The aim and purpose of the model determines the scale used for the modelling – this is a key starting point for designing the geomodelling workflow. As mentioned above, small-scale features may influence fluid flow and its properties on a larger scale, so the smaller-scale aspects have to be analyzed and included in the larger object by performing upscaling. A first estimation whether small-scale heterogeneities are important can be obtained by analyzing the grainsize contrasts and associated porosity and permeability values at cm and dm scale. If the contrasts are statistically relevant, they need to be included in the modelling process.

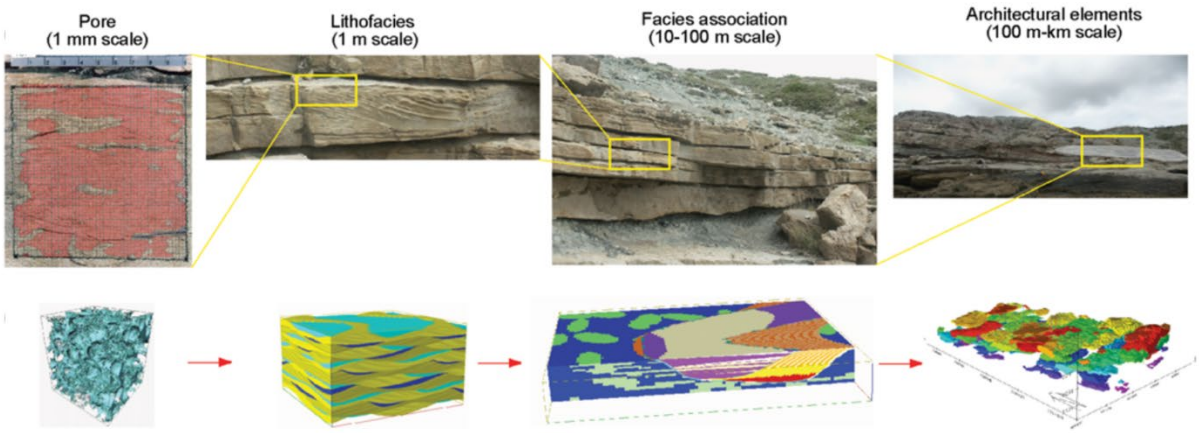

Figure 2. Examples of successive scale of sedimentary heterogeneities (Keogh et al., 2014)

Upscaling is an averaging operation to approximate effective properties of a fine-scale model to a coarser-scale model. In other words, it is an attempt to give an effective property value to a heterogeneous region which is composed of fine grid cells. Upscaling is operated for each of properties on every cell in chosen grids for reservoir flow simulation. Some different methods are available but choosing the proper one depends on properties that are going to be upscaled. Some properties are simple to upscale while others are complicated. For example, porosity is sufficient to be upscaled by basic weighted averaging. On the other hand, permeability is much more difficult to upscale than porosity because of its intrinsic directional dependent nature. No exact analytical solution exists to value an absolute permeability, except for a very ideal model, and it is a challenge to choose a relevant upscaling technique. The size of the grid chosen is also crucial since the upscaled values depend on the upscaled volume. The concept called Representative Element Volume (REV) (Bear 1972; Nordahl & Ringrose, 2008) was utilized to define a proper volume size used to represent a sedimentary feature in a particular scale.

The REV represents a volume or area which is large enough to capture the heterogeneity of the rock. If a model or sample is smaller than the REV, any property calculations extracted from them really depend on the sizes and positions of the models or samples. Some variations can be recognized as small changes in sample positions and/or volumes are applied. In the REV size, the variations are minimized, and an effective property for the model or sample can be measured (Nordahl & Ringrose, 2008; Nordahl *et al.*, 2014). REV between properties may be different since each property has their own characteristics. In this study, the sizes of the models were chosen based on the size of the sedimentary structures contained in each lithofacies. Once the models were built, REV analysis were conducted to obtain volumes that were used to make samples for effective property calculations which were input in facies association modeling.

Another tool that is crucial for multiscale modeling is the analysis of a relevant outcrop analogue. As subsurface reservoirs are only scarcely sampled, and sampled at a number of discrete spatial scales, additional information is required to obtain a better understanding of the interwell area at sufficient resolution (that is, better than the resolution that can be obtained from seismic). Thus, an outcrop analogue can be used to understand the 3D facies geometry, connectivity, the stratigraphic development and architecture, etc. This information is can often be directly applied as valuable input to the geomodelling processes. Besides, outcrops can provide qualitative and quantitative data of rock heterogeneity (properties – porosity, permeability) at various scales, especially at facies and facies association scale. Uncertainties associated with the three-dimensional shape at each scale need to be specified and quantified

when possible. Integrating outcrop analogues with subsurface understanding and advanced modelling techniques using the appropriate software has the potential to produce better representations of the reservoir heterogeneity distribution.

2.2 Overall Workflow Outline

The goals of this study are to build detailed geological models of the tide-influenced channels complex of Åre 6.2 and investigate if the thief zones affect the upscaled properties and flow simulation. To achieve the goals, the workflow of the study was established as shown in Figure 3. There are five general steps which are literature study, core observation, reservoir characterization, multiscale reservoir modeling, and flow simulation. Each step consists of several output which are illustrated in the chart at the right side of the figure.

A literature study was the first step which aims to provide background knowledge of the formation and to find useful techniques for geological modeling and simulation. After doing the literature study, the available data were prepared for the next analysis. The data used in this study were core data, well logs, and outcrop analogue. The core data were obtained by doing core observation while the outcrop analogue data was provided by published previous research.

The reservoir was characterized based on the available geological data. In this case, there are two different model scales that are investigated, the lithofacies and facies association scale. The sedimentary elements in both scales are related to each other because facies associations are composed of a particular lithofacies set that represent a certain depositional environment. Besides, the relation between all the facies associations in every well needs to be defined by correlating the wells. This is useful to interpret the depositional environment which is a foundation to build a conceptual model. The conceptual model includes an understanding of how the sedimentary sequences are formed and the relation between lithofacies contained in facies associations. Based on the conceptual model, a modelling strategy was subsequently established, and the geological models for both scales (lithofacies and facies association) can be constructed.

Lithofacies (LF) and Facies Association (FA) models were developed by using two integrated softwares which are SBED™ and ReservoirStudio™. SBED™ was used to model synthetic bedforms which are models of lithofacies scales whereas ReservoirStudio™ was useful to create numerical models of the facies associations. In this modeling part, porosity and permeability were distributed in the models stochastically, so every cell in the grid of the model was represented by a properties value. Assigning a value from a finer cell to a coarser cell was done by using the upscaling method. In this case, values from LF models were upscaled to larger cells (REV size) and used as input in FA scales. Subsequently, FA models were applied as a simulation grid which was used for flow simulation. Streamline simulation approach was chosen for the simulation instead of finite-difference simulation since it results in high accuracy and suitable with the objective of the study.

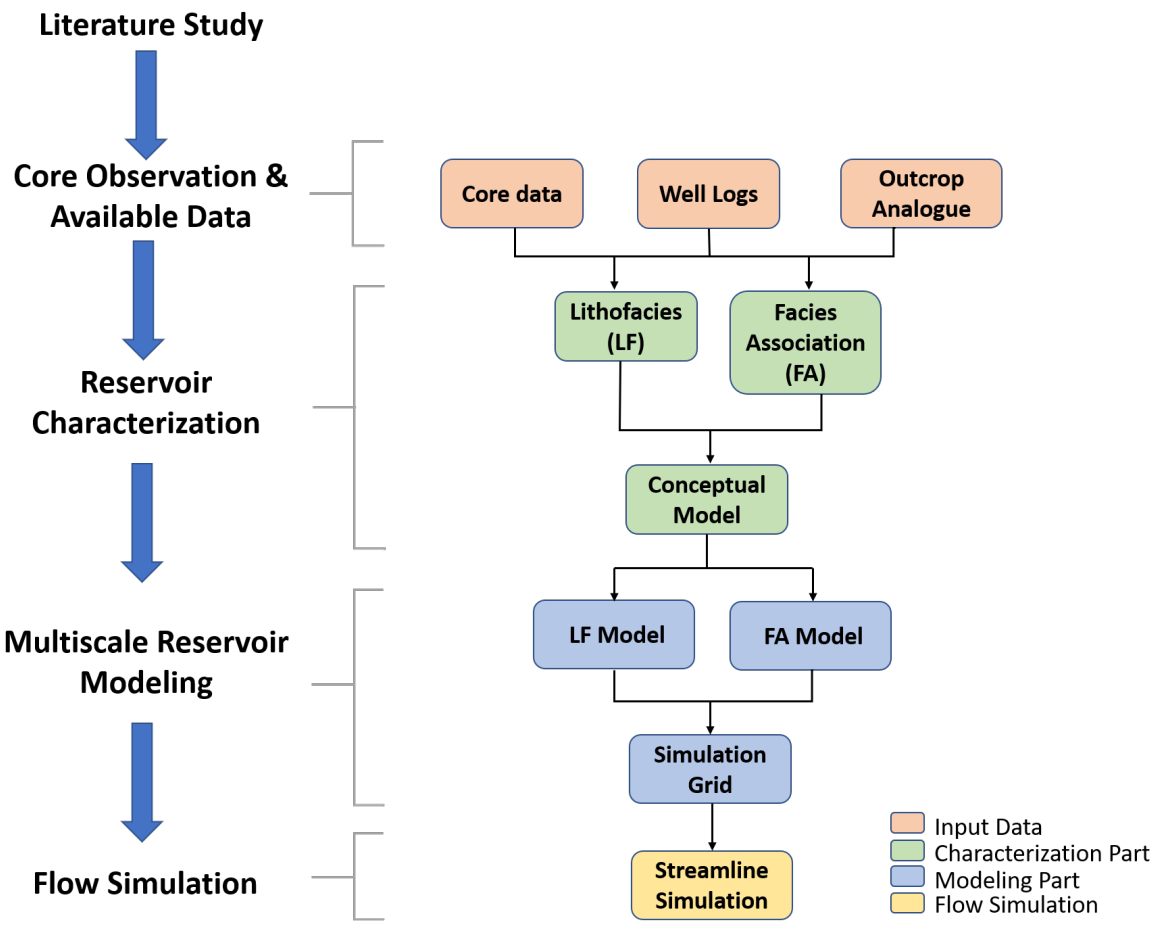

Figure 3. General workflow for this study and the processes within each step

2.3 Data Used for the Study

The data used in this study are core data and well log data obtained from seven wells within Heidrun Field (Table 1); the location of the wells is shown in Figure 4. The wells were chosen because they are the only ones in which core data are available in Åre 6.2 Zone. This study focuses on a specific heterogeneity type (high permeable 'thief sands'), thus core data is crucial for detailed sedimentary analysis. Core observations were conducted in the core laboratory in Stavanger (Norway) to describe and identify the characteristics of the zone. This included the identification of lithofacies that were later grouped into facies associations and also the thief zones. Overall, the rocks are well preserved, although in a few intervals, core gaps are present caused by either drilling issues or the fact that it was decided to not take core in these intervals during drilling operations. In particular, large core gaps are found in Well 6507/7-2 and 6507/7-5 with core gaps of 1.9 and 5.4 meters respectively while the other core gaps are only around 10-20 cm.

Special core analysis of plug data was also performed. This analysis produces values of actual permeability and porosity at a certain depth along the well trajectory. The resulting values obtained from plug data are reliable as they are measured directly on the formation. However, plug data are only available at certain depths which is quite limited because some of the zones are composed of unconsolidated sands.

From the core data, identifying rock characteristics is important for the interpretation and correlation purposes. Lithofacies term is commonly used as the first step to classify the rock from the core. A lithofacies is defined as a body of rock with specific characteristics that reflects the conditions where the rock was formed (Reading and Levell, 1996). The term facies has become important in modern stratigraphy for understanding the depositional environment and the characteristics of sedimentary rocks. A number of facies types exist but here the focus is on lithofacies (litho means rock).

Table 1. List of Wells Used in the Study

Well Name	Core Depth (m)	Thickness (m)
6507/7-2	2414 - 2427.20	13.2
6507/7-3	2642 -2648	6
6507/7-4	2756 - 2766.7	10.7
6507/7-5	2589 - 2604	15
6507/7-A-22	3006 - 3021	15
6507/7-A-40	2884 - 2898	14
6507/7-A-46	2671 - 2687.94	16.94

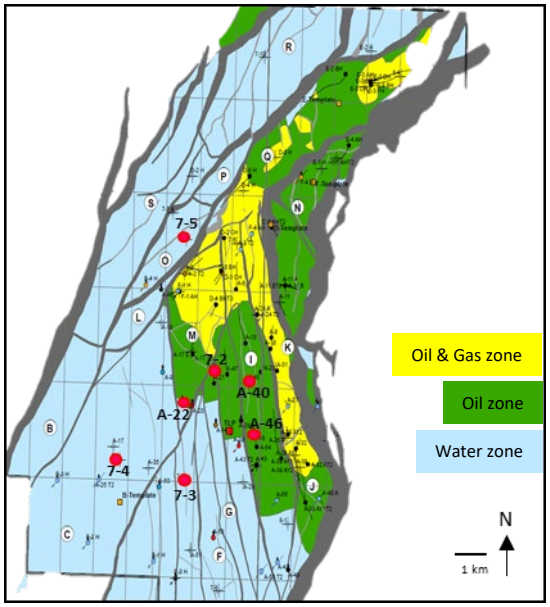

Figure 4. Locations of the wells used in this study indicated by red dots

In this study, core data was used for lithofacies analysis. It includes the determination of the lithofacies which is later used in defining the facies associations. The lithofacies were determined by categorizing the rock based on the lithology types and the dominant sedimentary structures observed in the rock. To define a lithofacies, the rock has to be distinguishable from the others. The typical features of the rock are used to name the lithofacies. For example, one of the lithofacies defined in this study is cross-stratified sandstone which is sandstone where cross stratification is the dominant structure. In this study, the lithofacies classification scheme was adopted resulting from a previous study which was conducted by Statoil in collaboration with a sedimentological consultant named Ichron Ltd. Table 2 lists all the lithofacies identified in this study with their abbreviation. The geological symbols used for lithofacies and facies association schemes can be found in Figure 5.

Once lithofacies have been prepared, the next step is to classify them into facies associations. A literature study was performed in order to understand the possible facies associations contained in tidal influenced estuarine area where the Åre 6.2 zone was formed (Thrana *et al.*, 2014). A facies association is mainly determined by looking at a typical lithofacies order which characterizes a particular depositional feature such as a channel, shoreface or something else. Some lithofacies make up a general organization of lithofacies in which the location of its occurrence is essential to define a facies association. Besides, other sedimentological aspects such as lithology, grain size, sedimentary structures, bioturbation, and erosional surfaces are important for supporting the interpretation. Physical processes control these aspects during the deposition of the rock, so that implicitly indicates the environment. There are five facies associations identified in this study which are:

- tidal channel
- distributary channel,
- tidal flat,
- upper shoreface, and
- lower shoreface.

These facies associations will be explained in more detail in Chapter 4.

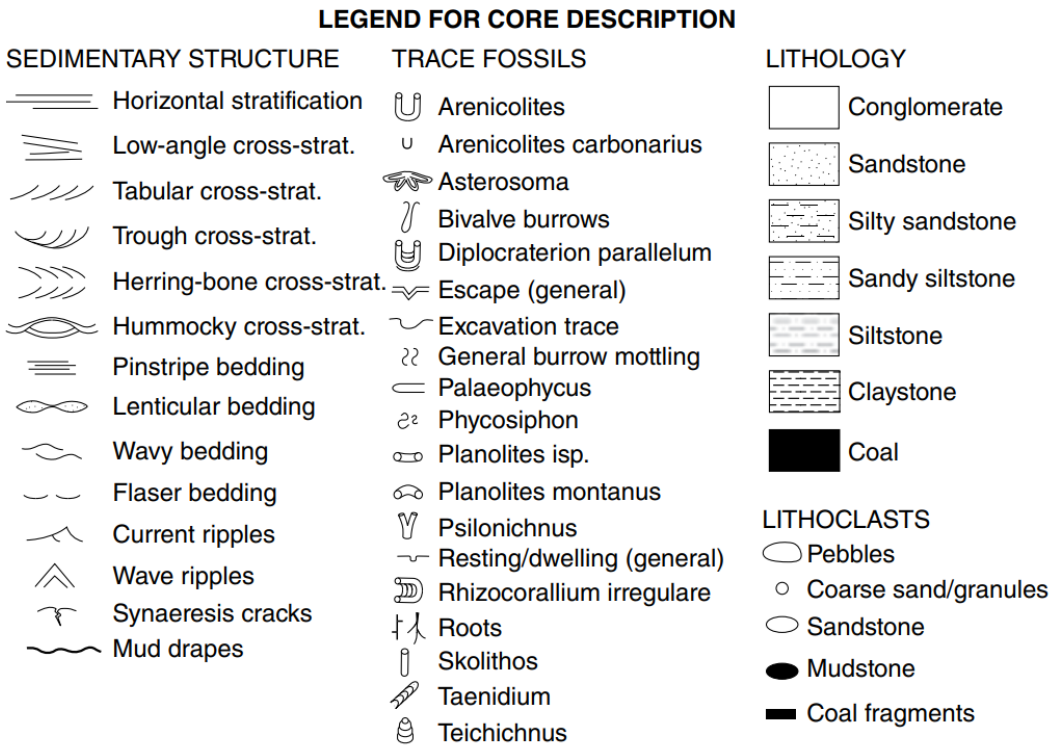

Figure 5. Legend for the lithofacies and facies association (Thrana et al., 2014)

Table 2. List of Lithofacies (adapted from Thrana et al., 2014)

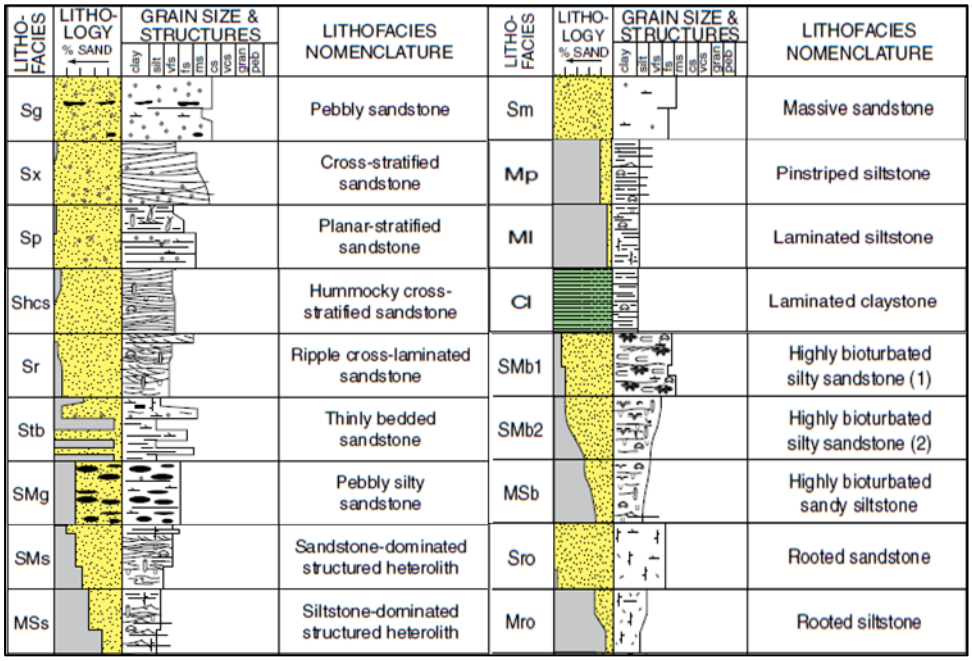

2.4 Streamline Simulation in General

Streamline simulation is an alternative technique to traditional finite-difference simulation for reservoir simulation which provides a rational balance between computational power and the complexity of the model. This simulation is a relatively simple method to understand the geological variability and complexity by running experiments of flow in the geological models (Gilman *et al.*, 2002). Streamline simulators represent fluid front propagation at numerous times and measure volume of oil swept for a defined geological model with an assigned well configuration. Simplicity is attached to this method since it converts the 3D domain to a series of 1D streamlines and thus gives computational advantages. Moreover, to produce high accuracy, the technique maintains sharp flood fronts from the displacement processes and lower the effects of grid orientations (Lolomary *et al.*, 2000). Because of its efficiency, a wide range of reservoir utilizes 3D streamline simulation to capture the displacement of the resident oil volume and path of fluid flows representing the dynamic connectivity from injection to production wells. Figure 6 shows an example of streamline simulation between two wells which is also to this study to test the fluid flow in the built models.

A more commonly used reservoir simulation technique is to apply finite-difference to a simulator. However, this approach suffers from computational efficiency, especially for a large reservoir model with a large number of grid blocks. The number of wells and production history has also been a challenge. Despite computer power development, the geological modeling tools have grown and allowed creating of detailed heterogeneities geological models with tens of millions of cells. As a better alternative to the previous finite-difference method, the streamline simulation is implemented with the time-of-flight concept which measures the interaction between the heterogeneity and the flow applied to the model, reflecting a reasonable oil recovery estimation (Idrobo *et al.*, 2000). The generated flow paths represent the producible oil geometry based on the well perforation placement and the permeability distribution. The flow paths can be a reliable indication of potential sweep zones which is

useful for field development strategy. Several examples from the various field have proven that the implementations of streamline simulation have been successful and beneficial (Lolomary *et al.*, 2000).

The streamline simulation was utilized in this study to evaluate if the interpreted thief zones affect the fluid flow distribution in the models. The effect is expected to be the concentration of flow path in the thief zones since they are very permeable which enable any fluids to flow through them. Petrel software was used to run and visualize the simulation result. A built-in streamline simulator called FrontSim was chosen rather than standard finite-difference reservoir simulator due to its simplicity and benefits mentioned above. To run the simulation, some initial conditions are needed such as fluid and reservoir properties. Such requirements will not be emphasized because the main focus is to observe the flow lines and not evaluating the full-field reservoir performances. A particular fluid and reservoir conditions were used to enable the streamline simulation to be applied to the models.

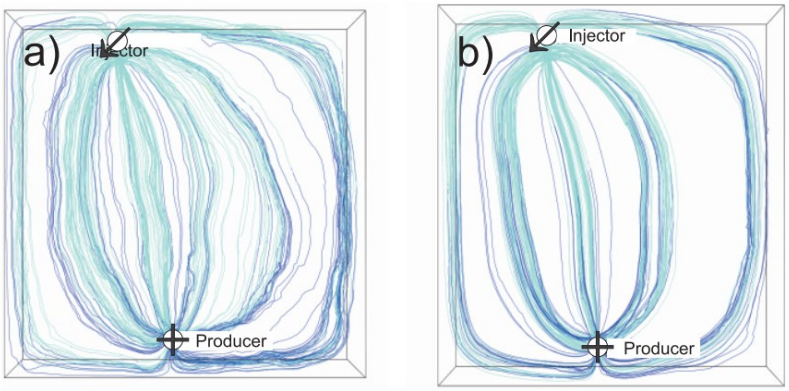

Figure 6. Simple illustration of streamline distribution between two wells, comparing (a) a well swept realization and (b) restricted swept realization (Brandsæter *et al.*, 2001).

3 Regional Geology

3.1 Regional stratigraphy of the Jurassic period in the Halten Terrace area

The reservoir rocks in the Heidrun field were deposited during the Late Triassic to Middle Jurassic. The rocks were formed in a rift basin with initial rifting initiated in the Triassic and later rifting phases occurring during the Jurassic. Sediment was derived from the Norwegian mainland as well as from a western source area (Ziegler, 1988). In addition, sediment was derived from rift shoulders. The rifting forced Fennoscandia and Greenland to drift away from each other, thereby gradually opening up a seaway in between these two continents connecting the northern Boreal Ocean with the southern Tethys Ocean. During Early Jurassic, multiple relative sea level changes occurred causing transgression in the area where the Heidrun field is located. A number of retrogradational and progradational sedimentation packages were formed which consist of continental alluvial and fluvial deposits as well as coastal to shallow marine deposits, all within the of Båt Group of which the Åre Formation is part. This group is overlain by the overall regressive sequence of the Fangst Group which was deposited in Middle Jurassic. The stratigraphic framework for the mid-Norwegian Continental Shelf is illustrated in Figure 7.

The oldest main reservoir unit of the Båt Group in Halten Terrace is the Early Jurassic Åre Formation which succeeded the Triassic continental sediments called the Red Beds and Grey Beds. The Rhaetian to Sinemurian Åre Formation is composed of alternating sandstone, claystone, and a number of interbedded coals with high organic content which were extensively developed in non-marine, fluvio-deltaic, and possibly lacustrine environments (Dalland *et al.*, 1988). During the Pliensbachian, the overlying Tilje Formation was formed during a regional marine incursion when the rate of subsidence versus sediment supply (sediment deposition) was increased. The Tilje Formation is very heterolithic and deposited in a marginal marine, intertidal/subtidal, to shallow marine setting.

The Tilje Formation is overlain by the marine mudstones of the Ror Formation which was deposited during the Toarcian. This transition from the Tilje delta to the muddy marine facies was caused by a regional transgression that moved the delta in a more landward direction. Locally on the Halten Terrace, coarse sands and conglomerates of the Tofte Formation interfingered with the mudstone deposition. These coarse sediments are interpreted as fan-delta deposits which formed as a result of erosion and local uplift near the Sklinna Ridge in the Western Halten Terrace (Ehrenberg *et al.*, 1992; Gjelberg *et al.*, 1987).

Subsequently, during the Middle Jurassic period, hydrocarbons were trapped in the Garn and Ile Formations. These formations are part of the Fangst group together with marine mudstone Not Formation intercalated between the Ile and the Garn formations. The Fangst Group is an overall sand-dominated deposit which was deposited during a lowstand of sea level and it is marked as an equivalent unit to the Etive Formation which is part of the Brent Group in Northern North Sea. The Ile Formation, the oldest stratigraphic unit of the Fangst Group, was

deposited in a low-gradient tide-influenced delta and comprises heterogeneous sandstone-rich facies such as tidal channel and subtidal flat deposits (Martinius *et al.*, 2005). During a transgression that influenced the entire Halten Terrace area, the Not Formation was formed overlying the Ile Formation with a sharp boundary and remarkable ravinement surfaces. The formation was mainly composed of shallow marine shales and sands, but it is considered as a non-productive unit.

The Garn Formation, stratigraphically located in the upper part of the Fangst Group, is assumed to have been deposited as an extensive shallow shelf sand controlled by waves and tidal currents. It forms a thick succession of relatively homogeneous sand, and the Garn package provide the highest quality of reservoir sandstones on the Halten Terrace, specifically in the Heidrun field (Hemmens *et al.*, 1994).

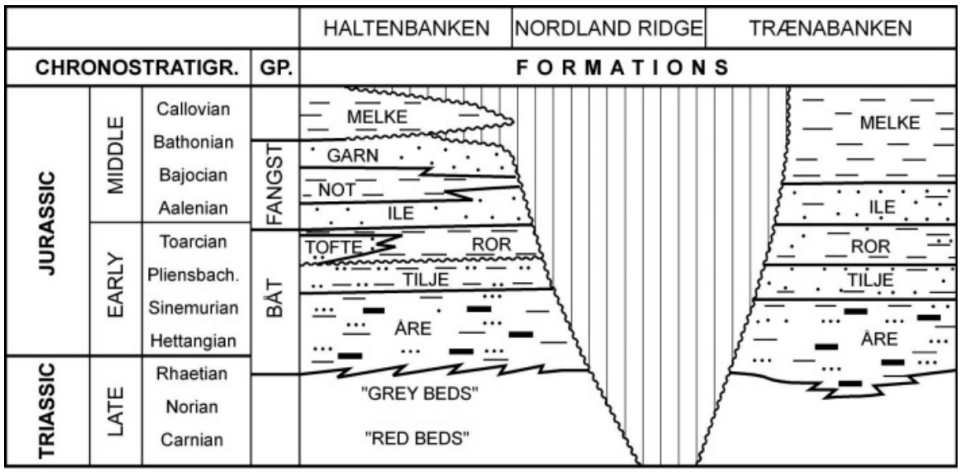

Figure 7. General Stratigraphic Column of mid-Norwegian Continental Shelf (After Dalland et al., 1988)

3.2 Structural and Basin Setting in Halten Terrace

Rifting in the North Sea Region initially started in the Triassic as the result of thermal subsidence and crustal extension which separated the Norwegian and Greenland continents. The development of the rift caused rift propagation in a north-south direction forming, among other structures, the Viking and Central Graben (Ziegler, 1988). These extensional structures controlled the geometry and setting of the Jurassic Basins (Osmundsen & Ebbing, 2008). Structural styles were also affected by the presence of a salt interval in the Upper Triassic in the Halten Terrace.

A second rifting phase occurred in the middle Jurassic and culminated in the Late Jurassic during the Cimmerian tectonic phase. The extensional system and NE-SW trend of associated normal faults characterized the structural style of the Early Jurassic rifting and the high subsidence rates. In the early Middle Jurassic, most faults changed to a N-S trend due to structural relaxation. However, a gradual increase of tectonic activity is recorded in the late Middle Jurassic caused by a reactivation of rifting (rifting phase 3). These processes caused widespread uplift, erosion, and tilting of the already existing Jurassic fault blocks which resulted in the formation of structural traps now identified in several hydrocarbon fields including the Heidrun Field (Whitley, 1992) which is located at the transition between the Halten-Terrace and the Nordland Ridge (Figure 8). Because of the complex nature of these

structures and fault blocks, the field is divided by a number of extensional faults with a north to northeast trend and up to 100 m displacement. The faults split the field into several large-scale structural compartments (Segment A-T; Figure 9) with a large number of faults within each structural compartment.

Consequently, hydrocarbon accumulations on the Halten-Terrace are generally discovered within structural traps formed by fault blocks with the main closures formed by Upper Jurassic mudstone successions and/or by the Base Cretaceous Unconformities (BCU). The majority of these east-ward dipping Jurassic fault blocks and were tilted and slightly rotated during the Early Cretaceous, and as a consequence the major faults bounding the fields commonly have NE-SW trend.

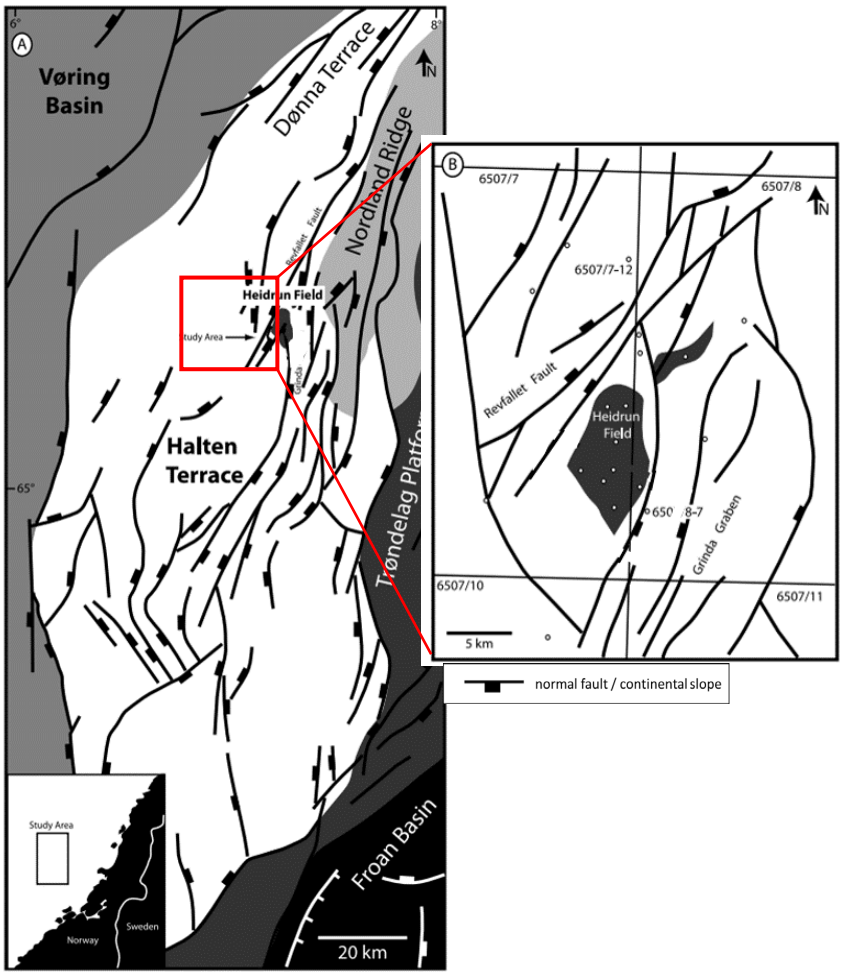

Figure 8. (A) Tectonic map of the Halten Terrace region including the location of the Heidrun Field (Moscardelli et al., 2013). (B) Close up view of the Heidrun Field.

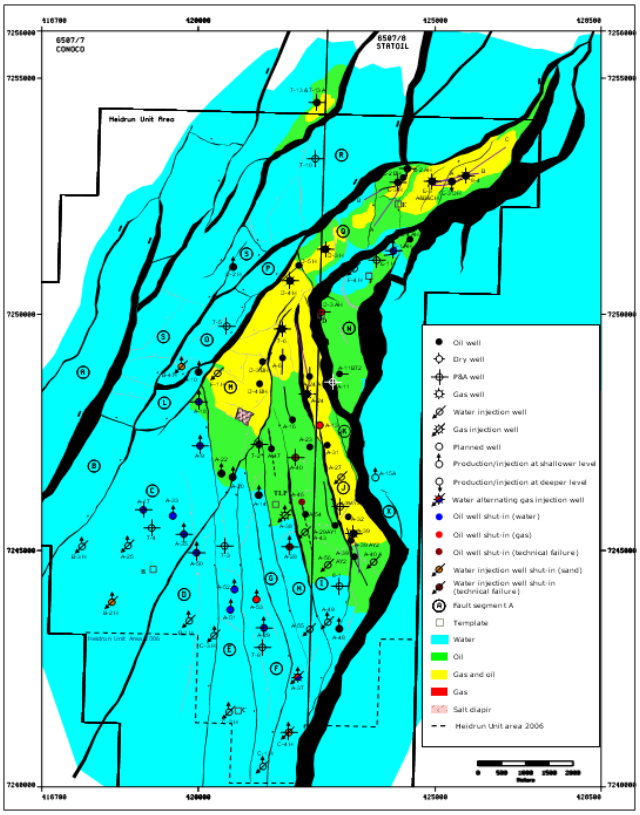

Figure 9. Schematic structural map of the Heidrun Field showing the main fault trends, structural compartments, distribution of hydrocarbons, and drilled wells (Internal Equinorl, 2014).

3.3 Petroleum Overview of the Heidrun Field

The Heidrun field was discovered in 1985 and is situated approximately 250 km north-west from Trondheim with water depths of around 350 m (Whitley, 1992). The first oil was produced in 1995 and the field is currently still producing oil and gas; however, production shows a gradual decrease over the last two decades. In total, the field has produced more than 150 x 10^6 Sm^3 oil and 40 x 10^6 Sm^3 gas with the estimated remaining reserves of oil and gas 38 x 10^6 Sm^3 and 26 x 10^6 Sm^3 respectively (Norwegian Petroleum Directorate website). The field is about 10.5 x 5.5 km in dimensions of which the hydrocarbon accumulation comprises more than 60% of the total area. The distribution of hydrocarbon is shown in Figure 10. The field is operated by Equinor together with ConocoPhillips, ENI and Petoro as partners.

The hydrocarbons in the Heidrun Field are found in two main intervals. The Fangst Group has high quality reservoirs whereas the Båt group is more heterogeneous *(*Hemmens *et al.* 1994; Welbon *et al.* 1997; for the stratigraphic position see Figure 7*)*. The sediment is formed by coarse clastic sediment derived from the Fenno-Scandian mainland, a micro-continent located to the west of the field, and from the elevated rift shoulders (Whitley, 1992). The Upper Jurassic Spekk Formation is the primary hydrocarbon source, with the coals of the lower Åre Formation as an additional source rock (the coaly beds contain high organic-rich material). The mature source rocks are located in 5 to 15 km southwest and west of Heidrun in a downdip direction. Therefore, the hydrocarbon migration paths are relatively long. In fact, some surrounding oil fields, such as Smørbukk, Smørbukk South and Trestakk, are linked to the same hydrocarbon migration system (Heum *et al.*, 1986). The rocks acting as seal are formed

by the marine shales of the Late Jurassic Viking Group as well as the Cretaceous shales of the Cromer-Knoll and Shetland Group.

The Heidrun field is a part of a large plunging horst block oriented to the SW. The area is highly faulted (see above) and tilted which is the result of extension that occurred during the Late Jurassic to Early Cretaceous (Schmidt, 1992; Hemmens *et al.*, 1994; Koch and Heum, 1995). They created structural compartments (Figure 10) and resulting different fluid contacts between the fault blocks. This might occur because of partially sealing faults (Hemmens *et al.*, 1994) and/or the dynamic behaviour of fault seal (Heum, 1996; Welbon *et al.*, 1997).

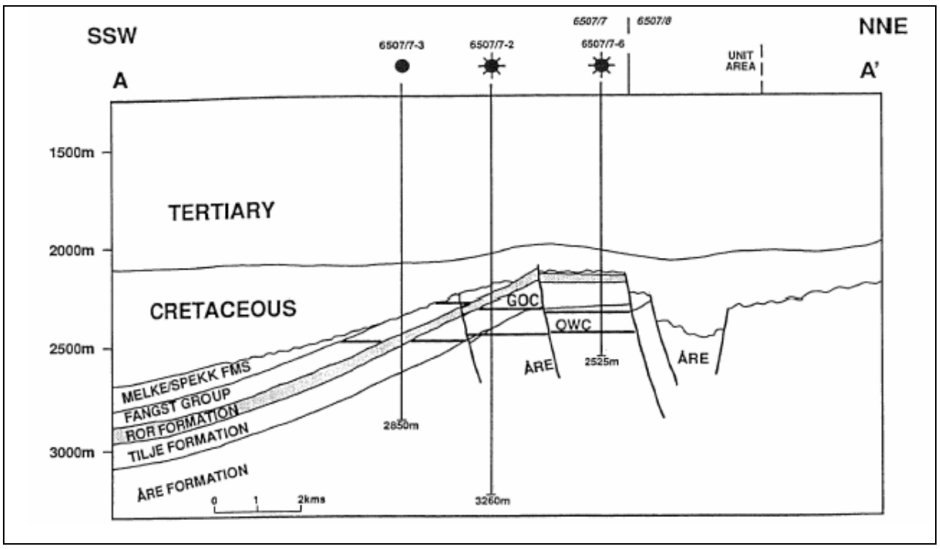

Figure 10. Illustration of Heidrun Field cross-section showing fluid contact differences in some reservoir blocks (Hemmens et al., 1994).

4
Reservoir Characterization

4.1 Stratigraphy and Well Correlation of the Åre 6.2 Zone

As described in the regional stratigraphy section, the Åre Formation (Åre is Norwegian for oar) is the oldest formation within the Båt Group. It consists of coastal plain to delta plain deposits which overlay alluvial Triassic age grey beds and is succeeded by tide-dominated Tilje Formation. Generally, the Åre Formation is divided into two members, Åre 1 and Åre 2. These members are separated by coal-bearing strata which indicates a transition from coastal plain deposits of the Åre 1 to marginal marine deposits of the Åre 2 (Dalland *et al.*, 1988; Svela, 2001). A more detailed study conducted by Thrana *et al.* (2014) identified seven reservoir zones in the Åre Formation (Åre 1 to Åre 7) and seventeen subzones (Figure 11). These zones represent four main depositional environment which from the base to the top are fluvial/alluvial coastal plain, lower delta plain/brackish-water interdistributary bay, mixed wave-and-tide-influenced estuary, and transgressive shoreface. The Åre Formation shows an overall transgressive succession in which a progressive switch to open marine is documented in the uppermost part (Åre 5, 6, and 7). This study focusses on the Åre 6.2 reservoir subzone which is interpreted as an estuary setting comprising tide-dominated facies of heterolithic channel sandbodies, and tidal flats.

The upper and lower boundaries of the zone are clearly identified and can be traced across the field. At the base, the Åre 6.2 overlies the Åre 6.1 which is mainly composed of bay-fill deposits. The transition is marked by a transition from wave-influenced bay-fill deposits to the tide-dominated facies of Åre 6.2. Form the core data, the boundary shows the change of a highly-bioturbated siltstone into a structured sandstone and sand-dominated heterolithic which forms a sharp-erosional surface overlain by channel facies of Åre 6.2 zone. This facies changes from the Åre 6.1 subzone composed of muddy bay deposit to the tide-dominated channel facies is interpreted as a basin ward movement of the depositional system and taken as a candidate sequence boundary (Thrana *et al.*, 2014).

At the top of the Åre 6.2 subzone, a transgressive shallow marine shoreface deposit is found that is part of the Åre 7.1 subzone. Unlike the Åre 6.2 subzone, wave-dominated sedimentary structures are found significantly more often in Åre 7.1. In addition, Åre 7.1 is composed of extensive calcite cemented horizons and a higher variation of trace fossils. These characteristics are used to distinguish the Åre 6.2 from the Åre 7.1 subzone and to define the boundary between the two subzones. The ichnological assemblage changes from low diversity to a relatively high diverse assemblage confirming that the depositional environment has changed to more salinities associated with more open marine environments (Thrana *et al.*, 2014). In some cored wells, the basal surfaces of Åre 7.1 is observed. This basal surface erodes in the underlying Åre 6.2 and forms a lag of granule-pebble clasts. This erosive surface is interpreted as a transgressive ravinement surface (TRS).

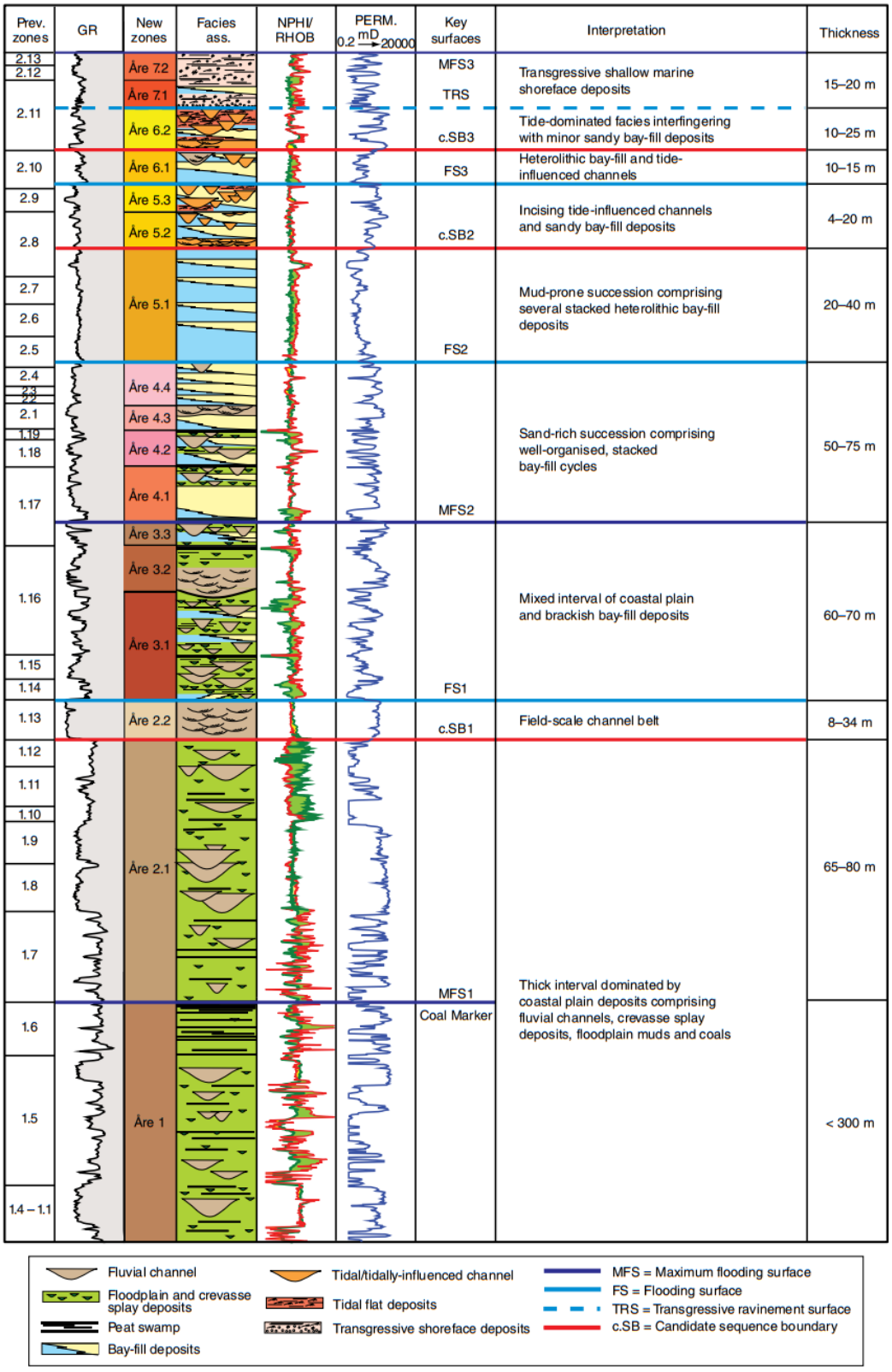

Figure 11. The updated reservoir zonations of Åre Formation in Heidrun Field showing logs and sedimentary characteristics (Thrana *et al.*, 2014)*. The traditional reservoir zonation is indicated in the left column. The logs shown in the table are GR (Gamma Ray), NPHI (neutron porosity), RHOB (density porosity), and PERM (permeability)*

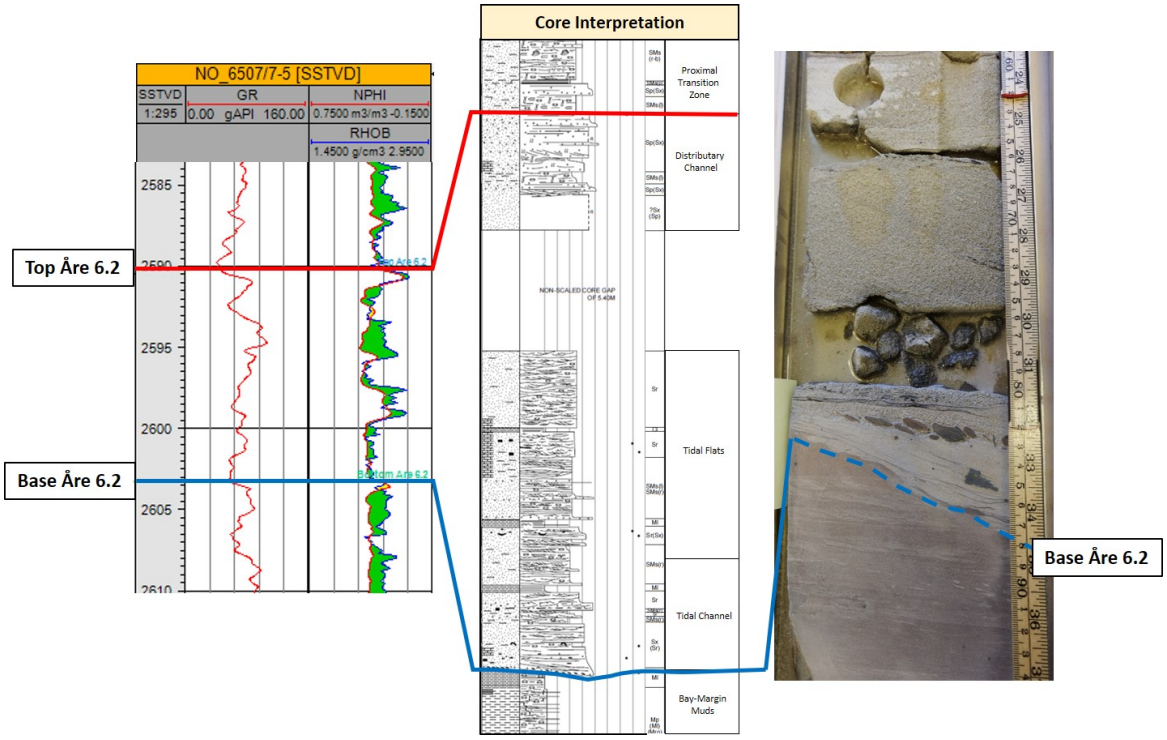

Figure 12. Well log and core log from well 6507/7-5 showing the boundary of Åre 6.2 Zone. The core image (at 2602.8m MD) shows sharp-erotional surface as a base of Åre 6.2. Core desription provided by Ichron Ltd and for the key to the sedimentary symbol see Figure 5.

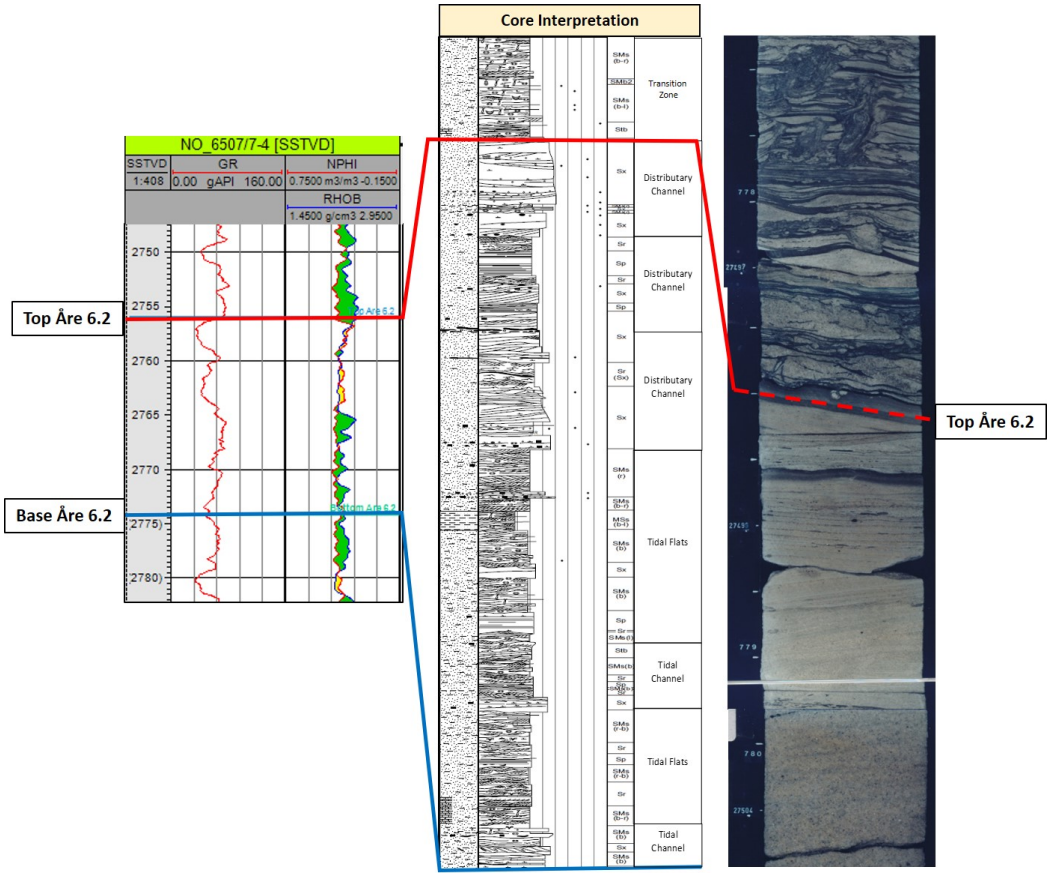

Figure 13. Well log and core log from well 6507/7-4 showing the boundary of Åre 6.2 Zone. The core image (at 2750.2m MD) shows a shallow marine deposit with high amount of trace fossils (upper part), indicating the shift of Åre 6.2 to Åre 7.1. Core desription provided by Ichron Ltd and for the key to the sedimentary symbol see Figure 5.

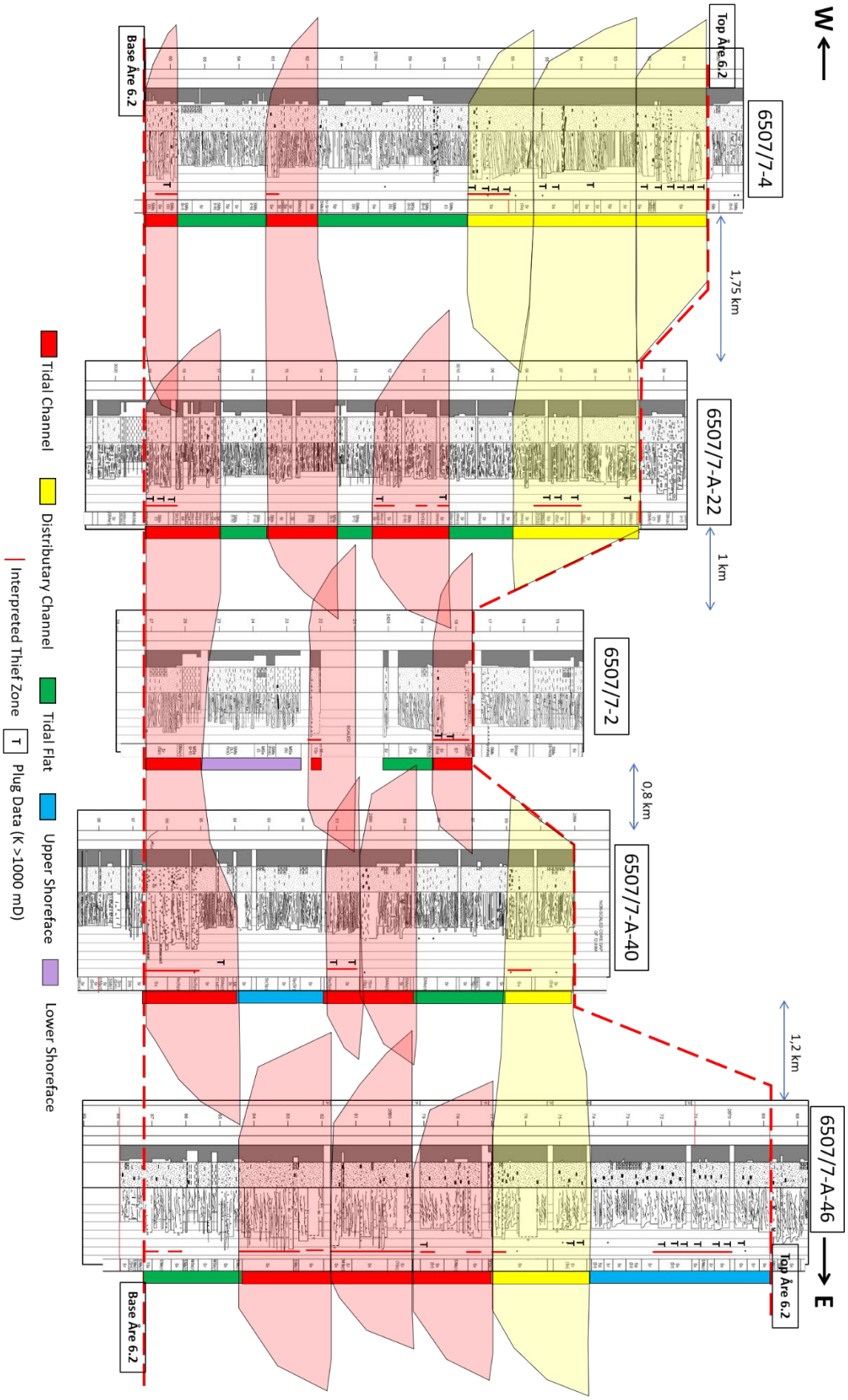

Figure 14. West to East Well Correlation. Individual core descriptions provided by Ichron Ltd and for the key to the sedimentary symbol see Figure 5.

4.2 Lithofacies Descriptions

Åre 6.2 is mainly composed of structured sandstones and heterolith facies. The observed sedimentary structures are cross-bedding, ripple lamination, and parallel lamination. Current and wave action, represented by different types of ripples, are identified in these structures. Identification of sedimentary structures is essential because it is one of the key ingredients used to classify the lithofacies. Besides, a large volume of heterolithic facies is identified in Åre 6.2. They are mostly formed by tidal processes as indicated by different types of mud layers (more than 1 cm thick) and drapes (less than 1 cm thick) as well as bi-directional current indicators. The heterolithic lithofacies are divided into two lithofacies based on the dominant composition of the rocks, which are sandstone-dominated structured heterolith (SMs) and siltstone-dominated structured heterolith (MSs) – see the lithofacies classification scheme adopted from the Statoil-Ichron study (Table 2).

There are many lithofacies identified in Åre 6.2, but only five types of sandstone lithofacies were discussed; they are: planar-stratified sandstone (Sp), ripple cross-laminated sandstone (Sr), Cross-stratified sandstone (Sx), Sandstone-dominated structured heterolith (SMs), and Siltstone-dominated structured heterolith (MSs). These lithofacies are the dominant lithofacies in Åre 6.2 and will be modeled in the SBED software to analyze rock heterogeneities at lithofacies scale, which is explained in the next chapter. The five main lithofacies are described and interpreted as follows. The other lithofacies were not modeled since their occurrences are local and considered insignificant for this study.

1. Ripple Cross-Laminated Sandstone (Sr)

   This lithofacies consists of fine to very fine grained and well sorted sandstone, showing ripple cross-lamination (Figure 15). The ripple structures were mainly formed by current processes indicated by one directional ripple migration. Some bipolar cross-laminations are present, suggesting tidal influnce (cf. Dalrymple and Choi, 2007; Van den Berg *et al.*, 2007). This lithofacies is interpreted to be a deposit produced by a relatively slow flow according to a bedform stability diagram (Nichols, 2009). In contrast, climbing ripples are observed in some core sections. This feature is formed by rapid sedimentation in which additional transported sediments exceeds the ripple's forward movement (Nichols, 2009). Some cemented calcite layers and few bioturbation indications are found in this lithofacies.

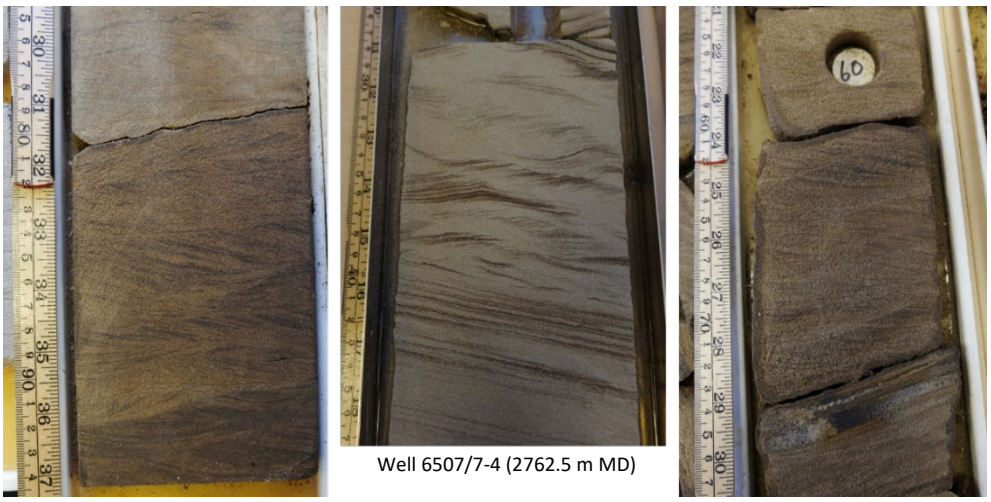

Well 6507/7-A-40 (2884.9 m MD) | Well 6507/7-4 (2762.5 m MD) | Well 6507/7-A-40 (2894.8 m MD)

Figure 15. Core interval of Sr lithofacies

2. Cross-Stratified Sandstone (Sx)

Moderately to poorly sorted, and coarse to fine-grained sandstones characterize this lithofacies. A sharp and erosive base with pebbles and mud clasts is common. In contrast with the Sr lithofacies, the size of the sediment structures of the Sx lithofacies can be up to several meters, and therefore the full geometry of the structures is not clearly seen in the cores. Low- to high-angle cross stratification is one indication to recognize this lithofacies. Locally, some sandstones are unconsolidated, causing poor preservation in the cores. Moderate to strong currents which occur at the base of the channel are intepreted to develop this lithofacies. Bioturbation is absent.

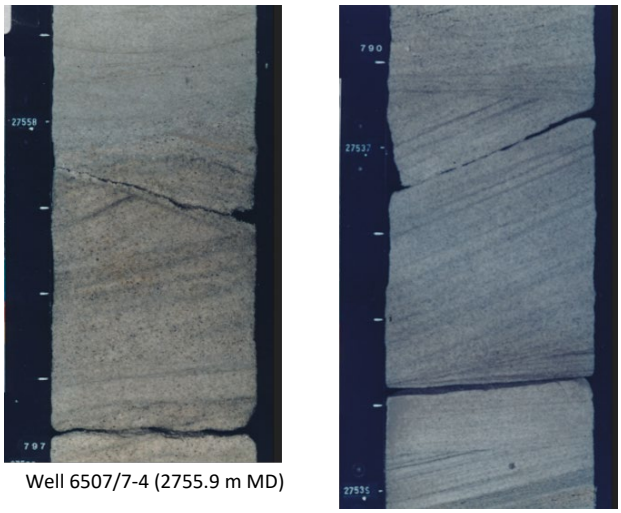

Well 6507/7-4 (2755.9 m MD) Well 6507/7-4 (2753.5 m MD)

Figure 16. Core interval of Sx lithofacies

3. Planar-Stratified Sandstone (Sp)

This lithofacies is characterized by planar stratified, well sorted, very fine to fine grained sandstones. Because of the paralel structures, the structure dip in this lithofacies represents the actual dip of the rock bedding. In this study, most Sp lithofacies shows horizontal or gently inclined bedding (<5˚). The planar stratification is formed by either coarser sands that are transported in relatively low flow velocities or by finer sediments transported in fast flow (cf. Nichols, 2009).

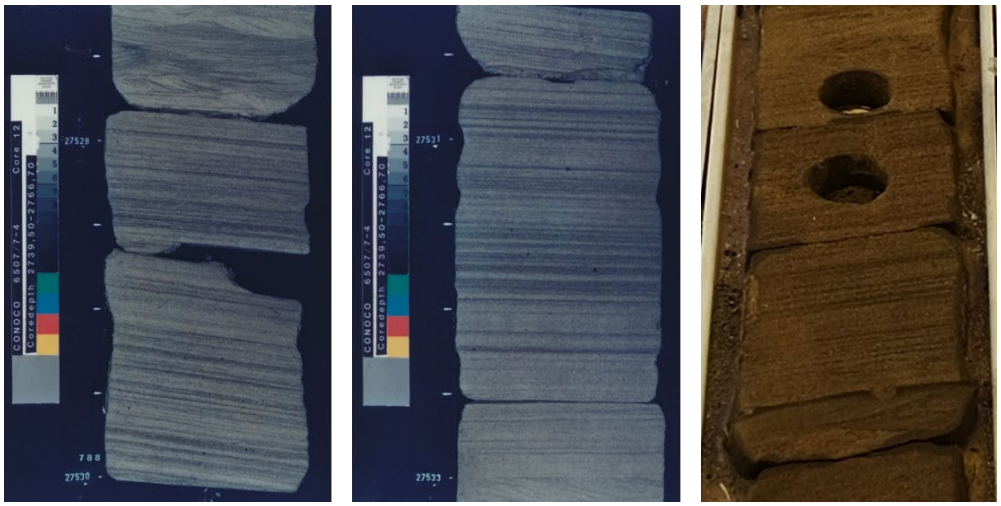

Well 6507/7-4 (2753.0 m MD) Well 6507/7-4 (2753.3 m MD) Well 6507/7-A-40 (2886.5 m MD)

Figure 17. Core interval of Sp lithofacies

4. Sandstone-Dominated Structured Heterolith (SMs)

This hetorolitic deposit is dominated by sandstone with a sandstone:mudstone ratio between 90:10 and 60:40. This lithofacies is typified by current-ripple lamination, large-scale cross stratification, and interbedded mudstone laminas showing double-mud-drapes (those less than 0.5 cm thick). Mudstone laminas ranging from 0.5 cm to 1 cm thick are interpreted as fluid muds. All of these characteristics indicate that tidal currents had a significant influence on deposition. Bioturbation is sparse in this lithofacies. The sandstones contained in SMs are generaly fine to very fine grained and moderately to well sorted, although medium-grained and poorly sorted sandstones are also present; this would suggest the occurrence of higher river discharge periods.

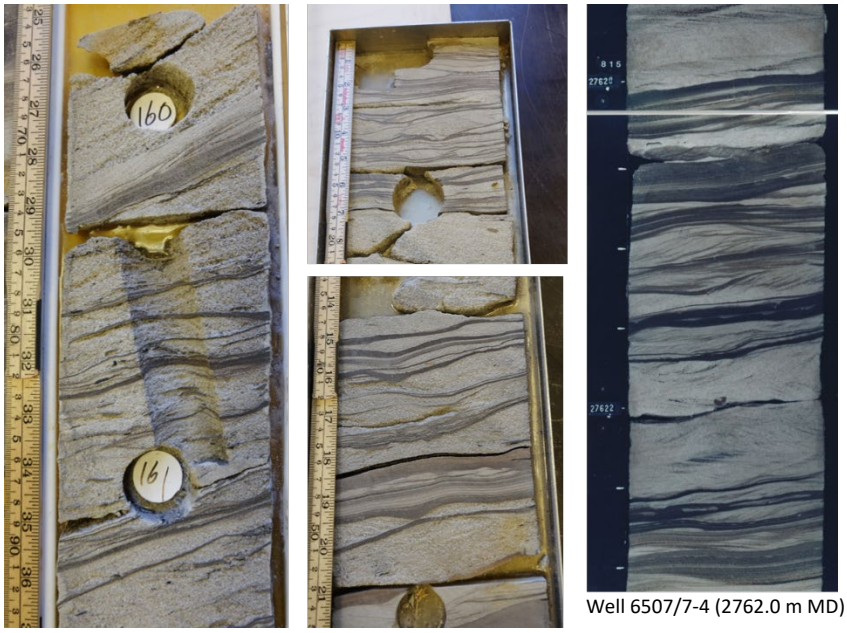

Well 6507/7-A-22 (2019.0 m MD) Well 6507/7-4 (2766.0 m MD) Well 6507/7-4 (2762.0 m MD)

Figure 18. Core interval of SMs lithofacies

5. Siltstone-Dominated Structured Heterolith (MSs)

This lithofacies is composed of lenticularly-bedded heterolithics. Mudstones interbedded with sandstone layers are pcommon, with mudstone dominating the rock composition and a sandstone:mudstone ratio between 10:90 and 40:60. The sandstones are very fine grained and well sorted. Sedimentary structures observed are ripple and parallel lamination. The ripple lamination is generally asymetrical which suggests unidirectional current indications. A large amount of mudstone clasts and sparse to moderate degree of bioturbation suggests that the depositions were formed by suspension processes during slow sedimentation in paleoenvironments with a somewhat restricted salinity.

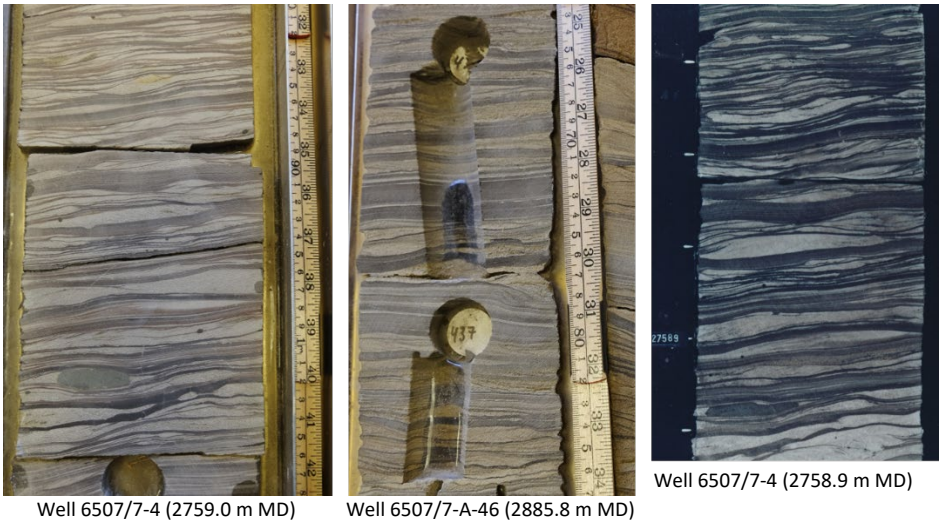

Well 6507/7-4 (2759.0 m MD) Well 6507/7-A-46 (2885.8 m MD) Well 6507/7-4 (2758.9 m MD)

Figure 19. Core interval of MSs lithofacies

4.3 Facies Associations Descriptions and Depositional Environment

Across the seven cored wells, five facies associations are identified with different abundancies and stratigraphic locations in each well. They are: tidal channel, distributary channel, tidal flats, upper shoreface, and lower shoreface. The facies associations are aligned with the interpretation which represents that the Åre 6.2 was formed as estuarine and bay-fill deposits (Thrana *et al.*, 2014). These facies associations are summarized in Figure 21 and the lithofacies legends can be found in Table 2.

1. Facies Association 1 (FA1): Tidal Channel

   FA1 consists mainly of structured sandstone and heterolithics that are arranged in stacked fining-upward successions (Figure 20). The base of FA1 is characterized by the sharp-erosional base and Sx lithofacies with medium to coarse grain size. Occasionally, rip-up mud clasts are found at the base indicating the erosional process of underlying mud layer. These deposits are overlain by SMs alternating with Sr or/and Sx which do not only occur at the base. The sandstone gradually changes into finer-grained sandstone followed by MSs and laminated siltstone (Ml) formed in the upper part of the FA1. This succession clearly shows and proves an upward decreasing grain-size (fining-upward profile). Locally, this facies association includes the unconsolidated sandstone which is considered as one of the thief zone's characteristics. Current and wave ripple structures are visible, and mud drapes are common which are indicative of tidal influence. Besides, structureless mud layers with thickness 0.5 – 2 cm were observed in this FA. These are interpreted as fluid muds associated with the area where the suspended sediment coming from the river is trapped due to the fresh and salt water mixing and tidal processes (Ichaso & Dalrymple, 2009). Fluid muds are typically formed in river mouths of either tidal-fluvial channels and proximal channel in deltaic environments. All of these characteristics are interpreted to indicate that the FA1 was deposited in a tidal channel.

   A tidal channel is one of the features that can be formed in tidal-dominated estuarine, specifically in the inner part of estuary where tidal process influences the area quite intensively. The sand bodies are deposited in the inner bank of the meandering belt by

lateral migrating point bars indicated by fining-upward succession. The deposition is showing generally the same point bar form as purely fluvial system with the exception of the products generated by the tides which include typical sedimentary structures, different sand body shapes and lithofacies distributions (this will be applied to the conceptual model and modeling part). The tidal channel usually dissected tidal flats with mud clasts and relatively coarse sands contained at the base of the channel sequence. Bidirectional cross-bedding and ripple laminations indicate reverse tidal current caused by ebb and flood current. The abundance of heterolithic facies represents sedimentation changes between suspension and traction due to flow velocities variation as the flow can decrease and increase with the tides (Payenberg & Lang, 2003).

2. Facies Association 2 (FA2): Tidal Flats

   FA3 is dominated by SMs and Sr that are shifting with a various thickness from 20 cm up to 100 cm. Unlike FA1, no medium and coarse-grained sandstone is observed in FA3. The grain size of the sandstone is smaller classified as fine to very fine sand, and the sandstone is well sorted. The mud content is high (Figure 20), which is an indication of lower energy sedimentation than in FA1. Other lithofacies found in this FA are Sx, Sp, MSs, Ml, and thinly bedded sandstone (Stb). These lithofacies occur disorderly around the dominant lithofacies SMs and Sr. The base of FA3 is not always visible. It can be recognized by a sharp grain size change or the lithofacies change into SMs. However, in some cases, the base of FA3 is not well defined especially when the underlying facies association consists of relatively similar sandstones. The high abundance of heterolith and the mud draped sedimentary structures in this FA are indications that tidal process formed a significant control on deposition. Therefore, FA2 is interpreted as tidal flats because of high tidal influence and low energy deposition. Tidal flats are the area adjacent to the channel that are submerged during high tide and exposed at low tide.

3. Facies Association 3 (FA3): Distributary Channel

   FA2 is generally composed of types of lithofacies that are contained in FA1. However, the proportions are different. For example, heterolithic sandstone and tidal-generated sedimentary structures occur much less frequent in FA2 than in FA1. It implies that FA2 is situated slightly away from the tidal movement and subjected to influences from fluvial energy. At the base of FA2, Sx is underlain by the erosive based surface in which pebble mud clasts can be present. These clasts may be introduced by erosion of channel banks. The Sx lithofacies is commonly followed by Sr which is frequently found in FA2. Locally, Sp and SMs are observed alternating with Sr or Sx lithofacies. This lithofacies succession indicates a fining-upward grain size profile in the FA. The sedimentary structures at the base of the FA indicate the importance of bedload currents which were most likely present in the deepest part of channels. In addition, tidal-generated structures such as mud drapes occur here. Combined with the presence of the heterolithic facies, it is suggested that FA2 represents the product of fluvial-dominated process with a little tidal influence that may occur in the most landward area of estuary but still within a tidal range in the area. The finning-upward grain size profile is an indication of product of meandering channels such as estuarine distributary channels. Figure 20 shows that Sx predominate the FA2 and the channels are amalgamated indicated by two FA2 on top of each other with erosional bases.

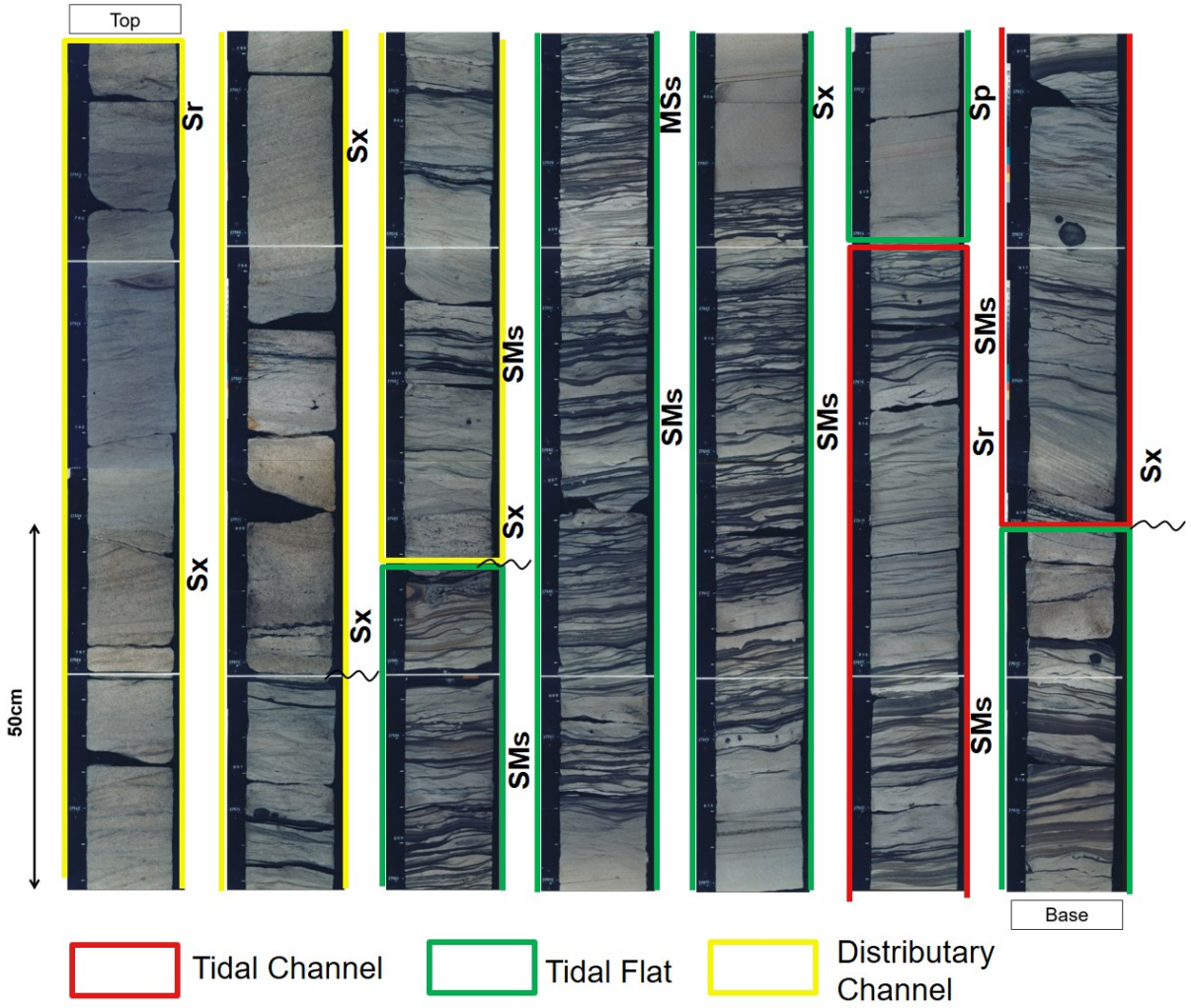

Figure 20. Facies Association FA1, FA2, and FA3 within well 6507/7-4 (2763.5 – 2755.1 m MD)

4. Facies Association 4 (FA4): Upper Shoreface

   FA4 is an association that does not have a wide lateral extent in Åre 6.2 because it is only found in well 6507/7-A-40 and 6507/7-A-46 in different stratigraphic level. These wells are located at the center-east part the Heidrun Field which might be explained by an irregular form of the shoreline since mainland is regionally interpreted to be in the west part. FA4 is predominantly formed by sandstone which contains cross- and planar stratification. At the base, FA4 consists of Sr characterized by very fine to fine-grained sandstone indicating low energy conditions. The Sr lithofacies is overlain by Sx and then followed by Sp. SMs is occasionally present as an indication that tidal processes affect this association, but wave-generated structures are dominant. All of these characteristics are interpreted to indicate that FA4 is deposited in a relatively low energy environment with limited influence by tidal activity. Therefore, FA4 is interpreted as a shoreface deposit that is related to the overall transgressive sequence of Åre 6.2 Sub-Zone.

5. Facies Association 5 (FA5): Lower Shoreface

   FA5 is mainly composed of SMs and MSs in which the sandstone is moderate to well sorted with a very fine to fine grain size. At the base, SMs is observed, which is overlain by MSs. This succession is repeated until the upper part of the FA. Although ripples are mainly formed by wave-generated processes, some current ripples and mud drapes occur formed as fluid muds in areas where salt and fresh-water mixed, which allows for including some tidal activity in the environmental interpretations. Besides, this association commonly shows low-angle laminated or Hummocky Cross Stratification (HCS) which represents high energy wave influence such as storms. Consequently, this structure is interpreted to be developed at the area between the fair-weather wave base and the storm-weather wave base,that is a lower shoreface environment.

The interpreted FA above show the characteristics of some elements that are suggested to be part of a compound estuarine valley fill. The position of these facies association within the estuary system are shown in Figure 23. This interpretation is aligned with the updated stratigraphic study of Åre Formation conducted by Thrana *et al*. (2014). An estuary is a seaward portion of the drowned valley which is influenced by the marine processes (Dalrymple *et al.*, 1992). The valley is flooded with seawater when relative sea level rise or during transgression period. The estuary receives sediment from both fluvial and marine, and the sediment are deposited with the effect of the tide, wave, and fluvial process. Delta environment differs from estuary as the sedimentation in delta build out into marine (prograding) while estuary represents the drowned valley. The estuary of Åre 6.2 is categorized as a tide-dominated estuary since the lithofacies formed by tidal processes are prominent.

A tide-dominated estuary is most commonly formed in mesotidal and macrotidal coastal regime where tidal current energy can be greater than wave energy at the funnel shape of the estuary. The tidal energy from the estuary mouth to the tidal limit decreases to zero. In contrast, the river current increases landward as it has less interaction with marine processes. This shift between marine and river current energy leaves the estuary to have three zonal patterns which are marine-dominated, mixed-energy, and river-dominated (Figure 22).

The area near the mouth of the estuary, which is a marine-dominated part, is dominated by tidal sand bar deposition, but this typical feature is not observed in Åre 6.2. This most distal section of the palaeo-estuary is most likely not covered in the Heidrun Field within the Åre 6.2 stratigraphic zone, but it may possibly be found in the underlying or overlying zones. Instead, the tidal and distributary channel in Åre 6.2 is interpreted to be deposited in the mixed-energy and river-dominated area. The estuary zonal patterns are used to differentiate between these two channel types. Distributary channel occupies the river-dominated zone whereas the tidal channel composes the central mixed-energy area of the estuary. Figure 22 shows that the mixed-energy area consists of a meandering channel which represents the tidal channel. The channel style changes to straight as it reaches the river-dominated zones. The distributary channel in this study is interpreted to be deposited in the river-dominated zones but still with a meandering channel style. This difference may be caused by the low-gradient morphology which tends to generate more meandering channels.

Facies Association	% Sand	Lithology	Grain Size and Structures	Lithofacies	Descriptions
			silt vf f m c vc		
Lower Shoreface (FA5)	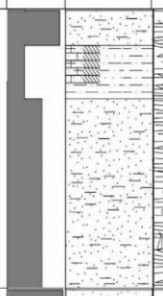			Sms, Mss, Hcs	Mainly composed by heterolith lithofacies, both sand and silt dominated heterolith with medium and small scale of cross stratifications. Cross bedding and ripple lamination are also present. Wave-influenced structures are dominated.
Upper Shoreface (FA4)	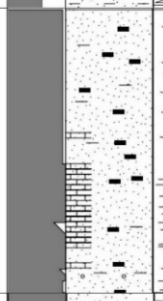			Sr, Sp, Sx minor: SMs	Fine to very fine grained and well-sorted sandstone with cross and planar stratifications. Locally, sand-dominated heterolithic and mud drapes are present. Mainly composed by alternating lithofacies Sx, Sr, Sp.
Distributary Channel (FA3)	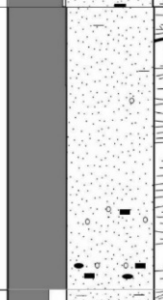			Sx, Sr minor: Sms, Sp	Medium to very fine sandstones showing fining-upward profile with sharp contact and lags of mudstone at the base. Sedimentary structures are dominated by cross bedding, current and wave ripples, and parallel laminations. Sand-dominated heterolithic and mud drapes are visible but not common. Composed of moderate-to-well-sorted grains and amalgamated sandstone may occur. Locally, coal fragments are present.
Tidal Flat (FA2)	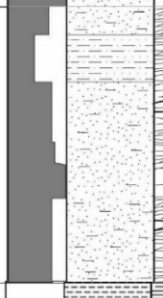			Sms, Mss, Sr minor: Sx, Sp, Stb, Ml	Sand-dominated heterolithics intercalated with ripple-laminated sandstones. The sands are fine to very fine-grained size and well sorted with mud drapes, current ripples, wave ripples, parallel laminations, cross beds. Strong tidal influences and very heterolithic.
Tidal Channel (FA1)	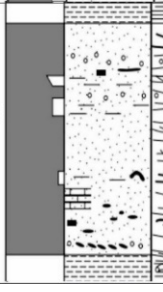			Sx, Sr, Sms, Mss, Ml, Stb	Sand dominated heterolithics and structured sandstones arranged in stacked fining-upward successions. Coarse to very fine grain size and moderate to well sorting. Some sandstones are unconsolidated. Cross bedding, current ripples, wave ripples, mud drapes are common. Sharp-erosional base composed by pebbly sandstone or basal rip-up mud clast, overlain by cross-bedded sandstone and followed by ripple laminated sandstone and sand-dominated heterolithics.

Figure 21. Facies Association descriptions observed in Åre 6.2 (core description from the Statoil-Ichron study). For the key to the sedimentary symbol see Figure 5

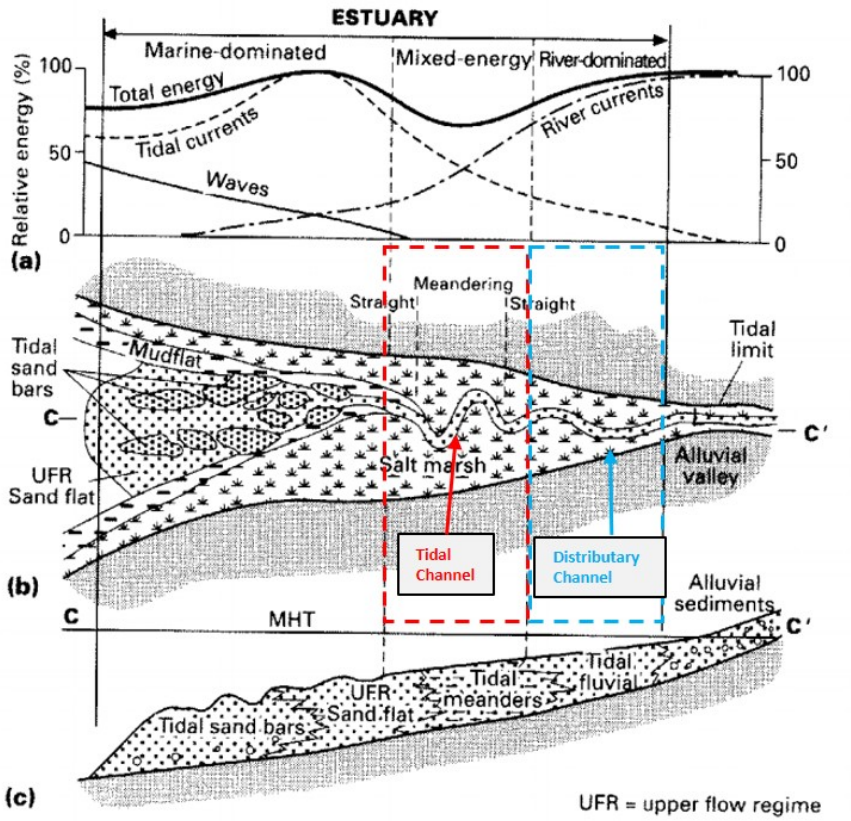

Figure 22. Distribution of tide-dominated estuary regarding (a) energy type, (b) morphology and (c) sedimentary facies. After Dalrymple et al. (1992).

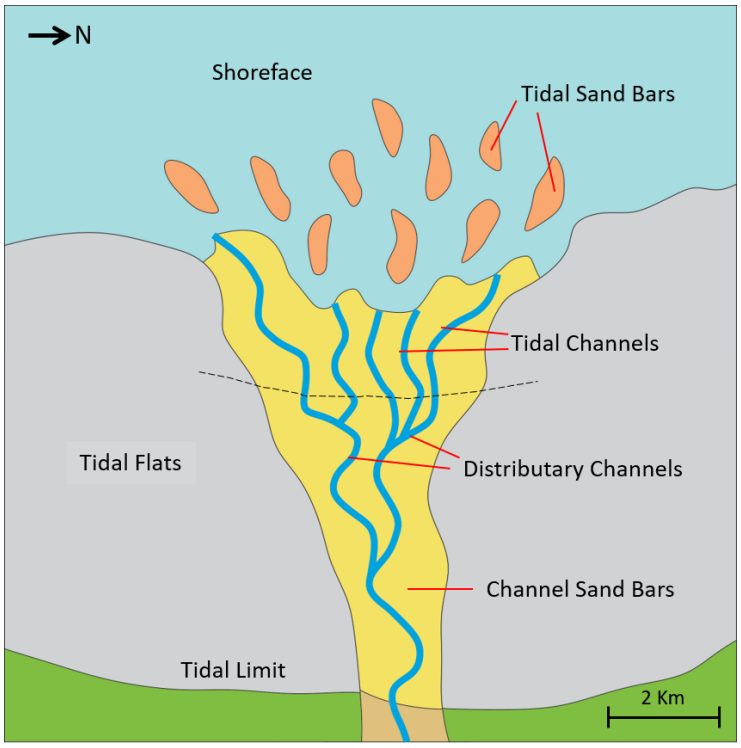

Figure 23. Estuary model for Åre 6.2, showing the location of the interpreted facies associations. Note that the distributary and tidal channels are connected but the tidal channel is subjected to more tidal processes

Along the side of the channel, there is an area alternately submerged and subaerially exposed by changing tidal level, called tidal flats. The associated tidal deposits can be found widely in intertidal areas. Therefore, their extension will depend on tidal range, sediment supply, and gradient of the shoreface. Macrotidal setting and low-gradient coastlines generate the most prevalent occurrence, so that tidal flats may contain a major portion of the delta or estuary plains. In this study, the tidal flats are mainly composed of very fine-grained sand-dominated heterolithic facies with some ripple laminations. This characteristic reflects the deposition occurred in the range of sand flats and mud flat zone in intertidal area as shown in Figure 24 (Dalrymple *et al.*, 1992). The intertidal area is situated in between high and low tide levels.

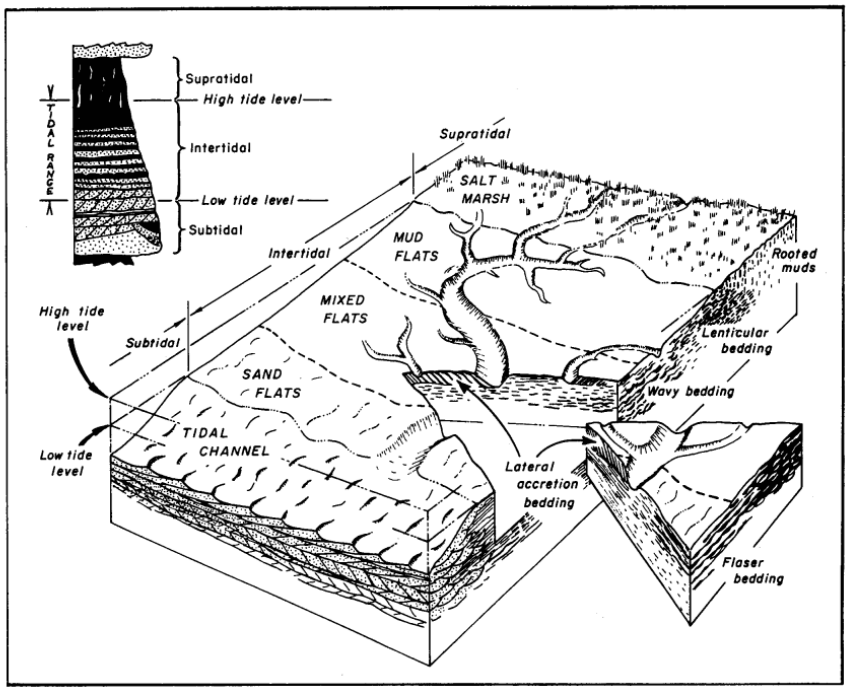

Figure 24. Block diagram of a typical siliciclastic tidal flat (Walker et al. 1992).

A study of Åre Formation by Thrana *et al*. (2014) also suggests that estuary model of the upper part of the Åre Formation can be equated to estuary model of the lower part of the Tilje Formation in the Heidrun Field explained in a paper by Martinius *et al.* (2001). The estuary model is described as a shallow and wide morphology which was shaped during a rapid sea level fall and the following rise. The overall succession shows typically fluvial dominated channels at the base, representing the initial incision of the valley. It is followed by flasser-bedded sandstone interval formed by landward-directed sediment transport. This interval is interpreted to be deposited in the outer part of the funnel-shaped estuary as mid-channel accretionary bars and subaqueous channel banks which was formed after initial flooding and the during the succeeding valley drowning. At the top of succession, wavy-bedded heterolithics which are parts of tidal point bar deposits were observed. This is interpreted as the heterogeneous fill of tide-influenced channels. The Åre Formation, specifically Åre 6.2 Zone which mainly consists of tidal and distributary channels with high heterolithic contents, may be referred to this top succession or a filling the late stage part of the estuary. This estuary evolution is illustrated in Figure 25 (Martinius *et al.*, 2001), where Åre 6.2 can be represented by the mostly filled estuary Stage B.

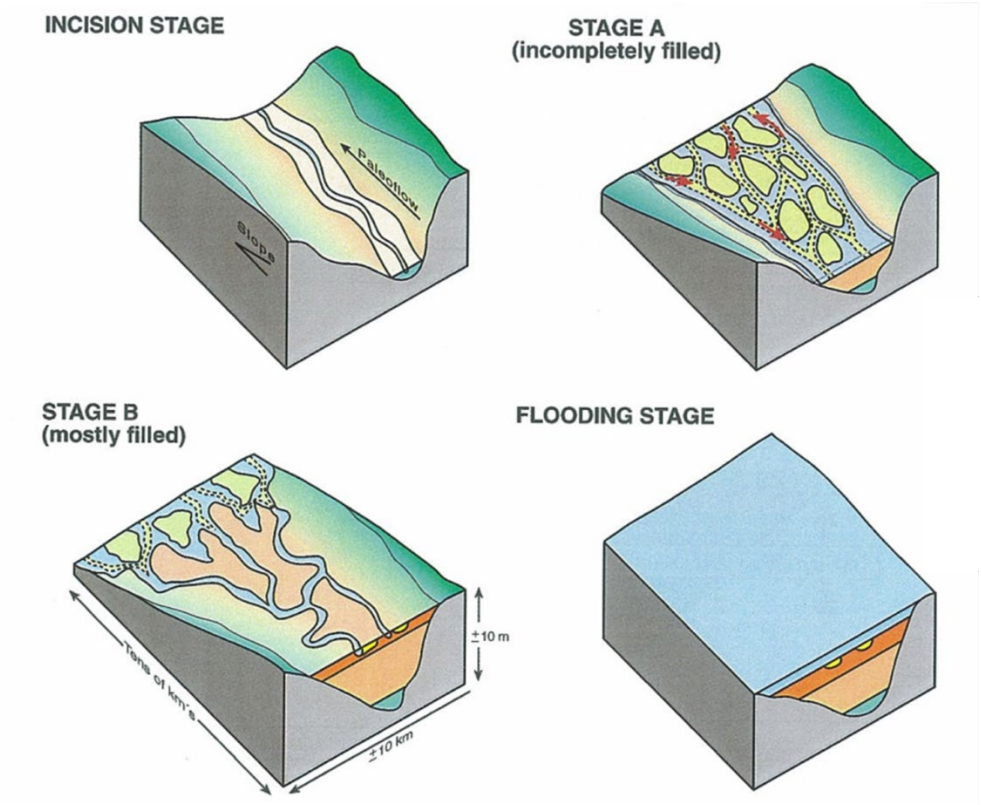

Figure 25. Estuary evolution models during transgression, interpreted from the lower part of Tilje Formation (Martinius et al., 2001). Channel complex in Åre 6.2 can be reffered to the mostly filled estuary (Stage B)

4.4 Thief Zone Characteristics

Bane (1994) defined a thief zone as a laterally continuous stratigraphic unit of relatively high permeability and large pore radius, which may approach residual oil saturation. The thief zone can give a different impact from one reservoir to another depending on the specific conditions. On one side, the high permeability can be favourable because a high rate of oil production can be extracted from a layer with a high permeability. On the other hand, the high permeability layer can cause unstable flood front motion and an abnormal well-production profile (Moore, 1989). This negative impact can lead to early water breakthrough and poor sweep efficiency since the thief zone can transmit a large quantity of water. This is the situation in the Åre 6.2 reservoir zone in the Heidrun field. Therefore, their characteristics and effects on the models and flow properties are important to note.

In this study, a thief zone is determined to be a relatively thin layer (0.5 to 2 meters thick) which has a high permeability greater than 1 Darcy (can be up 10 Darcy) while the permeability of the surrounding facies is generally around 0.3 Darcy or even lower in mud-rich facies. The plug data are used to obtain an indication of permeability, but they are limited because they sample a small rock volume and, in addition, some core intervals with thief zone facies are unconsolidated and cannot be sampled. Thus, thief zone identification was also performed based on visual core observation and handled through the conceptual model input to the geomodel. The thief zones have to some extent variable characteristics, but generally, they are characterized by relatively immature medium to coarse-grained sandstone with moderate to poor grain sorting (Figure 26). The unconsolidated sandstone is mainly composed of medium to coarse sand which is also considered to be a thief zone (and production data

support this assumption). The thief zones are present both as part of a heterolithic interval as well as of structured sandstone. Cross stratification in particular, but also and ripple lamination, are sedimentary structures that are common in the thief zone intervals.

Thief zones were identified in all seven wells that are used for this study. Table 3 lists the characteristics of the thief zones and their depth occurrences in the wells, linked to the lithofacies and facies associations. Based on the core observation and plug data, the high permeability layers are mostly found in the channel facies associations, both tidal channel and distributary channel. This shows that the thief zones were formed by a process that has a significant impact on the channel's palaeo-depositional conditions.

Most thief zones are situated at the bottom or the lower part of the channel succession. This might be because the lower part comprises the base channel deposits with the highest energy levels and with the coarser-grained cross-stratified (Sx) sandstone fractions (higher than in the middle and upper parts). The coarse material influxes may be the result from a significantly larger influx of fluvially-derived sediment during high water discharge into the channel (river floods, possibly seasonal). The distributary channels are found to be directly affected by these high discharge periods because the resulting deposits are of fluvial origin. In some occasions, the coarse fluvial sands can also be transported all the way to the coastline by the fluvial flash floods and further distributed into the tide-dominated channels.

Another type of thief zone is found in the upper shoreface facies association. Examples are those found in the upper part of the Åre 6.2 zone in well 6507/7-A-46. These thief zones occur in the middle of the facies association and they are characterized by cross-stratified (Sx) very fine to fine grained sandstone, moderate to well sorting, and sub- to well-rounded grains. These grainsize characteristics are commonly found in beach environments and are interpreted to have formed in response to the back-and-forth movement of sediment caused by wave processes which are typical for beaches. Therefore, it is deduced that the thief zones in the upper shoreface result from sediments formed on beaches or the areas near shorelines.

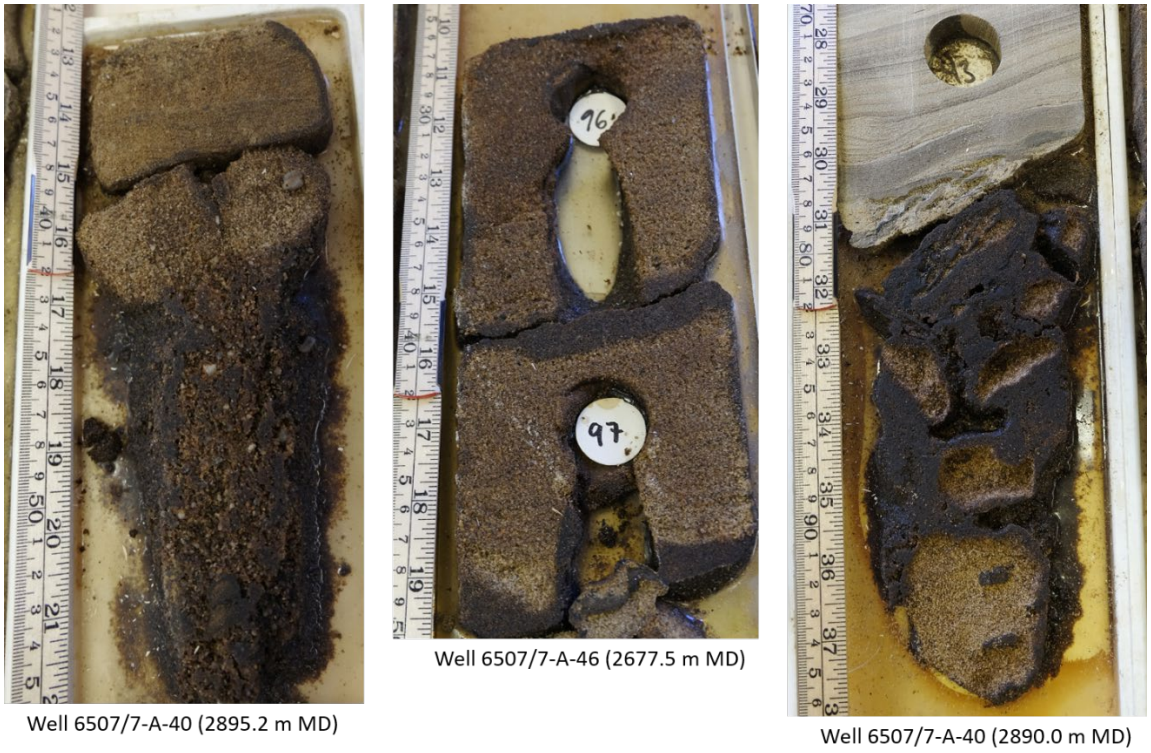

Well 6507/7-A-40 (2895.2 m MD)

Well 6507/7-A-46 (2677.5 m MD)

Well 6507/7-A-40 (2890.0 m MD)

Figure 26. Thief zones interval observed in the core

Table 3. Thief Zone's Presences in Each Well

Well	Facies Association (FA)	Stratigraphic Position	Lithofacies
6507/7-4	Tidal Channel	Middle	Sx
	Distributary Channel	Bottom	Sx
6507/7-A-22	Tidal Channel	Bottom, top	SMs, Sr
	Distributary Channel	Middle	Sr
6507/7-2	Tidal Channel	Bottom	unconsolidated
6507/7-A-40	Tidal Channel	Bottom, middle	Sx, Sr
	Distributary Channel	Bottom	Sx
6507/7-A-46	Tidal Channel	Bottom, middle, top	Sx, Sr
	Distributary Channel	Bottom, top	Sx, Sr
	Upper Shoreface	Middle	Sx
6507/7-5	Tidal Channel	Top	Sr
	Distributary Channel	Bottom, top	unconsolidated, Sr
6507/7-3	Distributary Channel	Bottom, middle, top	Sx

4.5 Conceptual Depositional Model

As explained in the previous sections, a facies association is a group of lithofacies with a typical order that represents a particular depositional environment. In this study, they are defined based on the vertical variation of lithofacies observed in the cores. According to the Walther's Law a vertical change of some facies is also present horizontally in comformable succession (cf. Posamentier and Allen, 1999). Thus, the vertical sequence implies the lateral distribution of lithofacies as well as a depositional environment (if no erosional or transgressive surfaces are present). This concept is the basis for understanding the spatial distribution of facies in sedimentology. Combined with the available data and the developed sedimentation model, conceptual depositional models representing the facies associations in Åre 6.2 are established.

As described in Table 3, the thief zones are mainly present in the tidal channel and distributary channel facies associations. Therefore, both facies associations become essential, and their conceptual depositional models need to be designed. The deposition of the tidal channel and distributary channel are dominated by current flow as asymmetry ripple laminations and cross-bedding are common. The current is interpreted to occur in the meandering channel complex in which fluvial and tidal processes contributing to the overall net current flow.

This study will model two types of bars representing the distributary and tidal channels respectively. Both bars generally have the same process regarding lateral migration which occurred similarly in both systems. However, they are different in terms of the shape and the growth direction of the bar.

- Distributary Channel
  This channel is a branch of the main river channel that is connected to the sea. The characteristics of this channel are relatively similar to a lower delta plain meandering fluvial system. The flow direction and the sediment sources of this channel are from land towards the sea. Moreover, deposition also occurs in the point bar which is the area inside the bend of the stream. Sediments are inclined layers of lateral accretions which record gradual migration of the point bar. The difference between the distributary

channel and fluvial channel comes from the tidal processes that may influence the current flow and the deposition.

Based on the point bar model of Nichols (2009) and the lithofacies comprised in the distributary channel, a conceptual deposition model for distributary channel in Åre 6.2 zone was developed (Figure 27). The model shows a meandering tidal channel with its bars in which deposition occurred. Each lateral accreting beds consist of five different lithofacies which are Sx, Sp, SMs, Sr, and MSs (ordered from the base to the top). The cross-stratified sandstones (Sx) are present at the bottom of the channel as it is observed in the core. It is followed by planar-stratified sandstone (Sp), sandstone-dominated heterolith (Sms) and ripple-laminated sandstone (Sr). Heterolith lithofacies in distributary channel represent tidal influences, but its occurrence is not extensive since the deposition is dominated by fluvial activity. At the top of the channel, fine-grained sediment is found that drapes the accretion surfaces downward towards the base of the channel. This sediment is represented by the siltstone-dominated heterolith (MSs).

- Tidal Channel
  This channel is shaped by bidirectional flows generated by flood and ebb flows from tides that control the hydrodynamics in the channel. Although the tidal channel shows relatively similar morphological characteristics as the fluvial channel or distributary channel, it has significant differences in the processes that play important roles and affect deposition. The differences are reflected by the sedimentary structures, the shape of sand bodies, and the growth direction of the bar.

  Unlike the distributary channel, heterolithic lithofacies (SMs and MMs) containing double mud drapes are more abundant in the tidal channel. Those structures implicitly show that the deposition is dominated by a tidal mechanism which tends to form heterolithic facies. Ripple lamination (Sr) and cross-bedding (Sx) are common while parallel lamination (Sp) is rare. Based on the core observation, Sp is barely found in tidal channel FA, so it is excluded from the model. In addition, the tidal bar accretions typically migrate obliquely because of a combination of the dominant current and the subordinate currents which flow in opposite directions (Figure 28). This combination creates typical low-velocity zones where sediment can be deposited, resulting in oblique growth bars and elongated morphologies. This characteristic is one the differences between a tidal bar and a point bar that have to be captured in the geomodel.

  Similar to the distributary point bar, the elongate tidal bars migrate laterally. The lateral migration occured because the oblique-oriented tidal bars allow erosion on the stoss side and deposition on the lee side which results in bars migrating towards the downflow direction. Besides, the tidal bars are formed in the inner part of channel bend which is identical to the point bars. The lithofacies arrangement is also similar except the fact that lithofacies Sp does not exist, which changes the SMs composition.

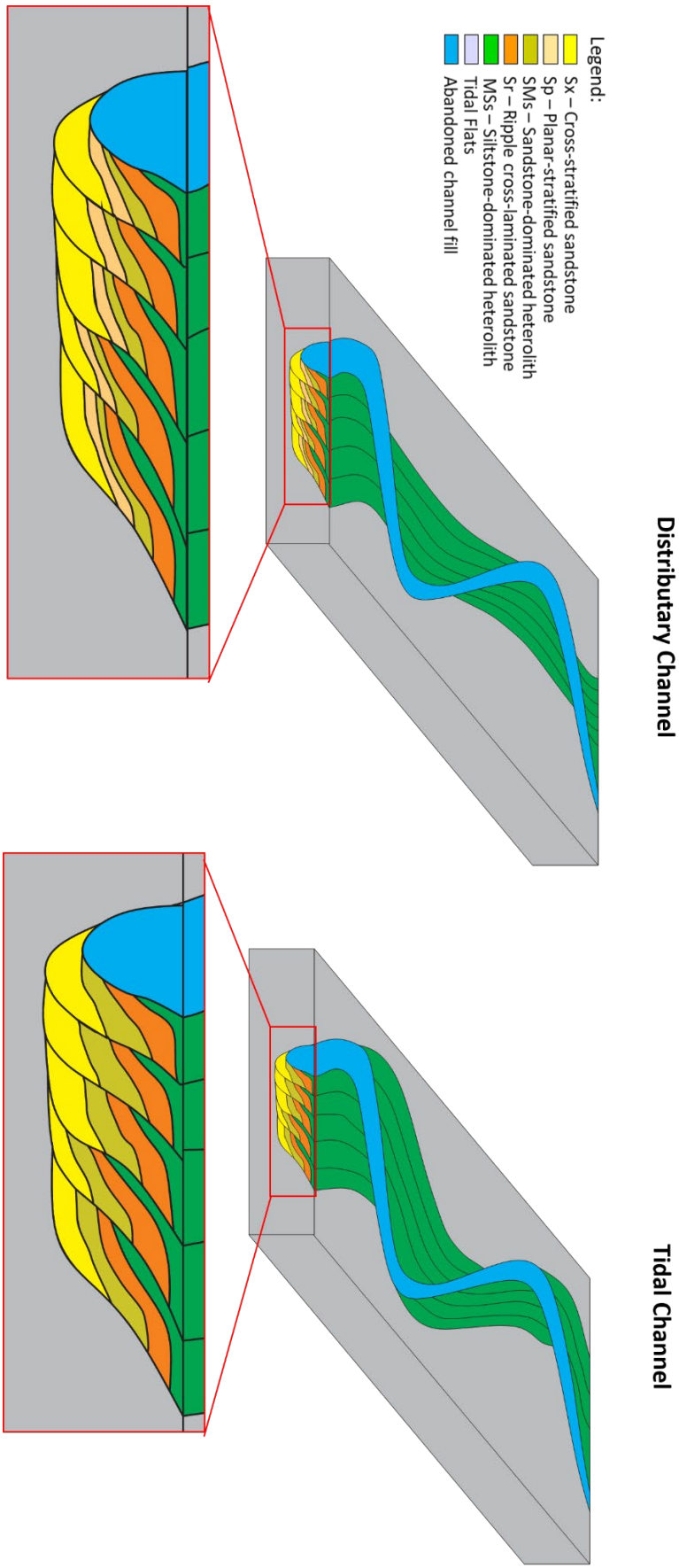

Figure 27. Conceptual Models of a Distributary Channel and a Tidal Channel as defined in this study.

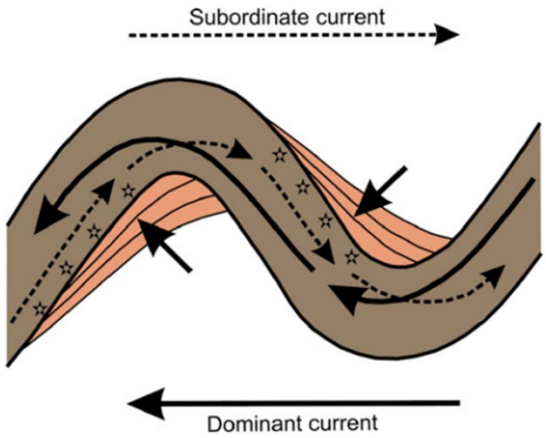

Figure 28. Flow patterns in a tidal meandering channel showing the dominant and subordinate currents flows in an opposite direction (Mutti et al.,1985). The stars indicate the point-bar surface in a low-speed zone and the oblique direction of the lateral migration is indicated by the short black arrows.

5 Multiscale Modeling and Simulation

5.1 Lithofacies-Scale Modeling

SBED™ is a geological modelling software which is used to build a small-scale lithofacies model by applying 3D numerical and process-oriented computation. A synthetic bedform model can be constructed which will represent the sedimentary structure and heterogeneity that exists in the rock. The approach is to make a realistic model by providing input parameters such as migration attributes, amplitude of ripples, and lamina thickness based on characteristics observed in the cores or representative outcrops. It is considered as an important part in geological modelling in certain depositional environments because previous studies have shown that these small features influence flow characteristics such as porosity and directional permeability in reservoir simulation scale (Kjønsvik *et al.*, 1994; Nordahl *et al.*, 2014) The overall workflow for lithofacies scale modelling is illustrated in Figure 29.

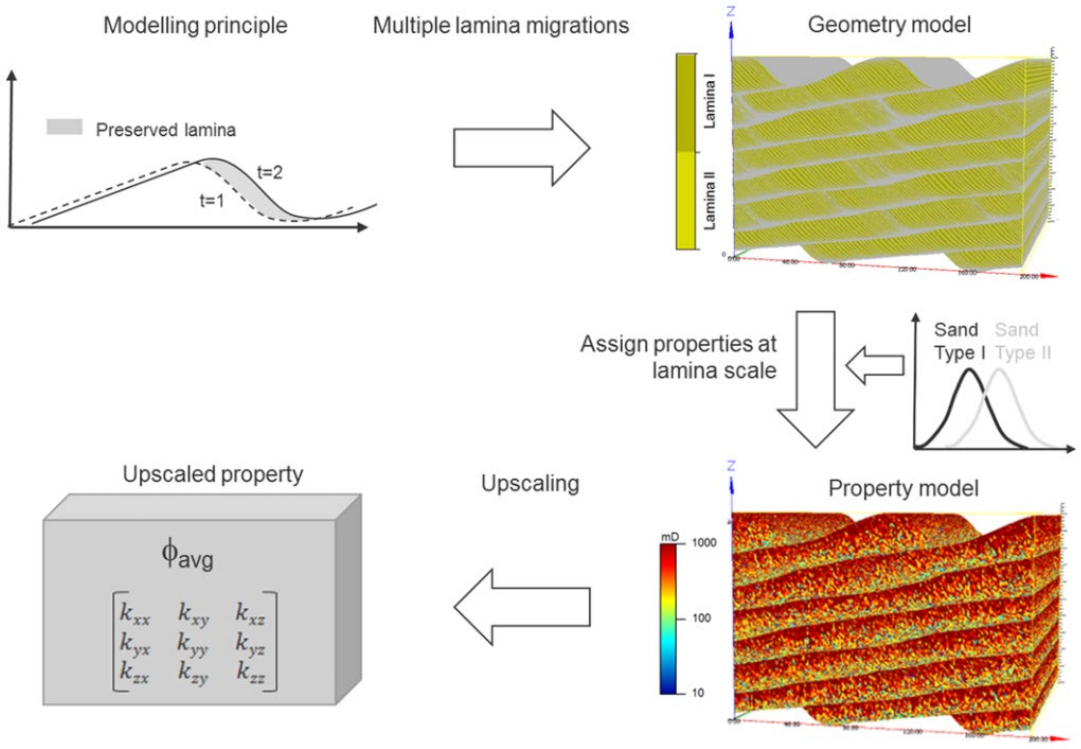

Figure 29. Lithofacies modeling workflow in SBED (Nordahl et al., 2014)

5.1.1 Geometry Modeling

The first step in building a lithofacies model is constructing a geometrical model that represents the sedimentological features of the rock. In this step, sedimentary structures have to be designed and a number of laminas contained in the model need to be defined. The model grids size depends on the size of features that needs to be captured. In this study, the models were built with a size of 30 x 30 x 15 cm, except for Sx lithofacies which has dimension of 200 x 200 x 100 cm because of larger size of cross bedding structures. The chosen dimensions of the models must capture the geometry of the sedimentary structures and cover Representative Element Volume (REV) concept (Bear J., 1972).

The REV represents a volume or area which is large enough to capture the heterogeneity of the rock. If a model or sample is smaller than the REV, any property calculations extracted from them would really depend on the sizes and positions of the models or samples. Some variations can be recognized as small changes in sample positions and/or volumes are applied. In the REV size, the variations are minimized, and an effective property for the model or sample can be measured (Nordahl & Ringrose, 2008; Nordahl *et al.*, 2014). REV between properties may be different since each property has their own characteristics. In this study, the sizes of the models were chosen based on the size of the sedimentary structures contained in each lithofacies. Once the models were built, REV analysis were conducted to obtain volumes that were used to make samples for effective property calculations which were input in facies association modeling.

The SBED™ tool provides some geometrical model templates that are already built in the software. Various template types of cross and planar stratifications, heterolith, and others are available. They are useful to give basic framework to the modeller when building a certain model. Many parameters can be set up to achieve realistic models matched to the core or outcrop images. The parameters include lamina modelling principles such as bedform geometry, migration, and deposition characteristics. Wavelength, amplitude, steepness, thickness, and number of laminas can also be defined within the modelling tool. To show the natural variation, the software gives options of random components that can be applied to the model. All these attempts are done by giving some values to the adjustable parameters which represents multiple lamina migration process. A number of trials were performed until the proposed model is produced.

Some lithofacies in the interested zone were modelled; they are Sx, Sr, Sp, SMs, and MSs (Figure 30). These lithofacies were chosen because they have a significant thickness and comprise majority of lithofacies in Åre 6.2. Moreover, their particular orders are able to be representatives of the facies association. Every lithofacies model is created based on characteristics observed on the core. Any possible features such as bedding set thickness and the dip angle were identified and tried to be implemented to the model. The models are expected to replicate the lithofacies observed on the cores. The cores, however, can only provide 2D views of the rock, so it is often difficult to apply them to a 3D model. In the lithofacies scale, the models can be built as generic model which represent some features identified on the core data. Conceptual model from several sources were also applied to give a guidance on geometry of the sedimentary structures.

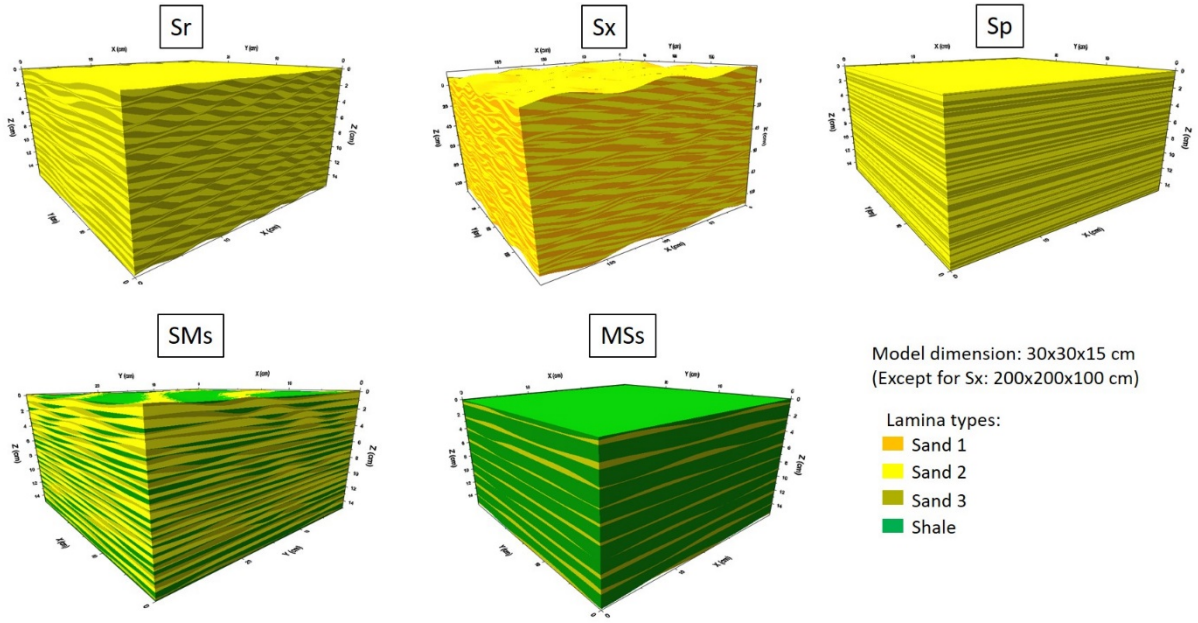

Figure 30. Geometry models of Lithofacies defined in this study.

5.1.2 Property Modeling

Once the geometrical models are constructed, the next step is property modelling. In this study, porosity and permeability are the petrophysical properties which are populated to the model. The statistical distributions of both parameters from a number of samples are required for the modelling process. The data were taken only from routine core analysis from core plugs. Data from well logs were not used since it represents predicted value and does not reflect real value of each properties. Mini-probe permeability data are usually helpful to generate permeability statistics, but such data are not available for the studied cores.

Each geometrical model consists of two or three lithological components which are called laminas. A lamina is a small unit of the rock with the same lithology and characteristics. To illustrate a lamina, Sx lithofacies model is composed of two different laminas which both are sandstone but different in terms of grain size and grain sorting. There are four lamina types identified in Åre 6.2 (Sandstone 1, 2, 3, and shale), described as follows:

Sandstone1: medium to coarse-grained sandstone, moderately to poorly sorted, sometimes unconsolidated. It is mainly present in Sx lithofacies and shows very high permeability values. This is an important lithofacies in the context of this study as it represents the thief zone.

Sandstone2: very fine to fine-grained sandstone, well sorted, light brown. This lamina is a typical sand that exists in every lithofacies, but it locally shows high permeability which can be found in Sr lithofacies.

Sandstone3: very fine-grained sandstone or siltstone, well sorted, dark brown which indicates silt or shale contents.

Shale: dark brown shale, present in the rock as a part of heterolith which is alternating with sandstone.

Each lamina type has to be assigned a statistical distribution of porosity and permeability that are required as input for the modeling part. Looking at the core images and the core plug location it is important to decide whether a sample can be used as representation of one of the lamina types. Some core plugs containing mixed-lamina type, such as in heterolithic zone, are neglected because the samples should reflect property values for a particular lamina type. Thus, only core plugs taken in pure lithologies were selected to property statistics calculations. The stochastic property modeling requires statistical values such as mean and standard deviation for each property in every lamina type. The property values used in the property modeling are listed in the Table 4.

Table 4. Input for Petrophysical Modeling of Lithofacies

Lithofacies	Lamina Type	Porosity (fraction)		Permeability (mD)	
		Mean	StDev	Mean	StDev
Sx	Sandstone 1	0.30	0.08	2431.65	2256.39
	Sandstone 2	0.31	0.06	723.63	767.80
Sr	Sandstone 2	0.31	0.06	723.63	767.80
	Sandstone 3	0.25	0.06	123.59	90.65
Sp	Sandstone 2	0.31	0.06	723.63	767.80
	Sandstone 3	0.25	0.06	123.59	90.65
SMs	Sandstone 3	0.25	0.06	123.59	90.65
	Sandstone 2	0.31	0.06	723.63	767.80
	Shale	0.15	0.04	2.78	5.12
MSs	Sandstone 3	0.25	0.06	123.59	90.65
	Shale	0.15	0.04	2.78	5.12

With regard to petrophysical input, there is only one type of permeability applied to the models. In this case, only horizontal permeability was utilized to build the lithofacies property models. Although some vertical permeability data form core plugs are available, they were not included to the property modeling processes since there is not option to add them. This becomes one of the software limitations found in the property modeling. The software does not differentiate permeability according to the direction despite the anisotropy characteristics. Due to this limitation, the calculations might overestimate the vertical permeability of the models.

The porosity and permeability fields are simulated in a different distribution model. A normal distribution is used for porosity model whereas permeability is modeled by using a log-normal distribution. The permeability has to be modeled log-normally because the data shows an asymmetric distribution which has a tail and a high concentration in a particular group of value. A spherical variogram model is also implemented in modeling process for which the sill and range are set to be 1 and 5 cm respectively. However, for Sx lithofacies, a range of 10 cm is used in the variogram because Sx is larger than in the other models and contains larger sedimentary structures. The relation between porosity and permeability was included in the simulation by adjusting coefficient correlation obtained from core analysis which is 0.75. Based on all of these inputs, lithofacies property model were built (Figure 31 and Figure 32).

Once the petrophysical properties were distributed to the models, the upscaling process was the next step to obtain a representative value of each lithofacies model. However, before doing so, the models needed to be compared with the core plug data and also the rock volume that should be used for upscaling needed to be defined. The following sections explain these required procedures and show the representative upscaled values for each lithofacies model.

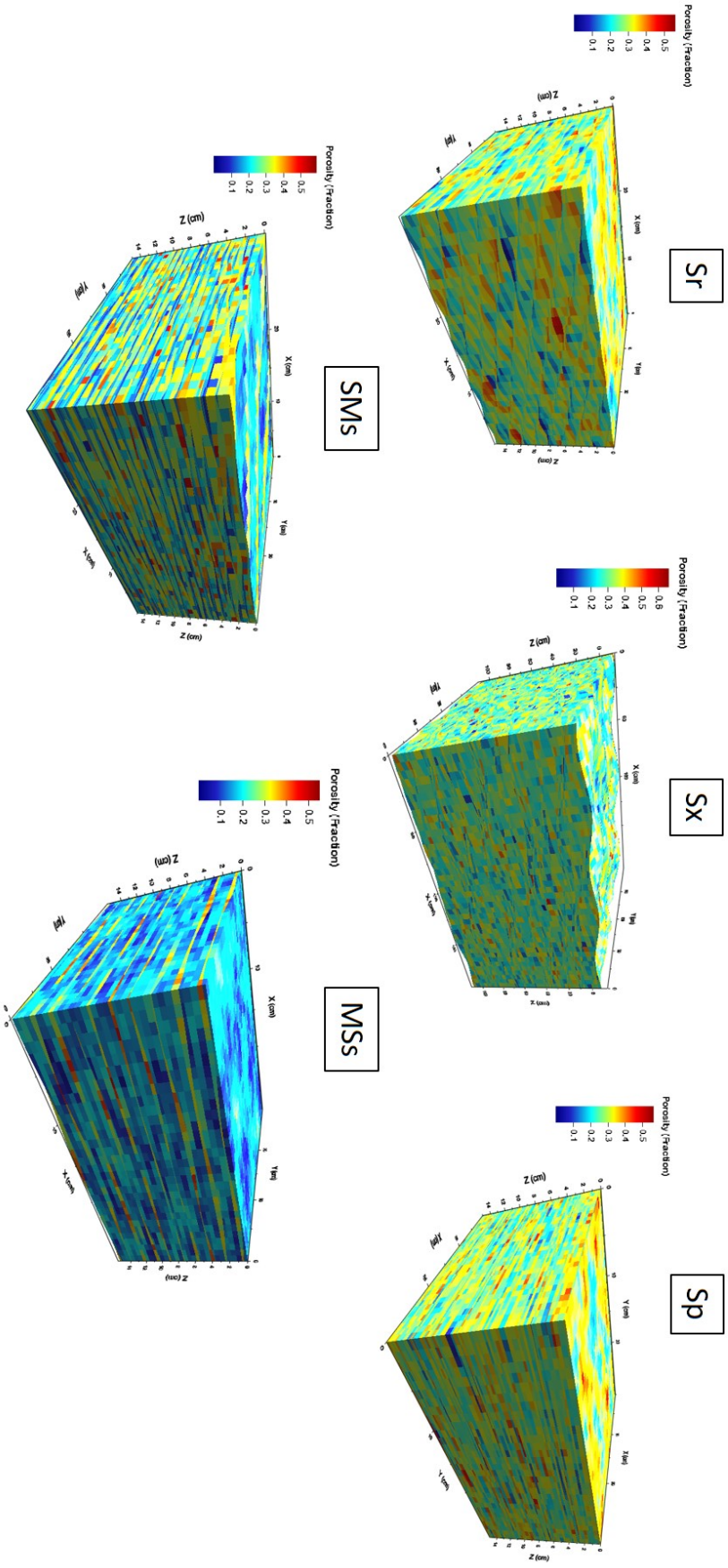

Figure 31. Porosity models of the lithofacies defined.

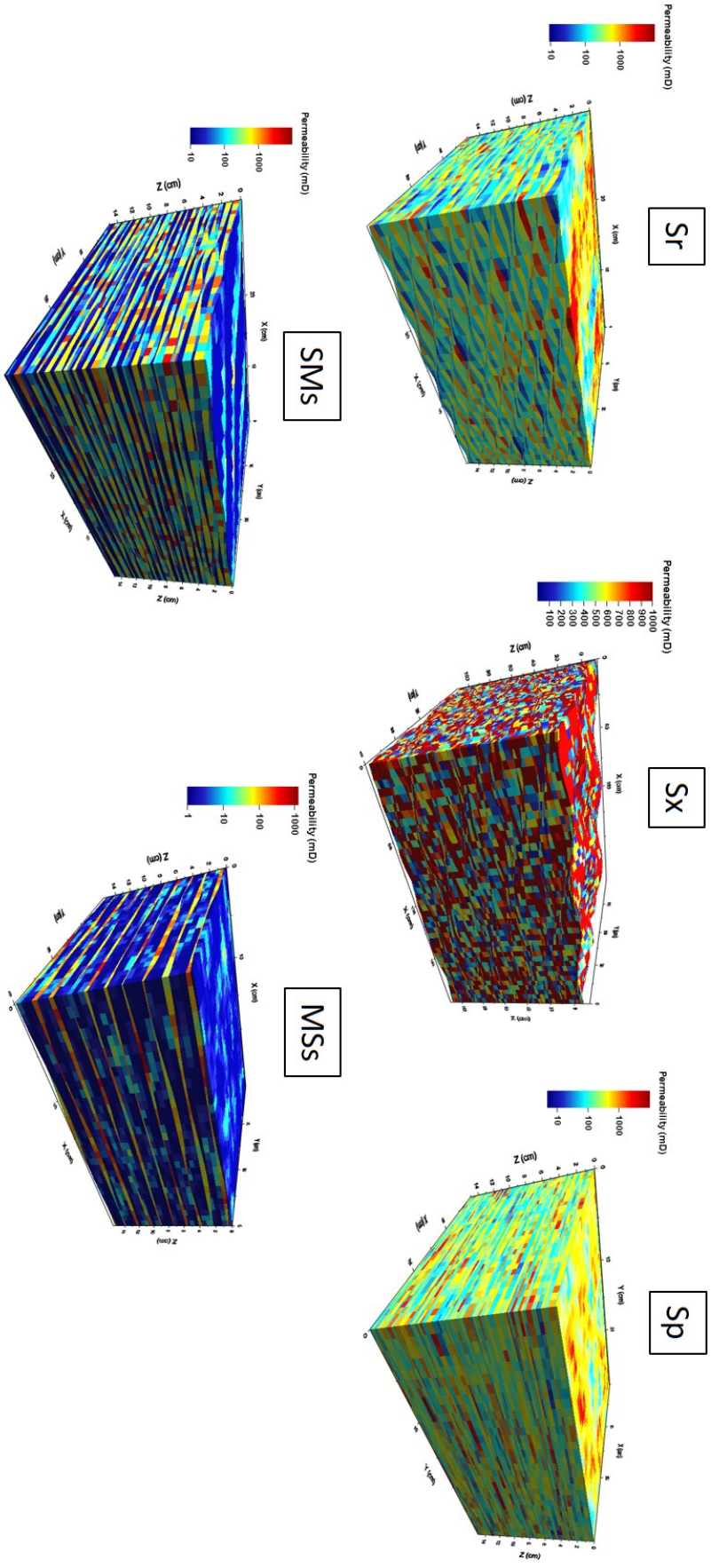

Figure 32. Permeability models of the lithofacies defined.

5.1.3 Validation of lithofacies models

Before the generated lithofacies models are used as input to the next hierarchical modeling level, they need to be quality checked to ascertain whether they honour the real rock measurements represented by the core plug data. This validation was done by taking subsamples from the models at the same size as the core plug size. An open source tool, called cpchop from Open Porous Media (OPM) project (https://opm-project.org), applied with fixed boundary conditions, was performed to obtain subsamples and their upscaled petrophysical values. Fifty subsamples were compared to the available core plug data by using cross-plot of porosity and permeability. Figure 33 shows comparisons between the synthetic and the actual core plug data for each lithofacies model. They both have equivalent distributions which indicate that the models give realistic lithofacies-scale models.

Several iterations for property modeling were conducted to achieve well-matched distributions with the actual core plug data. Slight modifications were made to the input of property modeling because in some lithofacies, the models using the initial input generated a significantly different distribution or trend in the porosity versus permeability distribution plot. Although there are only limited core plug data such as for Sp and MSs lithofacies, general patterns in the cross-plot can still be recognized and be used for this model validation.

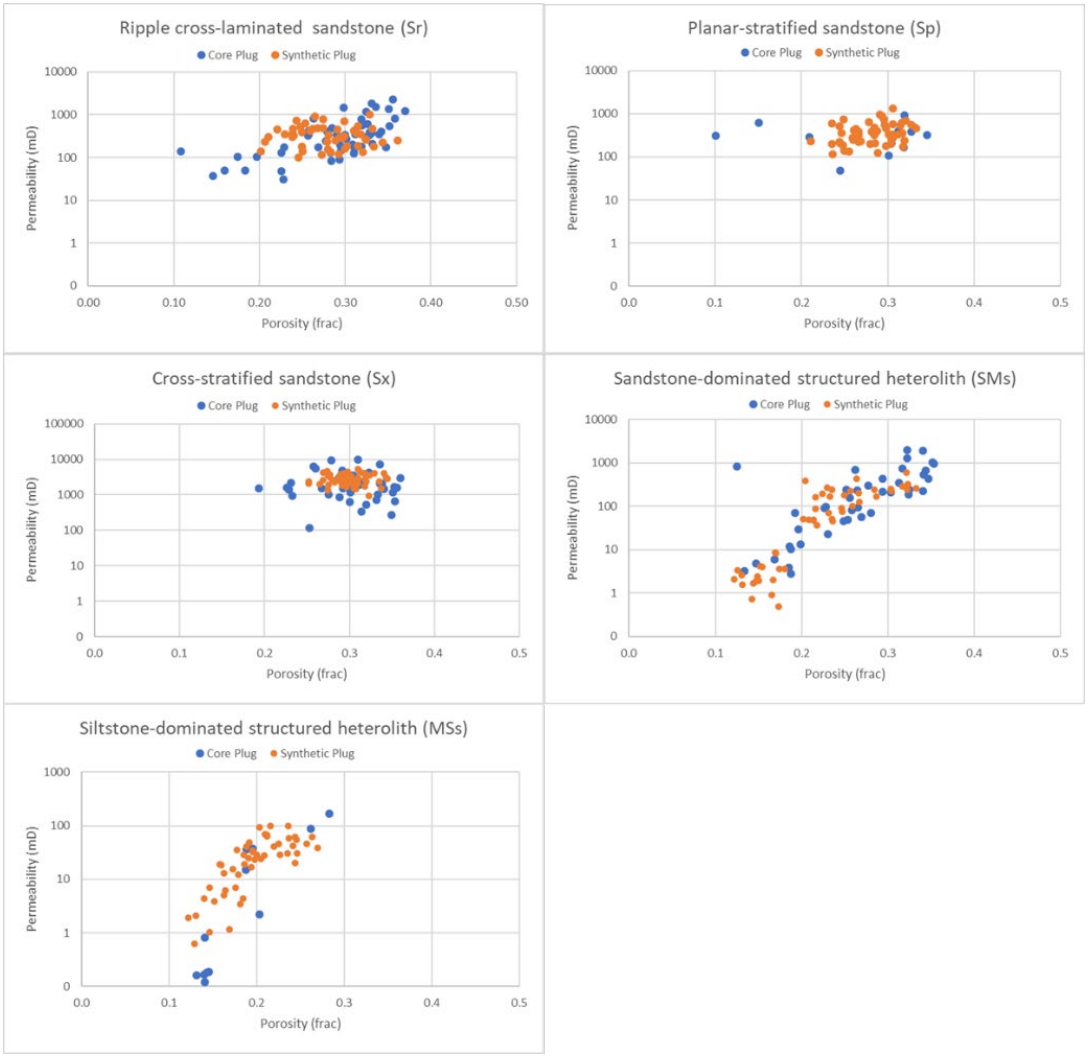

Figure 33. Cross-plot of porosity versus permeability for core plug and synthetic core plug data derived for each lithofacies model. The similarities and differences can easily be detected.

5.1.4 REV analysis and Upscaling

REV analysis was performed to obtain a minimum volume that is still large enough to capture the characteristics of the specific heterogeneity type (object). By using the REV volume, it is expected that the upscaled value is a proper representation of the heterogeneity type. To build the lithofacies models, a rather large dimension (larger than the REV) was chosen to make sure that the size of the sedimentary structures was covered. The REV will be used as the optimal sample size to achieve a representative porosity and permeability of each lithofacies model. The sample is then upscaled and the mean of 50 upscaled values obtained from model multiple realizations for each lithofacies are applied as input data to run property modeling on the facies-association scale (the next hierarchical heterogeneity scale). The REV of the pore scale is also present in a sedimentological hierarchy, investigated by Bear (1972). However, because this study is focusing on bedform scale, the pore scale REV is assumed to have been attained by the core plug data representing properties within a lamina.

REV analysis for lithofacies model was done in the SBED™ software. The software can generate multiple upscaling calculations at various sample sizes which can be assigned using a gradually increasing sample volume. The initial and final sample size in x, y, z directions had to be set up with a number of steps and iterations included for the analysis. The more steps, realizations, and size differences, the longer time was needed to process the REV analysis. Several tests with different combinations were performed to obtain sufficient results within an acceptable processing time. The analysis is shown in the plot of Kx upscaled values as a function of volume supports (Figure 34). Kx is chosen because all models show a very large range of Kx values compared with the other properties. This indicates that Kx is the most variable property which typically has larger REV and should thus be able to cover other properties for all lithofacies models.

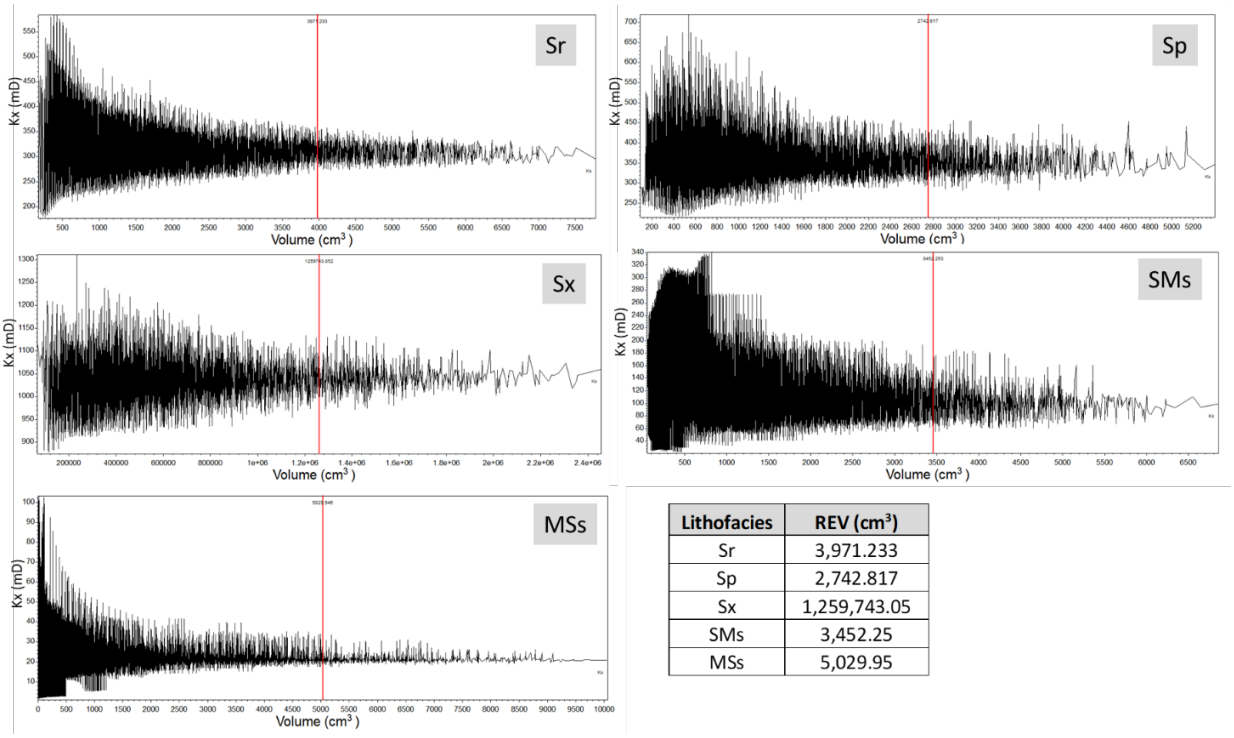

Lithofacies	REV (cm³)
Sr	3,971.233
Sp	2,742.817
Sx	1,259,743.05
SMs	3,452.25
MSs	5,029.95

Figure 34. REV analysis result of each Lithofacies

After the REV sizes for each lithofacies were defined, the lithofacies models were upscaled form the extracted REV-sized samples. REV size was used to obtain effective properties which represent each lithofacies type. The resulting upscaled values are listed in Table 5. The upscaled values of porosity range from 19% to 30%, in which Sx has the highest porosity. Sr and Sp have slightly lower porosity values which are 28%. SMs and MSs, however, only have a porosity of around 20%. This noticeable difference is caused by the shale laminae dominantly present in both heterolithic lithofacies which cause the upscaled porosity values to drop.

For permeability, the values for X and Y direction are almost identical, implying that a separation between X and Y direction of permeability for the models are not necessary. The vertical permeability (Kz), on the other hand, shows a significant difference compared with the horizontal permeability (Kx and Ky). The values may be only half of the horizontal permeability or even less. A greater contrast can be seen in heterolithic lithofacies in which the Kz values dropped to values as low as around 2 mD. The low permeability value is definitely the effect of shale laminae modelled in SMs and MSs as shale layers blocking the permeability or fluid pathway on the vertical direction.

Form the Table 5, Sx lithofacies has the highest porosity and permeability. The upscaled horizontal value is significantly higher reaching 1038.35 mD. This is to be expected because the Sx lithofacies is composed of medium- to coarse-grained sandstone (Sandstone1 lamina) which represents the thief zone. The other lithofacies do not contain Sandstone1 lamina which causes the upscaled permeability values to be much lower than Sx: around 300 mD for Sr and Sp, and 100 mD for SMs. MSs is the least permeable lithofacies typified by an upscaled horizontal permeability of 21 mD. Therefore, MSs is considered as a seal at the lithofacies-scale.

As described in the thief zone characterization part, the thief zones are mainly present in Sx lithofacies, but they are also observed in Sr and SMs to a lesser extent. The Sx model built using SBED™ clearly represented the thief zone which is indicated by a remarkably high permeability. Sr and SMs model might contribute to the thief zone, but the thief zones are not well-captured in the lithofacies models. Both models show permeability values which are lower than thief zone's permeability criteria (>1000 mD). There are also only a few core plug data showing unusually high permeability in Sr and SMs. Thus it is logical that both lithofacies cannot directly represent the thief zones.

Table 5. Upscaled Values of lithofacies models

Lithofacies Model	Porosity (fraction)	Kx (mD)	Ky (mD)	Kz (mD)
Sr	0.283	311.63	341.61	166.57
Sx	0.303	1038.35	1031.10	537.41
Sp	0.281	355.97	356.31	150.96
SMs	0.211	106.49	106.57	2.05
MSs	0.193	21.81	22.39	1.65

5.2 Facies Association-Scale Modelling

The next step in the static geomodelling workflow following lithofacies modelling is the facies association scale modelling. To achieve this, the lithofacies are organized into a characteristic (and conceptual) lithofacies order according to the sedimentological definition of the facies association as explained in Section 4.3 and 4.5, and a facies association model is created. The facies association model must capture the lithofacies relationships and the internal stratification which characterize the facies association. In this study, a software called ReservoirStudio™ (RS), which is closely linked to SBED™ was used to build numerical models of facies associations.

RS is a robust software to create facies association models which can be integrated into the multiscale reservoir modelling workflow (Wen, 2005). At facies association scale, RS is useful because it provides a pseudo process modelling tool that enables the construction of lateral and vertical stacking patterns of facies association, especially for meandering river system. For example, a variety of lithofacies can be distributed vertically and laterally to create lateral accretion packages in a point bar. The rules to set-up such a FA model must reflect the conceptual models as described in the characterization part. When the arrangements and input parameters have been set, the software then simulates channel migrations and point bar development through geological time.

This study focuses on understanding the distribution and flow properties of the thief zones as occurring in the tidal channel and the distributary channel facies. Therefore, the objective of this modelling part is to reconstruct both channel features by using process modelling tools in RS. Although various templates of channel models are built in the software, the modeller has to define conceptual models (explained in section 4.3) and use them as constrains when creating the FA model – which is the workflow followed in this study of the Åre 6.2 reservoir zone.

Outcrop analogues are needed in this modelling process for estimating the channel geometries and other information that cannot be obtained from cores (for example, lateral variations). For this purpose, the Gule Horn Formation of the Neill Klinter Group (East Greenland) was used in this study because it is considered as a suitable analogue for the Upper part of Åre Formation and Tilje Formation (Ahokas *et al.*, 2014; Eide *et al.*, 2016). As the tidal and distributary channels are considered to be meandering river forms, the point bar geometry and the lithofacies arrangement have to be assigned. Varying architectural elements such as lithofacies volume fraction is also feasible to measure the effects of parameter uncertainty in the reservoir volume and the fluid flow properties.

5.2.1 Geometry Modeling in Facies Association Scale

Geometry modeling at facies association scale aims to implement the conceptual model built for each FA as described in section 4.3 into numerical models. The purpose is similar to the lithofacies model scale but now it is at the next level of reservoir heterogeneity. The numerical FA models were constructed using a grid format that can be used for two purposes. The first is to to generate effective property curves for input in reservoir zone scale geomodels. The second is to analyze flow dynamics at the FA scale using dynamic property values assigned to the grid cells (FA scale flow simulation). Moving to the next level in sedimentary hierarchy which is facies association scale, the lithofacies models that have been built are used as an

input. The FA scale numerical models were set up using the conceptual model understanding of how individual lithofacies are organized spatially within a facies association. One of the challenges is to construct a FA model that reflect the conceptual model using the pseudo process modelling tools in the ReservoirStudio™ software package. Many parameters need to be assigned properly to produce realistic models. Some of them are related to the channel geometries and the lateral variations, and these were obtained from the outcrop analogue of the Gule Horn Formation.

Ahokas *et al.* (2014) and Eide *et al.* (2016) discuss the outcrop analogues used in this study. The tidal influenced channel complex of Åre 6.2 can be referred to Facies Association 6a (FA 6a; cf. (Eide *et al.*, 2016). FA 6a is a distributary channel facies association formed by tidal bars. The characteristics are generally the same as the distributary and tidal channels that form the focus of this study. Based on the outcrop observations, the thickness ranges from 2 to 10 m and the bodies of the facies association are several kilometers wide (can be up to 1.9 km width). The wide-spread bodies indicate that the channels migrated widely at a rather rapid rate. An abandoned channel was also identified with mainly claystone beds and minor ripple stratifications. These outcrop data combined with the core data were used to determine the reasonable dimension, channel and bar geometries applied in the FA numerical models.

Based on the facies geometries from the outcrop analogues, the dimension of the FA-scale numerical models was chosen to be 2000 x 2000 x 15 m. This model size was selected to accommodate the width of the sand bodies that has to be captured in the model. A single meandering channel with its sandstone bodies was modeled for each facies association. The depth of the bar and the abandoned channel was set to be 10 m. The width of the channel was estimated to be 180-200 m. The channel shape is sigmoidal, but the sinuosity of the channel is difficult to develop from well data and outcrop which introduces another uncertainty to the model.

Similar numerical model dimensions are used in the distributary and tidal channel FA (Figure 35). The width and the depth of the channel for both FA are also considered to be the same because the outcrop analogue can be applied to both FA. The differences between both FA are the shape of the bar and lithofacies composition as explained in the conceptual model descriptions (section 4.3). The sandstone bodies in distributary channel and tidal bar consist of lateral accretion packages encased in the tidal flat FA. The accretion packages comprise several lithofacies set in a typical order that represent the facies association and shows a fining-upward trend. Each lithofacies was placed in an accretion bed which was inclined a few degrees. For the base case, the lithofacies proportion contained in the FA models was set to be proportional, meaning that every lithofacies has the same quantity within the same FA model. The background facies in the models is the tidal flat FA which mainly consists of heterolithic facies. This FA is not a target in this modeling study, so for efficiency, the tidal flat FA is simply represented by SMs lithofacies. The abandoned channel fills are shown in blue which are characterized as a claystone.

In this study, there is only one single meandering channel representing each facies association. This is the first step to examine the flow properties of the channel facies associations. Another method that might be applied is to combine some channels in one model, showing the channel connectivity. The implications of transgressive and regressive sedimentary sequences can be represented by decreasing or increasing the amalgamation degree of the channels. However, this method is not included in this study because the result of a single-channel model is already able and sufficient to represent the facies association characteristics and the effect of the thief zones. The multiple-channels model might be more relevant to a full-field reservoir model.

Table 6. Dimension and Channel Geometry Used in the Model

Parameter	Value
Model Dimension	2000 x 2000 x 15 m
Number of Cells (i direction)	200
Number of Cells (j direction)	200
Number of Cells (k direction)	23
Total Number of Cells	920000
Channel Width	200 m
Channel Thickness	10 m
Point Bar Width	1000 m
Point Bar Thickness	10 m

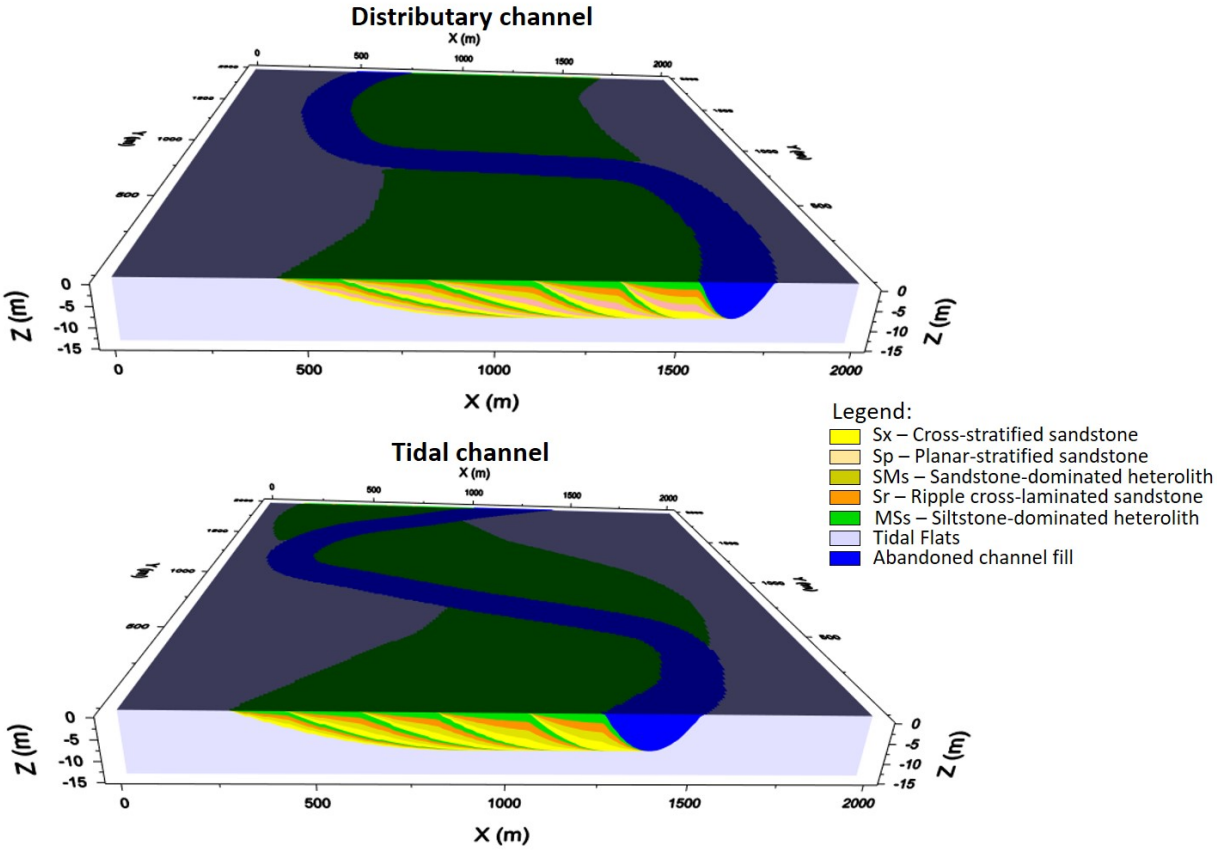

Figure 35. Facies Association Geometry Models applied.

5.2.2 Property Modeling and Upscaling

To distribute petrophysical properties in the model, the geometry model has to be arranged with the lithofacies placement as described in the conceptual model, so that the property distributions can be assigned based on the lithofacies. The property modeling process for FA was performed by using the same software, ReservoirStudio™. This software provides a tool which allows statistical parameters applied to each lithofacies. Mean and standard deviation are the basic input to populate properties to the model. These statistical values can be derived from upscaled values obtained from samples of lithofacies models. ReservoirStudio™ also provides the application of variogram parameter, but there is not a clear method to estimate the variogram. The effect of the variogram is also negligible compared with the impacts of the definitions of mean and standard deviation values, so variogram parameter was excluded in this study.

The upscaled values applied to the property modeling were obtained from the extracted REV-sized samples of lithofacies models. The REV upscaled values of lithofacies models are listed in Table 5. The REV-sized samples were used because it gave an accurate lithofacies representation (Nordahl & Ringrose, 2008) which is one of the concerns in multi-scale modeling. Since the upscaled values were taken from REV samples, the value variations were minimized, resulted in very low standard deviation values. Therefore, it can be assumed that a constant property value represents each lithofacies type in the model. It should be noted, however, that in this FA property modeling, similar to the lithofacies property modeling, only one type of permeability can be applied to the modeling process. Only the horizontal permeability (Kx) was used as the input and this gives another limitation to the accuracy of the models. The vertical permeability values were not included to the property modeling due to the software limitation.

The resulting model of porosity and permeability distribution for distributary and tidal channel FA are shown in Figure 36. As mentioned above, each lithofacies is represented by a constant property value, so the distributions of the properties are rather simple since they just follow the lithofacies distributions. From the permeability models, it can be seen that the basal part of the accretion packages contains red zones which is a noticeable high permeability (around 1000 mD). These remarkable high permeable features are representing Sx lithofacies which is where the thief zones are located. In the porosity models, the values vary between 0.18 and 0.3 which is similar to the range of upscaled lithofacies values. The permeability value of the abandoned channel fill is assumed to be 0 since it is interpreted as a claystone. (In reality, however, it will not be exactly zero but a very low permeability value due to sedimentary impurities in the abandoned channel fill. For the purpose of this study, the value has been set to zero.). The grid of these porosity and permeability model have not upscaled. Therefore, for flow simulations, grid upscaling might be needed to cope with the computational limitation.

Once the properties have been distributed to the model, the next step is flow-based upscaling of extracted volumes from each FA models. Similar to the upscaling at lithofacies scale, the extracted volume must be large enough to correctly represent the characteristics of the models. Sample size is important because of the scale dependency of upscaled values. The REV concept was subsequently applied to establish the most accurate size volume for the upscaling. However, because of some undetermined errors in the software, the REV analysis tools could not function properly. To cope with the problem, a relatively large sample size was chosen which was expected to accommodate the REV size. To ensure that the upscaled values taken in different locations are approximately the same (and thus indicate that the REV

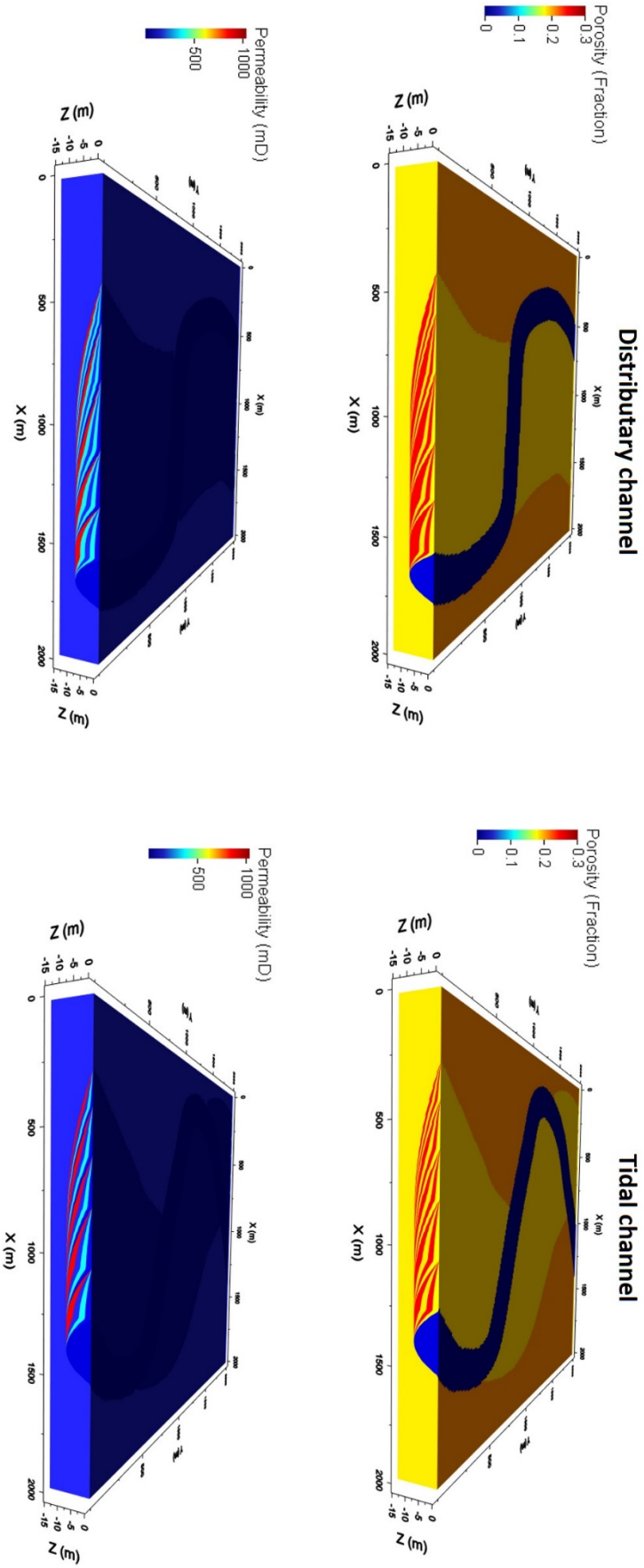

Figure 36. Porosity Model (upper figures) and Permeability Models (lower figures) of Distributary and Tidal Channel FA

size was reached), the sample position was moved multiple time and the upscaled values calculated. The sample dimension of 500x300X10m was chosen because it covers a relatively large volume of the barform and has upscaled values that are independent of a sample location. Therefore, the estimated REV for the FA models will refer to that volume size. The resulting upscaled values using the estimated REV are shown in Table 7. According to the table, the distributary channel has slightly higher values of porosity and three different permeabilities. The high proportion of heterolithic lithofacies in tidal channel FA is interpreted to reduce the property values. The vertical permeability (Kz), as expected, is much lower than the horizontal permeability (Kx and Ky) due to the direction of the flow that tends to cut through the layers, declining the result of the upscaling calculation. Moreover, the occurrences of heterolithic lithofacies can significantly lower the upscaled vertical permeability since they block the fluid flow in vertical direction.

Figure 37 summaries the changes of Kx values over the several scales from the lamina used in Sx lithofacies to the distributary and tidal channel FA models. Based on the figure, reductions in Kx values are observed when the models are upscaled, showing the upscaling effect at each scale. Sx lithofacies, representing cross stratified sandstone, is composed of two different types of laminae types, Sandstone1 and Sandstone2. Of these two, the very high permeability layers, formed by medium to coarse-grained sandstone, are defined as Sandstone1 lamina types. Core-plug property measurements are used to populate the lithofacies-scale model. Very high permeability values (>1000 mD) can still be recognized at the REV upscaled values of Sx model. This upscaling result implies that the Sx lithofacies can capture the thief zone characteristics and thus represent the thief zones at the next heterogeneity scale (facies association scale).

Moving to facies association scale, the thief zones were identified at the channel FA, the tidal channel and distributary channel. Based on the vertical succession as observed in the core and the conceptual models that were constructed, Sx lithofacies are placed at the base of the FA. Sx was genetically associated with three or four other lithofacies in a particular arrangement to depict the barform, representing the channel fills. Similar to the lithofacies scale, samples at REV were taken and upscaled to obtain properties which represent the FA models. The upscaling effect is significant, which causes Kx to fall to 319mD and 333 mD for the distributary and tidal channel models respectively. Because of this Kx reduction, the upscaled value of the FA models cannot directly represent the thief zones, so it is suggested that the thief zones should be determined in the models properly so that they can be recognized by the reservoir engineers and will receive the appropriate attention in the reservoir modeling and simulation processes.

Table 7. Flow-Based Upscaled Values of FA Models with using the estimated REV size sample (500x300x10 m)

Facies Association	Porosity (frac)	Permeability (mD)		
		Kx	Ky	Kz
Distributary channel	0.25	333.24	334.58	83.09
Tidal channel	0.24	319.16	321.71	72.51

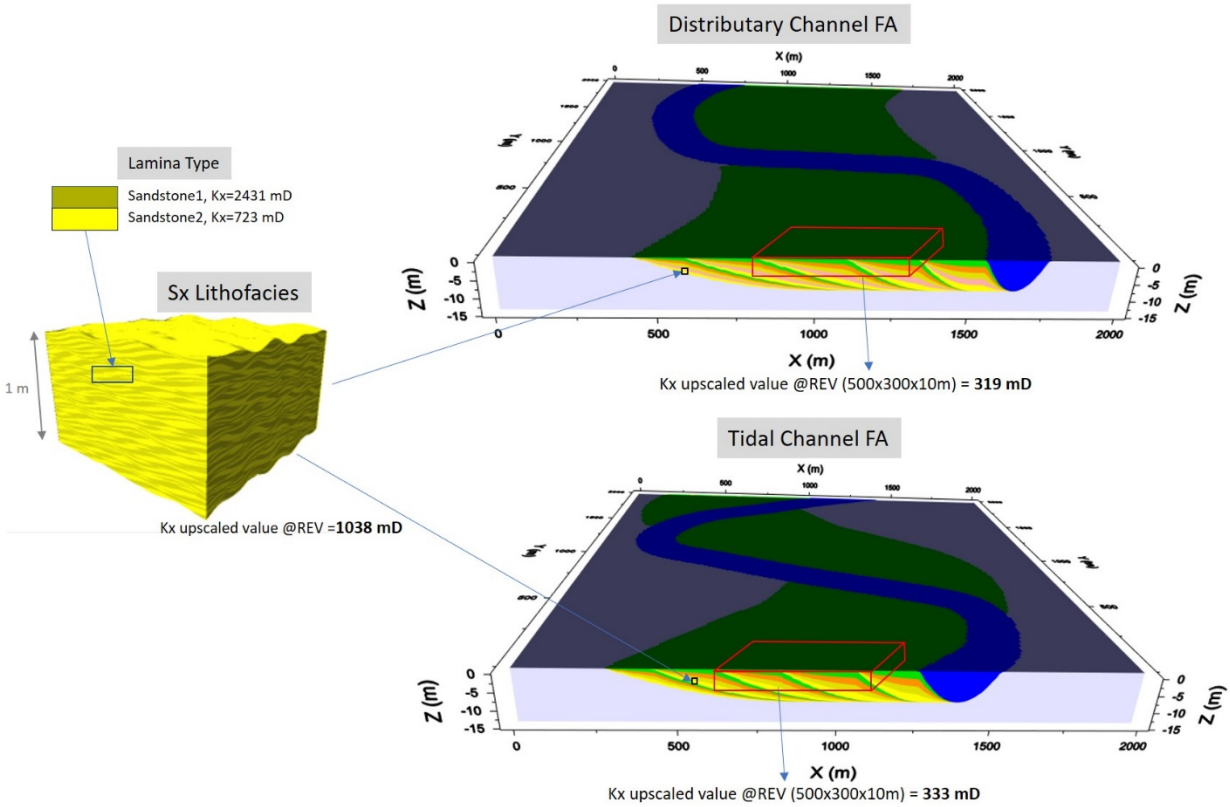

Figure 37. Comparison between Lithofacies and Facies Association Scale with the representation upscaled value.

5.2.3 Streamline Simulation

As mentioned in Section 2.4, streamline simulations can be performed to visualize fluid flow patterns which is used to investigate the effect of the thief zones in the models. This simulation uses a different computational approach which not only is faster but also more accurate than the traditional finite-difference simulator. For the generic channel FA models as built during this study, the streamline simulation method is suitable because of its capability to display flow line movement and its simplicity incorporated with the available data. A simple one-phase water flooding scenario was demonstrated in the simulation with certain key parameters and reliable assumptions.

The models used in the simulations are numerical grid model of facies associations built in ReservoirStudio™ (Figure 36). Each cell in the models consists of two properties which are permeability and porosity. These parameters are the main input derived from the models, and other inputs such as fluid and reservoir properties are also required to get the simulation run. However, the required additional parameters are not available in the dataset for this project, so some assumptions were made to define the fluid and reservoir conditions. Table 8 lists the parameters applied which represent simple properties for the fluid contained in the field. Besides, all the grids are initially defined with water saturation values of 0.18 and a pressure of 240 bar. These additional parameters of the models were manually added by using 3D property calculator tools in the software.

Another dynamic property setup for the streamline simulation is a rock physics function which includes functions of relative permeabilities and capillary pressures. These parameters are used to estimate the capacity of oil, water, and gas flow during a production period. Fluid

saturation (Sw and So) will change as the injected water replaces the resident oil. As a result, the relative permeability and the capillary pressure will change as well because these parameters depend on the fluid saturation. Defining these two parameters can be quite complicated because it may involve structure and chemistry aspects of the fluids and the reservoir itself (Christiansen, 2001). However, this study utilized a relatively simple example of physics function shown in Figure 38. The data used to the curves are attached to the appendix B.

Table 8. Reservoir and Fluid Properties

Parameter	Value	Unit
Reservoir Pressure	240	bar
Initial Water Saturation	0.18	fraction
Water Salinity	25,000	ppm
Temperature	93	℃
Bubble Point Pressure	56	bar
Oil Gravity	34	API

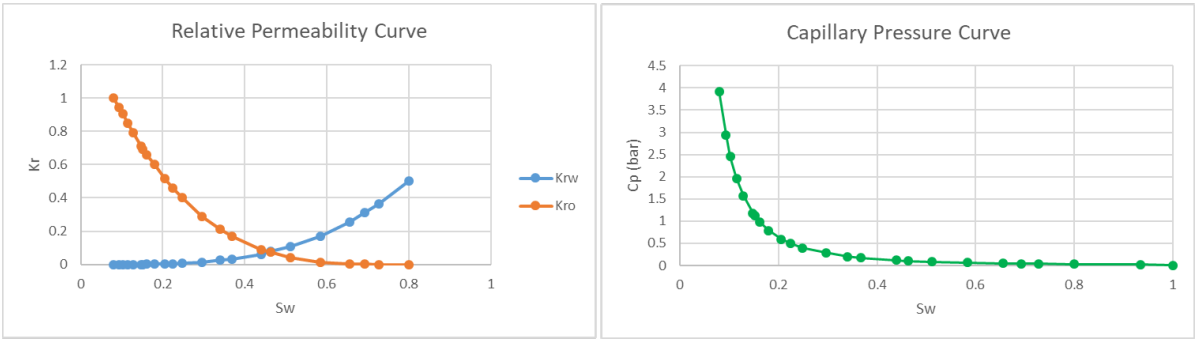

Figure 38.Rock physics function applied to the model for the simulation.

When the fluid and reservoir properties are defined, a well configuration needs to be decided for each FA flow simulation model. Since this study only aims to test the model with a simple simulation and identifies the possible fluid flow path, one injector well and one production well were placed in the model in one-point bar feature (Figure 39). This approach is chosen to directly represent the condition where the injector and producer are situated in a 700-meters distance within a connected sand body width, so that the streamlines can clearly be seen and evaluated without any barriers between the wells. The rates of the producer and injector were maintained by adding rate controls of 100 rm^3/day to both wells. The production lifetime was set to be five years which is rather short compared to an extensive full-field reservoir simulation. Longer production time can always be performed but the chosen5-year production time was sufficient to illustrate the concentration of flow through the thief zones.

The streamline simulations were performed in distributary channel and tidal channel FA models (Figure 40). A total of 200 streamlines, indicating the fluid flow paths form the injector to the producer, were shown together with a property slice of the models. It is evident that from the beginning of production, the streamlines tend to be concentrated in the lithofacies that has a significantly higher permeability (Sx, indicated by red colour). This type of features is typical for thief zones where the majority of the flow concentrated due to the very high permeability

contrasts with the other zones and/or lithofacies. Some streamlines are passing through other lithofacies than Sx, but those occurrences form a minority. A large amount of fluid flowing through one specific zone is not a favourable situation in terms of sweep efficiency because potential oil present in the other zones might not be appropriately swept and thus left behind. This would reduce the cost efficiency of the project. Both FA models generally exhibit the same result even though the reservoir geometry and the well locations are different.

The simulation also calculated water saturation in every cell which can also be displayed in 3D models. As expected, the water saturation model (Figure 41) shows that the interpreted thief zones have the highest water saturation values (around 0.80). This indicates that the thief zones are the first intervals to be fully saturated with water which supports the observation of the position of the streamlines; consequently, both illustrate the behavior of the thief zones.

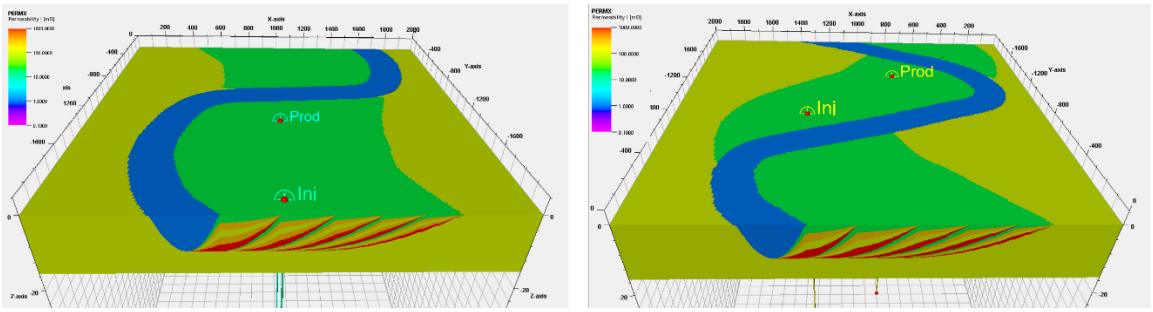

Figure 39. Well configuration for streamline simulation

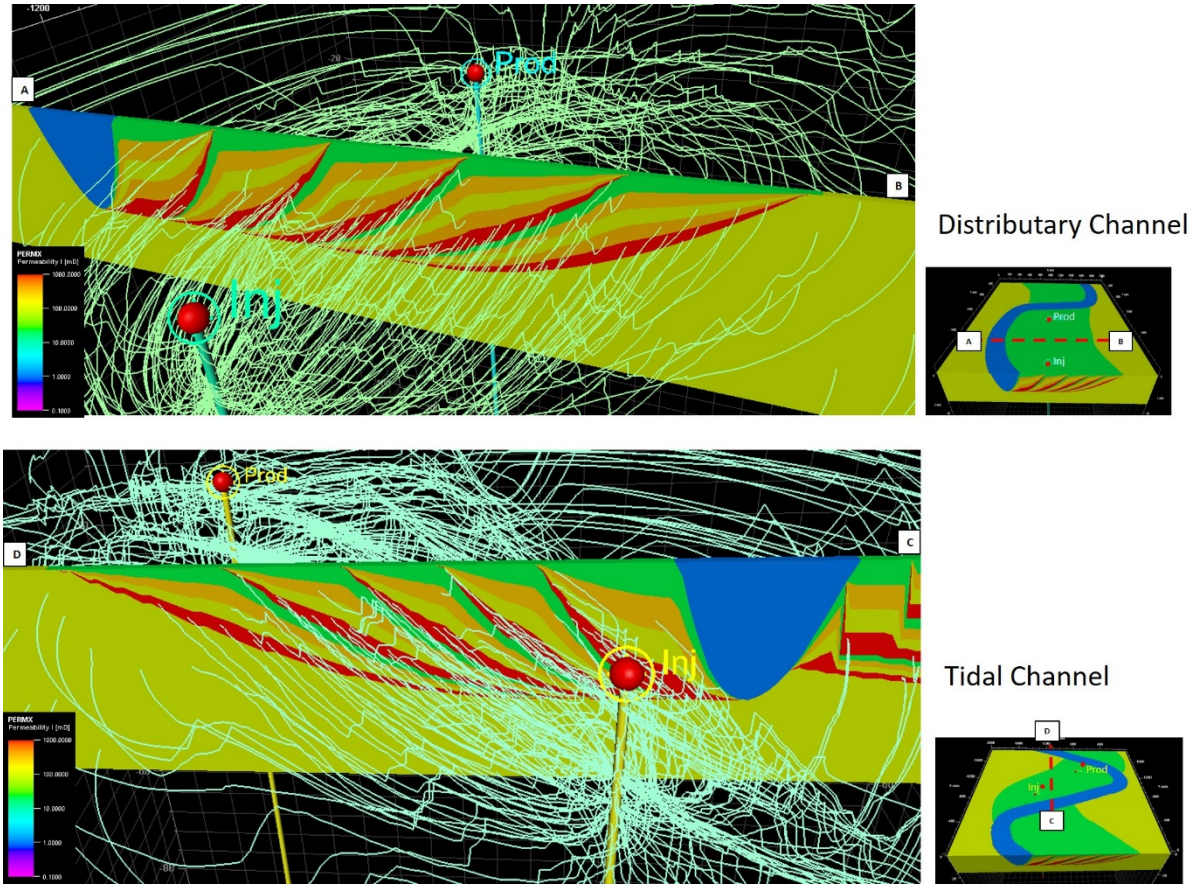

Figure 40. Resulting streamlines simulation in Distributary Channel (upper figure) and Tidal Channel (lower figure), showing the streamlines are concentrated in high permeable zones (in red).

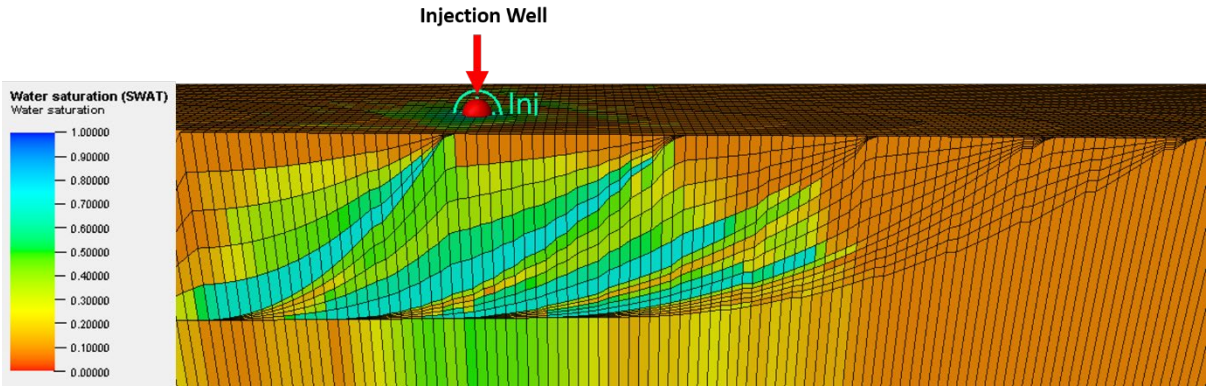

Figure 41. Slice of water saturation models near the injection well after a 1-year period of water flooding simulation. Turquoise layers indicate the high-water saturation grid cells which are contained in the interpreted thief zones.

6 Discussion

6.1 Volume Fraction Uncertainty

The proportion of each lithofacies assigned to a barform needs to be set as a fraction when building FA models. However, there is not a specific volume fraction configuration of lithofacies which can fit every channel. This is because the lithofacies distribution and proportion that occurs in channel barforms might naturally be different as they were subjected to different hydrodynamic conditions and received various types and amounts of sediment during its deposition. The lithofacies volume fraction might be estimated from core data or outcrop, but the exact number is uncertain because a wide variation of lithofacies relative proportions is observed. In Åre 6.2 Zone, for example, some channel facies associations identified from core data, have the same general lithofacies arrangement, but the individual lithofacies thickness and distribution vary from core to core.

A simple approach for FA modeling might use a proportional volume fraction for lithofacies composition. This was used in this study as an initial scenario when building the models and found useful to represent FA generically. This approach gives rather simple geometries which are rarely found in natural systems. To deal with the internal variability of the models and to evaluate the sensitivity of the property upscaled values with respect to the lithofacies composition, the lithofacies volume fraction input was varied and applied to the building of FA models.

In this study, five different volume fractions were introduced for each lithofacies in the built FA models. Each case resulted in a new scenario and an associated upscaled property value for each of the volume fraction combinations. The upscaled values for each lithofacies were then plotted as a function of fraction volume (Figure 42). It should be noted that when the volume fraction of a particular lithofacies is defined, the remaining fraction is divided over the remaining lithofacies proportionally. In other words, if one fraction of a lithofacies becomes higher, the other lithofacies fractions are decreased with equal proportion.

Figure 42 shows the variation in upscaled permeability values which were obtained from varying the volume fractions. The horizontal permeability (Kx) and vertical permeability (Kz) are plotted separately to allow the plots to display the trends in more detailed. According to the plots, the Kx values are more sensitive to the variation of Sx lithofacies volume fraction whereas the MSs lithofacies volume fraction has the highest impact on the Kz values. The steepest trendlines indicate those lithofacies that have the strongest influence as they show the most significant change of upscaled values when the lithofacies volume fraction are changed. The upscaled values for permeability in the y-direction (Ky) are not displayed because the permeability in the x and y directions are identical based on the upscaled calculation (Table 7).

For the horizontal permeability, the Sx trendline (light yellow lines) has the steepest gradient for both tidal and distributary channels, which suggests that Sx plays a major role in the upscaled values of horizontal permeability. The Kx value increases significantly as the Sx

volume fraction increases. This is considered logical because the Sx model has a much higher averaged permeability value than the others (1038 mD) while the second most permeable lithofacies, Sp, has a permeability of only 355 mD. In contrast, based on Figure 42, the other lithofacies show an inverse relation in which the increase of the Kx value is associated with a reduction of their volume fraction with a lower-gradient trendline. This is due to a decrease of Sx lithofacies that occurs when increasing any other lithofacies fraction. The least permeable lithofacies, MSs, contributes to a considerable degree to the decrease of the upscaled Kx value when the lithofacies fraction in the FA model is increased. The relation between Kx and all facies volume fractions in both facies associations are linear as the linear trendlines connect the scatter plots properly. This relation is aligned with the concept that the effective horizontal permeability is computed by using the arithmetic average when assuming that the sedimentary layers are oriented parallel to the flow.

The vertical permeability, on the other hand, shows different results in terms of dominant lithofacies and the relation between volume fraction and upscaled permeability values. It is evident from the graphs (Figure 42) that the MSs lithofacies (green lines) is the main factor in controlling the upscaled values of Kz. The upscaled Kz values increase rapidly with a decrease in MSs volume fraction while a decrease of other lithofacies indicates relatively slight downward permeability trends. All lithofacies other than MSs only have an insignificant effect on the upscaled Kz values compared to the MSs. Although tidal and distributary channels have a different lithofacies composition, they generally show the same results of permeability upscaled values with regard to the variation of lithofacies volume fraction. Moreover, the upward trend of Kz is better matched with an exponential trendline, indicating that the upscaled values change more rapidly when the MSs volume fraction becomes lower. Note that the trendlines represent harmonic averages which are commonly used for calculating effective vertical permeability, and in which the flow is perpendicular to the permeability changes.

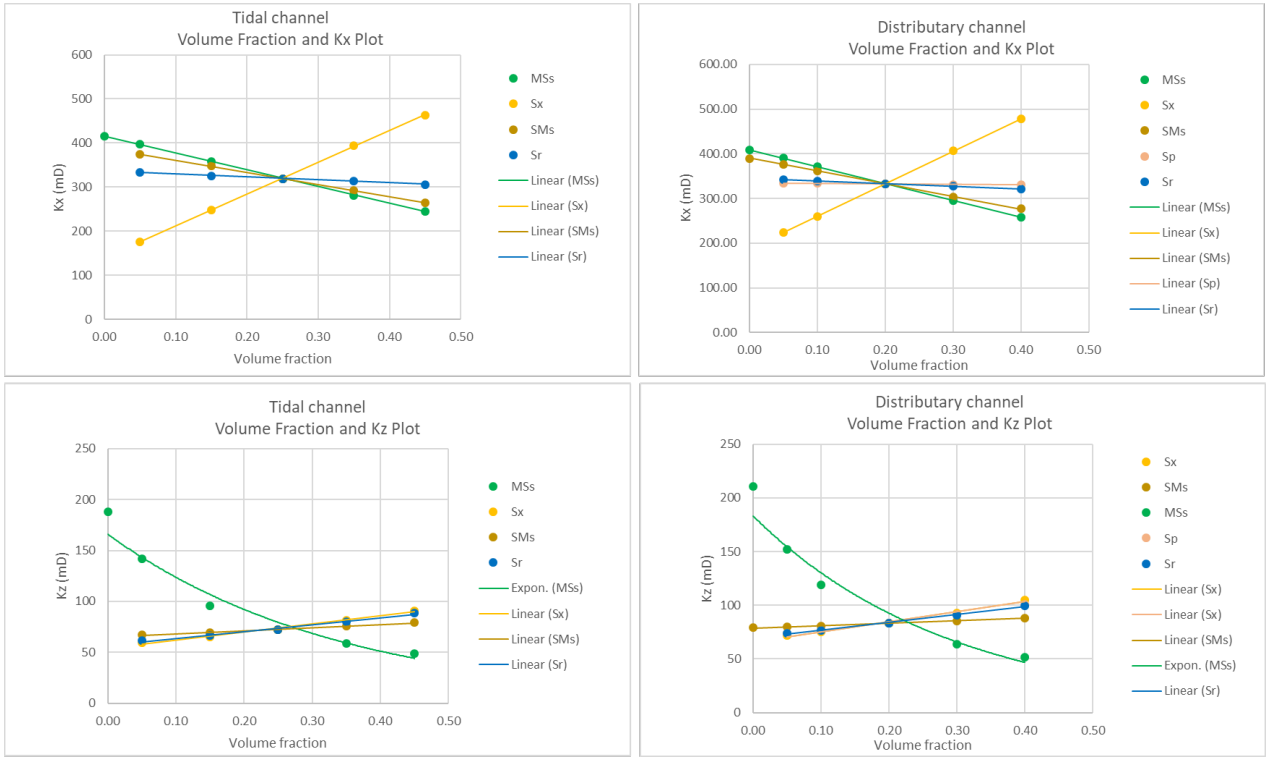

Figure 42. The plot of Upscaled permeability as a function of volume fraction.

The above analysis shows that Sx and MSs are the dominant lithofacies, which implies that the composition and relative proportions of these lithofacies in the core are essential to establish. Based on the core data from the seven wells, 20 occurrences of a channel facies association were identified, be it either tidal or distributary channels. Looking at the lithofacies composition of these 20 occurrences, the Sx lithofacies ranges from 20% to 90% of the total lithofacies fraction with an average of 52%. Lithofacies MSs, on the other hand, has much lower percentages than Sx, varying between 0% and 28%. It should be noted that the interpreted FA in the core are not as ideal and complete as the FA models. There are many deviations regarding lithofacies order and occurrences as the cores reflect the natural variability of preserved facies in the rocks.

Compared with the base scenarios of the tidal and distributary channel models, the Sx proportion from cores is larger while the MSs proportion might be lower. Sx is generally abundant in both tidal and distributary FA. It can reach as high as 90%, for example in wells 6507/7-3 and 6507/7-4 (Figure 14). In contrast, MSs are not identified in every channel FA, suggesting that having a MSs volume fraction equal to 0 is also realistic. Such a situation will generate a significant increase of Kz. Overall, it is expected that the upscaled horizontal and vertical permeability values are higher if the models are specifically linked to the observed FA in the core. For reference (and as explained earlier), the base scenario models use a proportional volume fraction to all lithofacies, so every lithofacies in one FA has the same relative proportion, which is 25% for all lithofacies occurring in a tidal channel and 20% for all lithofacies occurring in a distributary channel.

With reference to the conceptual models, the heterolithic lithofacies (SMs and MSs) are most likely formed in the tidal channel since the sandstone-mud variations and they mode of deposition are indicative of tidal processes. Therefore, the composition of those lithofacies in the tidal channel should be higher than in the distributary channel, resulting in the lower Kz because Kz is sensitive to the low-permeable lithofacies. Another difference between the two FA models is the occurrence of Sp lithofacies which is not present in the tidal channel FA. This is expected to only have a small effect on the upscaled FA values as illustrated in Figure 42. Sx lithofacies, controlling the Kx upscaled values, have the same possibility to be developed i both FA's. Sx is formed by the high-energy current which might occur in both tidal and distributary channels.

6.2 Grid Size Analysis

This study aims at constructing models at two different Hierarchical scales, individual lithofacies and facies associations. Each scale has typical sedimentological heterogeneities which need to be captured in order to achieve a better estimation of fluid flow properties (Keogh *et al.*, 2014; Nordahl *et al.*, 2014). The upscaling process then becomes crucial to accurately represent the smaller scale but important details as effective properties when modelling the larger heterogeneity scale. The appropriate volume at which upscaling can be performed is important to define, so that the extracted values can adequately be described to the stochastic modelling objects as used in reservoir modelling.

In this section, the distribution of core plug data and subsamples taken from different sizes and models are analyzed to determine how the distribution changes with the sample volume size. Box-whisker plot (Figure 43) is a useful approach to visualize the mean and variance of the samples used at a particular scale.

There are five different sample sizes shown in the box-whisker plot, which are core plug (3x3x5 cm) REV of lithofacies (10-100 cm), reservoir grid (50x50x1 m), simulation grid (100x100x2 m), and estimated REV of FA (500x300x10 m). The smallest data size is core plug which is the primary data source for porosity and permeability in this study. Synthetic core plugs were taken from the lithofacies models to match the model with the real core data. REV-size samples were examined to obtain a representative value for each model both at lithofacies and facies association scale. The remaining two sample sizes are at the scale of a geological reservoir grid and at the simulation grid scale. Different modelers might use different reservoir and simulation grid sizes, but the volume dimension of 50x50x1 m and 100x100x2 m were chosen here to be representative of the reservoir and simulation grid size as tested by the FA models. The reservoir and simulation grid sizes are important because, in the subsurface workflow as practiced in an operational asset, properties need to be assigned at these grid sizes.

Based on the distribution shown in Figure 43, it is evident that larger samples at each scale produce a lower variance. This is aligned with the REV concept (Bear, 1972; Nordahl and Ringrose, 2008) which states that variance of the samples reduces as the investigation volume increases.

However, at the lithofacies scale, there is a slight reduction in permeability variance from the core plug data to the synthetic core plug. This is not expected because these data types should show rather similar distributions as they were formed at the same scale and sample size. The synthetic core plugs, however, have a narrower range which indicates that the SBED™ models have a small range of variability compared with the core plug data. A possible cause for this can be that this occurs during calculations when conversion from the permeability value to the log-normal value resulting in a relatively low variance. Another reason for the narrower synthetic core plug might be a limited option for adding lamina types in lithofacies modeling. SMs and Sr lithofacies, for example, comprise some permeability values that are higher than 1000mD represented only by Sandstone1 lamina. However, in the property modeling, Sand1 lamina was not chosen to be one of the lamina types because Sandstone2 and Sandstone3 laminae are more dominant in that lithofacies. Moreover, from the core plug data it is obvious that there are some notably low permeability data which are few in number, but are still included in distribution, resulting in a wider permeability distribution of core plug data. Despite the above disadvantages, the SBED™ models are still acceptable because the core plug data and synthetic core plugs show the same general porosity-permeability relationship (Figure 33). In addition, upscaled lithofacies values at REV scale are also displayed in the figure, indicating that Sx and MSs, which have the highest and lowest upscaled permeability value respectively, are rather far from the mean value. Therefore, the presence of these lithofacies can produce noticeable effects in the upscaled values.

With regard to the facies association scale, every upscaled LF value was also displayed to Figure 43.B to show that they are the input data used for the FA property modeling. When comparing the sample distribution of the geological reservoir grid and the simulation grid, there is only a slight difference between both sample sizes where, as predicted, the simulation grid has a lower range of variability than the reservoir grid since its grid cell size is larger. This is consistent with the study by Nordahl *et al*. (2014) who found that the upscaling effect between reservoir and simulation grid is rather small compared with the upscaling effect from well data to reservoir model. This is interesting because, in general more effort is put into these problems than evaluating the upscaling effects from well data to reservoir models. In fact, based on the current study, larger distribution differences are identified when upscaling from well data (core plugs trough LF and FA models) to the reservoir models. Consequently, this study confirms that multiple scale geological modeling can improve the representation of the

porosity and permeability distribution in the reservoir model. Traditionally, only core plug data and well logs are combined and used to distribute properties directly to the reservoir model, neglecting sedimentological heterogeneity at the smaller scales. This may have substantial effects on the flow properties at the reservoir model scale.

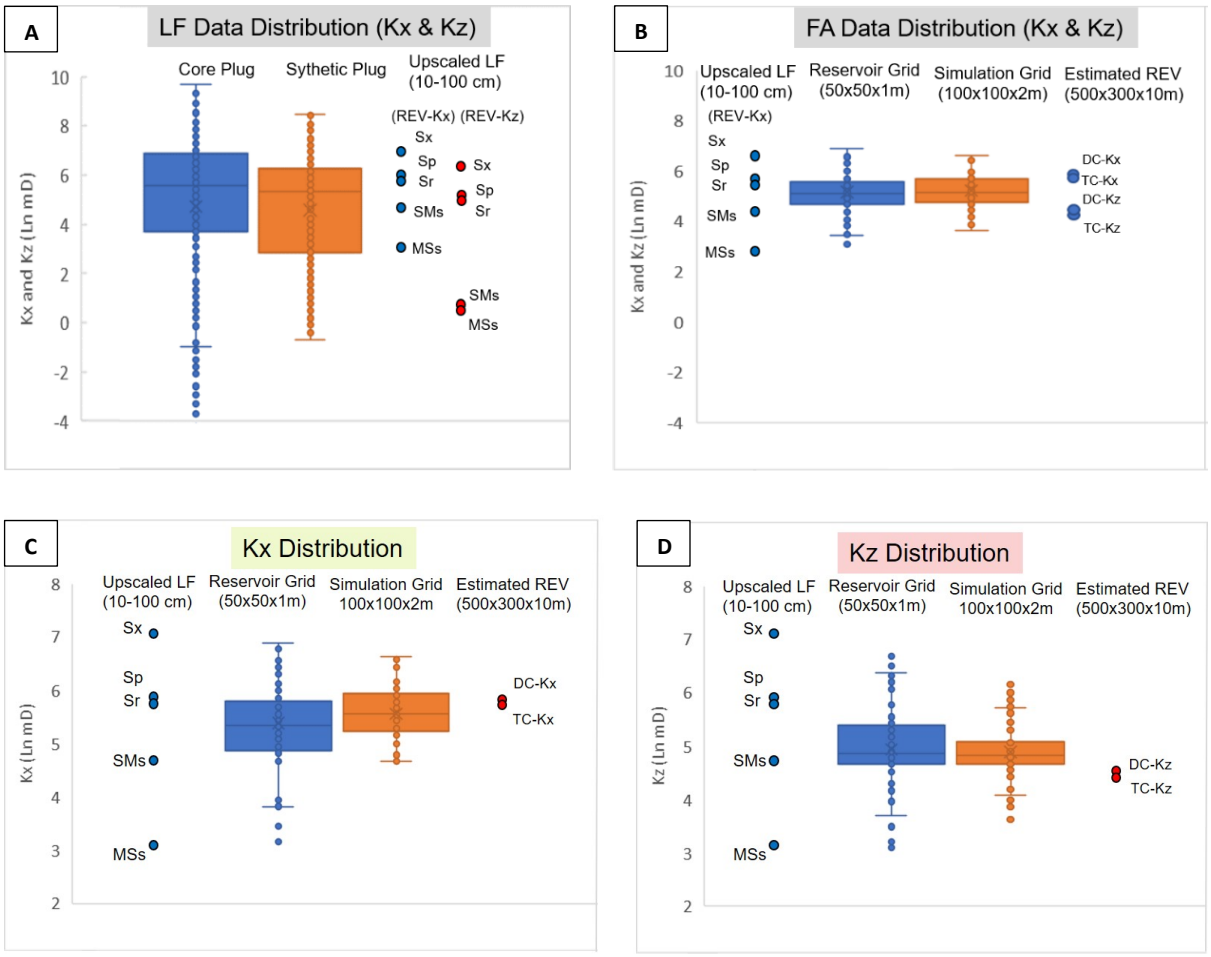

Figure 43. Box-Whisker plots showing the data distribution generated from different scales and sample sizes. (A) and (B) take into account horizontal and vertical permeability data (Kx and Kz) which were distributed in lithofacies and FA scales. In (C) and (D), the horizontal and vertical permeability data were separated.

In Figure 43.B, the upscaled FA values at the appropriate REV size are also shown. There is no significant difference between the tidal and distributary channel FA although the distributary channel FA has slightly higher Kx and Kz values. To evaluate the changes of upscaled values from different sample sizes in one particular permeability direction only, the Kx and Kz values were selected from the data set (Figure 43.A and 41.B) and visualized in additional box-whisker plots (Figure 43.C and 41.D). The chart shows that upscaled Kx values at the REV scale are higher than the mean of the permeability values at smaller scales while the Kz distribution shows lower values. This illustrates the consequences of taking samples below the REV size, that is, at sample volumes at which the data variance is still relatively high and the resulting distributions strongly depend on the sample positions. At the given reservoir and simulation grid size (50x50x1m and 100x100x2m respectively), a random sample taken cannot represent all lithofacies that are present in the FA models. It is often that they exclude Sx and MSs lithofacies, which are the main factor of influence in the upscaled values. Therefore, at REV scale, Kx is higher because it always contains Sx, and Kz is lower because MSs is always included in the REV-sized samples, reducing the Kz upscaled value.

Figure 43.D shows that the upscaled Kz values from both the tidal and distributary channel FA show a significant decrease at their REV sizes, revealing that the reservoir and simulation grid sizes may not represent the FA models accurately.

Upscaled Ky values are not included in the box-whisker plots because permeability in the y direction generally shows rather similar values as in the with x direction. However, looking in more detail, Ky actually has a noticeable larger upscaled values than Kx, reaching values of up to 50 mD higher. The higher Ky upscaled values are produced as the result of the internal barform geometry of the channels. To clarify, y is the direction which is parallel to the overall channel flow whereas the x direction is perpendicular to the channel flow and in the same direction as the lateral migration direction of the channel. Consequently, Kx crosses the dipping layers and is thus subjected to more lithofacies changes. In contrast, Ky tends to follow the same lithofacies along the strike of the dipping layers. The lithofacies variations observed across the dipping layers and recorded by the Kx in the samples thus result in a lower derived upscaled value. As a result, the Kx value is expected to be lower than the Ky value. Reservoir and simulation grid may also not cover the barform geometry since the geometrical object itself may be larger than the sample size.

Deciding the most suitable grid size for geological modeling is challenging due to the variation in kx-ky-kz upscaled values resulting from different sample sizes. Although applying smaller grid cells may produce more detailed reservoir models, it also creates a higher uncertainty regarding the property values added to the grids. As explained above, the internal barform geometry and lithofacies variation may influence the upscaled values which are extracted from smaller sample sizes (reservoir grid and simulation grid). Thus, the geometry and spatial distribution of the barform should be appropriately designed when using the smaller grid size. However, with the limited reservoir information and restricted capabilities of the modeling tools, this approach is not preferred. It is suggested that employing larger grid cells close to the REV might be a reliable option because it can capture the internal geometry better and gives a representative permeability value in each direction. Such a consistent upscaling technique with a proper sedimentological framework can better estimate the porosity and permeability for full-field reservoir models (Nordahl *et al*., 2014). In other words, one can further use the upscaled values FA model as input for reservoir zone model and include it in a field scale model.

Another method to assess the degree of the permeability variability is by measuring the Coefficient of Variation (Cv). The Cv is the ratio between the standard deviation and the mean of the samples. This variability estimation assesses the heterogeneity of the rock (Corbett and Jensen, 1992). Based on the Cv, heterogeneity can be classified into three classes: Homogenous ($0.0 < Cv < 0.5$), heterogeneous ($0.5 < Cv < 1.0$), and very heterogeneous ($1.0 < Cv$). It can be assumed that if the Cv is low, any quantities and sizes of samples are acceptable to represent a model as they represent measurably homogenous values, revealing that they are independent on sample locations. In this study, the Cv from the samples taken from the reservoir and simulation grid size were calculated and resulted in Cv values of 0.75 and 0.52 respectively. This indicates a high degree of variability of the samples and supports a high dependency on the sample location as described previously. Hence, using the size of these grids for reservoir modeling is not preferable, instead using larger grids representing values at the REV would give better estimations.

6.3 Possibility of Flow Diversion

The effects of the thief zones are made visible when deploying a streamline simulation using the FA models. The thief zones strongly funnel the fluids (water) through the model because of their much higher permeability. The injected water is mostly circulating in the thief zones, in which lithofacies Sx is dominant, and do not effectively sweep the oil in the other potentially hydrocarbon-bearing zones of the model (containing for example lithofacies Sr, Sp, and tidal flat deposits which have sufficient porosity and permeability). No effective fluid displacement is observed from the streamline simulation results. Similar situations described from the literature show that high water cuts and/or early water breakthrough may occur in production wells (Medeiros *et al.* 2004; Ding *et al.*, 2016; Li *et al.*, 2010; Li, Yang, & Lu, 2016). This phenomenon has been a serious concern in oil field development and have attracted much attention from geomodelers and reservoir engineers. The Heidrun interval subject to this study is such a case.

There are some possible solutions to control the thief zone effects. However, they depend on a large degree on the characteristics of the thief zones, the hydrocarbon properties, and also the field conditions. The idea is mainly to conduct a flow diversion with an approach to divert injected water to other zones by isolating or reducing the permeability of the zones which are preferable ways for fluid to flow (Muggeridge *et al.*, 2014; Fig. 40). Remedial efforts might include usages of chemical plugging agents such as polymer solutions, and also careful completion and perforation placement. If the treatment is successful, more injected water (or gas) will flow into adjacent oil-bearing zones and displace the oil therein.

According to Muggeridge (2014), to perform a flow diversion method effectively, the suspected thief zones need to be separated from surrounding oil-bearing zones by impermeable layers that cover the area between injection and production wells. This is because the impermeable layers block and prevent the injection fluid to enter the treated zones. If the impermeable layers do not exist or is not laterally extensive, the injected water might flow around the thief zone through the adjacent injection well area, but it might enter the thief zone again after passing the zone that has been plugged (Figure 44; Sorbie & Seright, 1992). Another possibility in the chemical plugging approach is that the polymer can flow into the hydrocarbon-bearing zones and thus reduce injectivity and oil production.

Looking at the thief zones in Åre 6.2, the heterolithic lithofacies (SMs and MSs) might act as the impermeable layers since they comprise mud layers with various thicknesses. Based on the conceptual model (Figure 27), the very permeable lithofacies Sx is present at the base of accretion packages of the distributary and tidal channel FA. This lithofacies erodes and creates an erosional base, separating a channel FA from the underlying FA which is commonly a tidal flat FA (see also the conceptual depositional model). Tidal flats mainly consist of mud-rich heterolithic lithofacies and very fine-grained sandstones, so it can be considered as an impermeable layer (almost zero Kx and very low Ky) underlying the thief zone. In the barform models, SMs is present overlying Sx. Although sandstones are more dominant than mudstones, intensive mudstone occurrences can be found in SMs lithofacies as laminas and fluid muds. It is suggested that these mud layers can form an impermeable layer which might isolate the Sx at the top part. Even though the facies association models built in this study are generic, all these observations provide evidence for the possibility that the flow diversion method can be effectively applied to the thief zones in Åre 6.2.

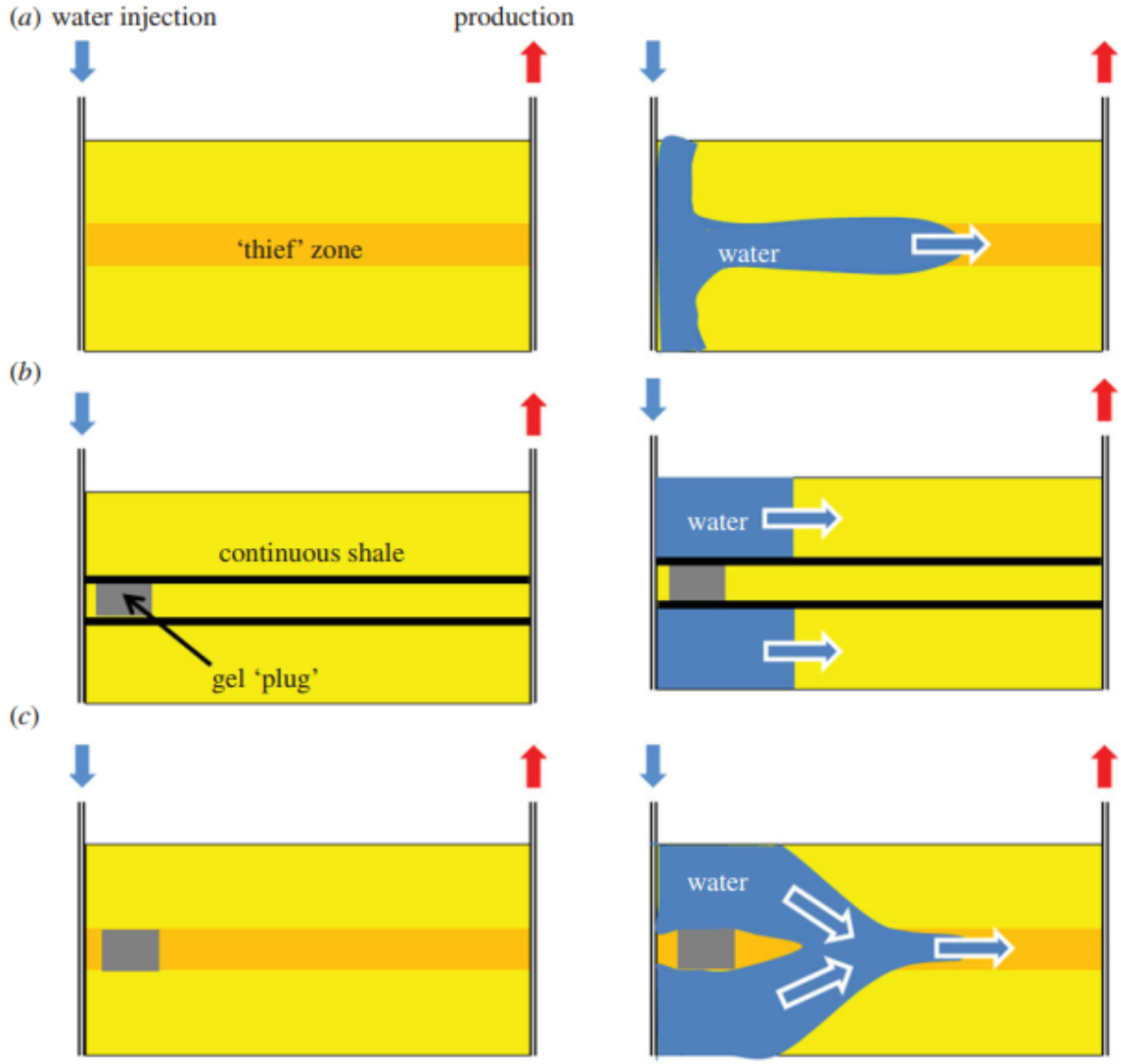

Figure 44. Illustrations of the effects of a thief zone. (a) water injection without any treatment to the thief zone. Water may only flow through the thief zone. (b) A gel plug between two continuous shale layers is successful because full isolation is achieved. (c) Partial improvement due to the absence of impermeable layers; the gel plug is circumvented (Muggeridge et al., 2014).

6.4 Suggestions for Future Research

Many different types of subsurface uncertainties are present in geological modelling processes, but the quantification and reduction of these is the primary objective of modeling procedures (Martinius *et al.*, 2005). With limited time and resources, one study cannot cover all relevant aspects. Therefore, some suggestions are provided for possible future work to further investigate the accuracy and evaluating other interesting aspects. The most pronounced uncertainties are related to the internal channel geometry such as channel sinuosity and the connectivity between channels. Such uncertainties result from the limited information gathered from the well data and difficulties adjusting the outcrop analogues to the models.

Channel Sinuosity Analysis

Identifying channel sinuosity is almost impossible by just studying the core data and thus this aspect is considered to be one of the main uncertainties. One approach that can be applied is to make different channel scenarios with a range of sinuosity. This may be useful to evaluate the effect of the channel sinuosity on some features such as FA upscaled values. Three different channel sinuosity scenarios have been made and analyzed in this study (Figure 45), but the result shows that there is no significant difference in upscaled porosity and permeability values between the FA models. This may be because the different sinuosity only generates slightly different barform geometry. The main differences appear to be the distribution of the sand bodies. A high sinuosity channel has noticeable wider barforms than a low sinuosity channel because a high sinuosity channel provides more spaces for sediment to be deposited (larger inner bank). This result suggests that channel sinuosity does not affect the FA upscaled values, but it shows a significant variation on barform distribution which is most likely associated with the connectivity between multiple channels and consequently also fluid flow between injection and production wells. Therefore, making multiple scenario of channel sinuosity and test these using streamline simulation might be a useful option for future. It should be noted that providing feedback to the way the conceptual model established is always important to ensure that the geomodels are realistic and capture the characteristics of the interpreted depositional setting.

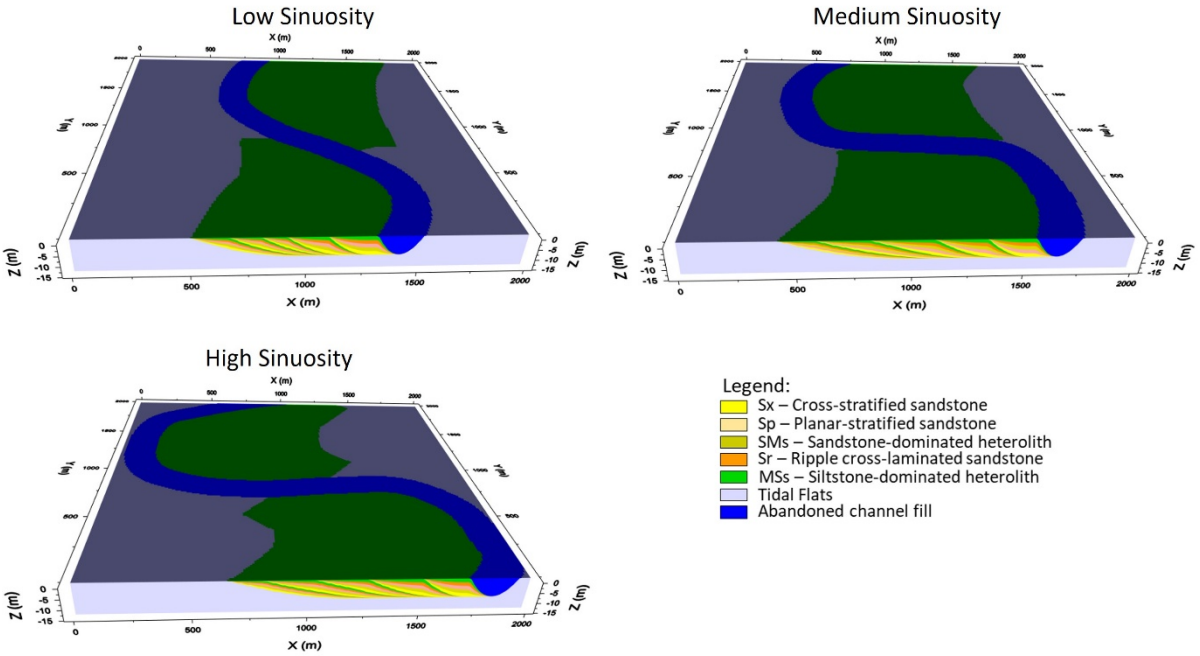

Figure 45. Example of channel sinuosity variation for FA models

Multiple-stacked channel modeling

ReservoirStudio™ software does not only allow the construction of a single channel model, but it does serve to make multiple channels models. It might yield a more realistic sequence of events of channel belt depositions as in reality a channel belt may consist of more than one channel. The multiple channel model is definitely more complicated to model since the modeler needs to design how the channels stacked on top of each other. The number of channels contained in the model is also challenging to define. Although this introduces another uncertainty, the number can be estimated by looking at the core data and the interpreted

channel FA. The interpretation in each well, combined into a well correlation interpretation (Figure 14), gives valuable information about the realistic estimation of channel quantity and also the degree of lateral and vertical amalgamation of the channels. This method is useful as guidance when building such models and can reduce the uncertainty of the models. Previous work by Nordahl *et al.* (2014) is a suitable example of how to design the multiple channel models (Figure 46). In the model, a laterally extensive amalgamated meandering channel fill occupies the lower part of the model. It is followed by a decrease of amalgamation of the channels upward, reflecting a period of lower sediment supply or high A/S ratio. This scheme is based on architectural analysis from core data - which has also been applied to the Åre 6.2 zone in this study.

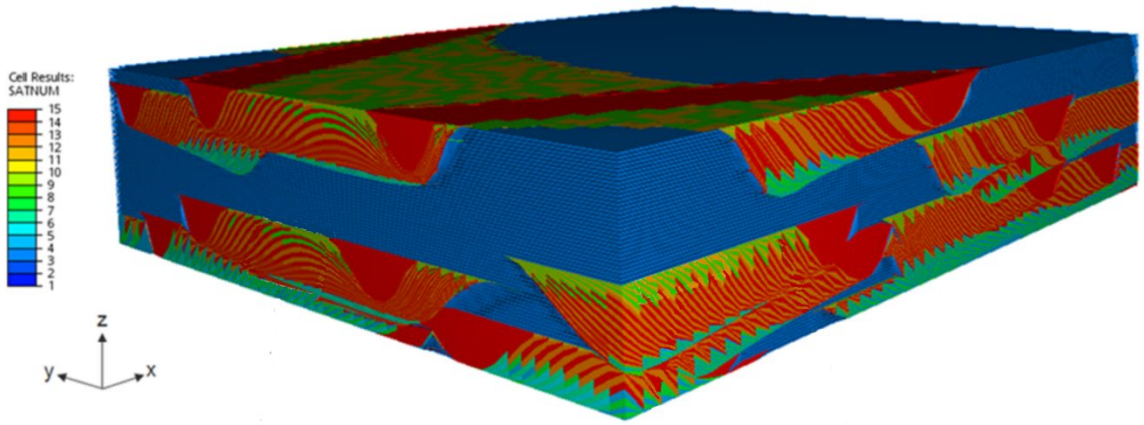

Figure 46. Example of multiple-stacked channel models (Nordahl et al., 2014)

7
Conclusion

The main goal of this study was to create detailed geological models used to examine the potential effect of the thief zones in Åre 6.2 (Heidrun Field) on fluid flow and consequently production. To reach this goal, an extensive sedimentary study has been performed. The study involved core observation to understand and validate the existing lithofacies description and to identify the thief zones characteristics.

Based on the lithofacies and literature on facies models (Thrana *et al.*, 2014; Martinius *et al.*, 2001; Dalrymple *et al.*, 1992; Reading and Levell, 1996), five facies associations were defined, which are tidal channel, distributary channel, tidal flats, upper shoreface, and lower shoreface. They represent deposition in a tide-dominated estuary with a wave-dominated offshore area and in which the distributary channel and the tidal channel form one continuum from the proximal part to the distal part. This depositional system becomes increasingly more tide influenced towards the outer part of the estuary while the fluvial energy contribution gradually decreases in the same direction.

The thief zones, defined as thin intervals with a permeability higher than 1 Darcy and strong permeability contrast with the surrounding rocks, are characterized by relatively medium to coarse-grained sandstone with moderate to poor grain sorting occurring in channels. The thief zones are mainly formed by a series of one type of laminae contained in Sx lithofacies and interpreted to be formed by a significantly higher influx of fluvially-derived sediment during high water discharge. At the facies association scale, the thief zones are situated in the tidal channels and distributary channels because Sx is one of the lithofacies characterizing both FA.

Geological models at lithofacies and facies association scale were built to be able to capture sedimentary heterogeneities at different dimensional scales. Very high permeability values (>1 Darcy) can still be recognized at the REV upscaled values of Sx model. This upscaling result implies that the Sx lithofacies can capture the thief zone characteristics and thus represent the thief zones at the next heterogeneity scale (facies association scale).

At the facies association scale, tidal and distributary geomodels were constructed based on the conceptual models developed for this study and were complimented by outcrop analogue data of the Gule Horn Formation (East Greenland). Flow-based upscaling with the estimated REV size was performed to produce the representation values of the FA models. The result shows that the upscaling effect is significant, which causes horizontal permeability (Kx and Ky) to fall to around 300 mD although both FA models comprise the thief zones. This reduction in Kx and Ky indicates that the thief zones should be determined at the FA scale specifically so that they can be recognized by the reservoir engineers and will receive the appropriate attention in the reservoir modeling and simulation processes.

When comparing the sample distribution of the geological reservoir grid and the simulation grid, there is only a slight difference between both sample sizes. In fact, based on this study, larger distribution differences are identified when upscaling from well data (core plugs trough LF and FA models) to the reservoir models. Consequently, this study confirms that multiple

scale geological modeling can improve the representation of the porosity and permeability distribution in the reservoir model which is consistent with the study by Nordahl *et al*. (2014)

There are a number of uncertainties identified during the model building process. At the lithofacies scale, limited geometrical information from core data can cause inaccuracy of the model geometry although generic sedimentary structure models from the literature can be used to complement the modeling process. Once the models were established, synthetic core plugs were taken from the models and matched with the actual core plug data to ensure that the models honour the actual core data. This validation was performed to minimize the lithofacies model uncertainty. Another uncertainty evaluation was applied at facies association scale. At this scale, volume fractions of lithofacies types composing the facies association might vary from one channel to another. Variations of lithofacies volume fractions were used, and the changes of upscaled values were identified in order to recognize the most influential lithofacies in the upscaled values. This analysis found that the quantity of lithofacies Sx, which are the thief zones, is the controlling factor for the horizontal permeability values while the vertical permeability is more sensitive to the volume of MSs lithofacies (more so than to the other lithofacies). The realistic range of these parameters can be derived from the core data and should be aligned with the conceptual models.

Simple streamline simulations were performed to the models to examine if the thief zones affect fluid flow. As expected, most flow paths were concentrated in the thief zones, revealing that the injected water tend to only sweep the oil in the thief zones. This will potentially reduce the overall sweep efficiency and increase the risk of early water breakthrough. Overall, this finding strengthens the idea that the thief zones affect the fluid flow in the reservoir zone and the distribution of the thief zones need to be assessed when designing well placement and perforation for further field development.

In conclusion, this thesis has provided a multiscale modelling workflow to assess the impact of thin thief zones of hydrocarbon production in tide-influenced and –dominated reservoirs, and has shown that the approach leads to results that can be quantified and used to assess and decrease production uncertainties.

Bibliography

Ahokas, J. M., Nystuen, J. P., & Martinius, A. W. (2014). Depositional dynamics and sequence development of the paralic Early Jurassic Neill Klinter Group, Jameson Land Basin, East Greenland: Comparison with the Halten Terrace, mid-Norwegian continental shelf. *In*: Martinius, A.W., Ravnås, R., Howell, J.A., Steel, R.J. and Wonham, J. (Eds) *From Depositional Systems to Sedimentary Successions on the Norwegian Continental Margin*. International Association of Sedimentologists Special Publications, 46, 291-338. https://doi.org/10.1002/9781118920435.ch12

Allen, G.P., Laurier, D. and Thouvenin, J. (1979). Etude sedimentologique du delta de la Mahakam: Compagnie Frangise des Petroles, Notes et Memoires 15, 156 p.

Bane, R.K., Parker, R.A., Storbeck, W.G., Sunde, R.L. (1994). Reservoir management of the Fullerton Clearfork unit. In: *Proceedings of the Permlan Basin Oil and Gas Recovery Conference*. Paper SPE 27640.

Bear, J. (1972). *Dynamics of Fluids in Porous Media*. New York: Elsevier.

Brandsæther, I., Wist, H. T., Næss, A. et al. (2001a). Ranking of stochastic realizations of complex tidal reservoirs using streamline simulation criteria. Petroleum Geoscience, 7, 53–63.

Choi, K.S., Dalrymple, R.W., Chun, S.S., Kim, S.P. (2004). Sedimentology of modern, inclined heterolithic stratification (IHS) in the macrotidal Han River delta, Korea. Journal of Sedimentary Research 74, 677–689

Christiansen, R. L. (2001). *Two-phase Flow Through Porous Media: Theory, Art and Reality of Relative Permeability and Capilary Pressure*. Petroleum Engineering Dept., Colorado School of Mines

Corbett, P. W. M. & Jensen, J. L. (1992). Estimating the mean permeability: how many measurements do you need? First Break, 10, 89–94

Dalland, A., Augedahl, H. O., Bomstad, K., & Ofstad, K. (1988). The Post-Triassic Succession of the mid-Norwegian Shelf. In A. Dalland, D. Worsley & K. Ofstad (Eds.), *A Lithostrategraphic scheme for the Mesozoic and Cenozoic succession offshore mid- and northern Norway* (Vol. NPD Bulletin no 4, pp. 5-42). Stavanger: Oljedirektoratet.

Dalrymple, R.W. (1992). Tidal depositional systems. In: Walker, R.G., James, N.P. (Eds.), *Facies Models: Response to Sea Level Change*. Geological Association of Canada, St. John's, pp. 195–218.

Dalrymple, R.W. and Choi, K. (2007) Morphologic and facies trends through the fluvial - marine transition in tide-dominated depositional systems: A schematic framework for environmental and sequence stratigraphic interpretation. Earth-Sci. Rev., 81, 135–174.

Ding, S., Jiang, H., Liu, G., Sun, L., Lu, X., & Zhao, L. (2016). Determining the levels and parameters of thief zone based on automatic history matching and fuzzy method. *Journal of Petroleum Science and Engineering*, *138*, 138–152. https://doi.org/10.1016/j.petrol.2015.09.010

Ehrenberg, S. N., Gjerstad, H. M., & Hadler-Jacobsen, F. (1992). Smorbukk Field: A Gas Condensate Fault Trap in the Haltenbanken Province, Offshore Mid-Norway: Chapter 21. AAPG special volumes, M 54: *Giant Oil and Gas Fields of the Decade* 1978-1988, 323-348

Eide, C. H., Howell, J. A., Buckley, S. J., Martinius, A. W., Oftedal, B. T., & Henstra, G. A. (2016). Facies model for a coarse-grained, tide-influenced delta: Gule Horn Formation (Early Jurassic), Jameson Land, Greenland. *International Association of Sedimentologists Special Publications*, 63, 1474–1506. https://doi.org/10.1111/sed.12270

Gilman, J. R., H.-Z. Meng, M. J. Uland, P. J. Dzurman and S. Cosic (2002). Statistical Ranking of Stochastic Geomodels Using Streamline Simulation: A Field Application. Annual Technical Conference and Exhibition of Society of Petroleum Engineers. Richardson, Texas.

Gjelberg, J., Dreyer, T., Høie, A., Lilleng, T., & Tjelland, T. (1987). Late Triassic to Mid-Jurassic sandbody development on the Barents and Mid-Norwegian shelf In J. Brooks & K. Glennie (Eds.), *Petroleum Geology of North West Europe,* Graham & Trotman, 1105-1129

Hemmens, P.D., Hole, A., Reid, B.E., Leach, P.R.L. & Landrum, W.R. (1994). The Heidrun Field. In: Aasen, J.O., Berg, E., Buller, A.T., Hjelmeland, O., Holt, R.M., Kleppe, J. & Torsæter, O. (eds) *North Sea Oil and Gas Reservoirs III*. Kluwer, Dordrecht, 1–23.

Heum, O. R., Dalland, A., & Meisingset, K. K. (1986). Habitat of hydrocarbons at Haltenbanken (PVT modelling as a predictive tool in hydrocarbon exploration). In: A. M. Spencer *et al.* (Ed.), *Habitat of Hydrocarbons on the Norwegian Continental Shelf,* Norwegian Petroleum Society, 259-274

Idrobo, E. A., M. K. Choudhary, A. Datta-Gupta and SPE (2000). Swept volume calculations and ranking of geostatistical reservoir models using streamline simulation SPE/AAPG Western Regional Meeting. Long Beach, California.

Ichaso, A. A., & Dalrymple, R. W. (2009). Tide- and wave-generated fluid mud deposits in the Tilje Formation (Jurassic), offshore Norway. *Geology*, *37*(6), 539–542. https://doi.org/10.1130/G25481A.1

Kempka, T., Norden, B., Ivanova, A., & Löth, S. (2017). Revising the static geological reservoir model of the upper triassic stuttgart formation at the ketzin pilot site for CO2storage by integrated inverse modelling. *Energies*, *10*(1559). https://doi.org/10.3390/en10101559

Keogh, K. J., Leary, S., Martinius, A. W., Scott, A., S. J., Riordan, S., Gowland, S. & Taylor, A. M. (2014). Data capture for multi-scale modelling of the Lourinhã Formation, Lusitanian Basin, Portugal: an outcrop analogue for the Statfjord Group, Norwegian North Sea. *In*: Martinius, A.W., Howell, J.A. and Good, T.R. (Eds) *Sediment Body Geometry and Heterogeneity: Analogue Studies for Modelling the Subsurface*. Geological Society of London Special Publications, 387, 27-56. https://doi.org/10.1144/SP387.11

Kjønsvik, D., Doyle, J., & Jacobsen, T. (1994). The Effects of Sedimentary Heterogeneities on Production from a Shallow Marine Reservoir - What Really Matters? *Proceedings of SPE Annual Technical Conference and Exhibition Paper 28445*, 27–40. https://doi.org/10.2118/28445-MS

Koch, J.-O. & Heum, O.R. (1995). Exploration trends of the Halten Terrace. In: Hanslien, S. (ed.) *Petroleum Exploration and Exploitation in Norway*. Norwegian Petroleum Society, Special Publications, 4, 235–251.

Li, B., Najeh, H., Lantz, J., Rampurawala, M., Gok, I., & Mohammed, A.-K. (2010). Detecting Thief Zones in Carbonate Reservoirs by Integrating Borehole Images With Dynamic Measurements: Case Study From the Mauddud Reservoir, North Kuwait. *SPE*

Reservoir Evaluation & Engineering, *13*(2), 193–202. https://doi.org/10.2118/116286-PA

Li, D., Yang, J., & Lu, D. (2016). Thief zone identification based on transient pressure analysis: a field case study. *Journal of Petroleum Exploration and Production Technology*, *6*(1), 63–72. https://doi.org/10.1007/s13202-015-0168-8

Lolomari, T., Bratvedt, K., Crane, M. *et al.* (2000). The Use of Streamline Simulation in Reservoir Management: Methodology and Case Studies. Paper SPE-63157-MS. http://dx.doi.org/10.2118/63157-MS

Martinius, A. W., Kaas, I., Næss, A., Helgesen, G., Kjærefjord, J. M., & Leith, D. A. (2001). Sedimentology of the heterolithic and tide-dominated Tilje Formation (Early Jurassic, Halten Terrace, offshore mid-Norway). *In*: Martinsen, O.J. and Dreyer, T. (Eds) *Sedimentary Environments Offshore Norway - Paleozoic to Recent*. Norwegian Petroleum Society Special Publications, 10, 103-144.

Martinius, A. W., Ringrose, P. S., Brostrøm, C., Elfenbein, C., Næss, A., & Ringås, J. E. (2005). Reservoir challenges of heterolithic tidal hydrocarbon fields (Halten Terrace, mid-Norway) *Petroleum Geoscience Thematic Set,* 11, 3-16.

Medeiros, R.S., Biswas, D., and Suryanarayana, P.V. (2004). Impact of Thief Zone Identification and Shut-Off on Water Production in the Nimr Field. Paper SPE 91665. doi: 10.2118/91665-MS

Moore, D.M. (1989) Impact of Super Permeability on Completion and Production Strategies. Paper SPE 17974. doi: 10.2118/17974-MS

Muggeridge, A., Cockin, A., Webb, K., Frampton, H., Collins, I., Moulds, T., & Salino, P. (2014). Recovery rates, enhanced oil recovery and technological limits. *Philosophical Transactions. Series A, Mathematical, Physical, and Engineering Sciences*, *372*(2006), 20120320. https://doi.org/10.1098/rsta.2012.0320

Mutti, E., Rosell, J., Allen, G.P., Fonnesu, F., Sgavetti, M. (1985). The Eocene Baronia tide dominated delta-shelf system in the Ager Basin. In: Mila, M.D., Rosell, J. (Eds.), Excursion Guidebook, 6th European Regional Meeting. International Association of Sedimentologists, Lleida, Spain, pp. 579–600

Nichols, G. (2009). *Sedimentology and Stratigraphy* (Second Edi). West Sussex: John Wiley & Sons.

Nordahl, K., Messina, C., Berland, H., Rustad, A. B., & Rimstad, E. (2014). Impact of multiscale modelling on predicted porosity and permeability distributions in the fluvial deposits of the Upper Lunde Member (Snorre Field, Norwegian Continental Shelf). *In*: Martinius, A.W., Howell, J.A. and Good, T.R. (Eds) *Sediment Body Geometry and Heterogeneity: Analogue Studies for Modelling the Subsurface*. Geological Society of London Special Publications, 387, 85–109. https://doi.org/10.1144/SP387.10

Nordahl, K., & Ringrose, P. S. (2008). Identifying the Representative Elementary Volume for Permeability in Heterolithic Deposits Using Numerical Rock Models. Math Geosci, 40, 753-771

Osmundsen, P. T., and J. Ebbing (2008). Styles of extension offshore mid-Norway and implications for mechanisms of crustal thinning at passive margins, *Tectonics*, 27, TC6016, doi: 10.1029/2007TC002242.

Payenberg, T. H. D., & Lang, S. C. (2003). Reservoir geometry of fluvial distributary channels - Implications for northwest shelf deltaic successions, Australia, Deltaic Successions. APPEA Journal, 325, https://doi.org/10.1071/AJ02017

Posamentier, H.W. & Allen, G.P. (1999) Siliciclastic Sequence Stratigraphy: Concepts and Applications. Society of Economic Paleontologists and Mineralogists, Tulsa, OK

Reading, H.G. & Levell, B.K. (1996) Controls on the sedimentary record In: Sedimentary Environments: Processes, Facies and Stratigraphy (Ed. Reading, H.G.). Blackwell Science, Oxford; 5–36.

Ringrose, P. S., Martinius, A. W., & Alvestad, J. (2008). Multiscale geological reservoir modelling in practice, From: Robinson, A., Griffiths, P., Price, S., Hegre, J. & Muggeridge, A. (eds) *The Future of Geological Modelling in Hydrocarbon Development.* The Geological Society, London, Special Publications, 309, 123–134. https://doi.org/10.1144/SP309.9

Schmidt, W.J. (1992). Structure of the mid-Norway Heidrun Field and its regional implications. In: Larsen, R.M., Brekke, H., Larsen, B.T. & Talleraas, E. (eds) *Structural and Tectonic Modelling and its Application to Petroleum Geology*. Norwegian Petroleum Society, Special Publications, 1, 381–395

Sorbie, K. S., & Seright, R. S. (1992). Gel Placement in Heterogeneous Systems With Crossflow. In *SPE/DOE Enhanced Oil Recovery Symposium*. Society of Petroleum Engineers. https://doi.org/10.2118/24192-MS

Svela, K.E. (2001). Sedimentary facies in the fluvial-dominated Åre Formation as seen in the Åre 1 Member in the Heidrun Field. In: Martinsen, O.J. & Dreyer, T. (eds) *Sedimentary Environments Offshore Norway – Paleozoic to Recent*. Norwegian Petroleum Society, Special Publications, 10. Elsevier, Amsterdam, 87–102.

Thrana, C., Ness, A., Leary, S., Gowland, S., Brekken, M., & Taylor, A. (2014). Updated depositional and stratigraphic model of the Lower Jurassic Åre Formation, Heidrun Field, Norway. *In*: Martinius, A.W., Ravnås, R., Howell, J.A., Steel, R.J. and Wonham, J. (Eds) *From Depositional Systems to Sedimentary Successions on the Norwegian Continental Margin*. International Association of Sedimentologists Special Publications, 46, 253–289. https://doi.org/10.1002/9781118920435.ch11

Van den Berg, J., Boersma, J., & Van Gelder, A. (2007). Diagnostic sedimentary structures of the fluvial-tidal transition zone – Evidence from deposits of the Rhine and Meuse. *Netherlands Journal of Geosciences, 86*(3), 287-306. doi:10.1017/S0016774600077866

Weber, K. J. (1986). How heterogeneity affects oil recovery. In: Lake, L. W. & Carroll, H. B. Jr. (eds) Reservoir Characterization. Academic Press, London, 487–544

Welbon, A.I., Beach, A., Brockbank, P.J., Fjeld, O., Knott, S.D., Pedersen, T. & Thomas, S. (1997). Fault seal analysis in hydrocarbon exploration and appraisal: examples from offshore mid-Norway. In: Møller-Pedersen, P. & Koestler, A.G. (eds) *Hydrocarbon Seals: Importance for Exploration and Production*. Norwegian Petroleum Society, Special Publications, 7, 125–138

Wen, R. (2005). SBED Studio – An integrated workflow solution for multi-scale geo-modelling, EAGE 67th Conference & Exhibition, Geomodelling Tools Workshop.

Whitley, P.K. (1992). The geology of Heidrun: A giant oil and gas field on the mid-Norwegian shelf. In: Halbouty, M.T. (ed.) *Giant Oil Fields of the Decade* 1978–1988. American Association of Petroleum Geologists Memoir, 54, 383–406.

Ziegler, P. A. (1988). Evolution of the Arctic-North Atlantic and the Western Tethys (Vol. 43). Tulsa, Okla.: American Association of Petroleum Geologists.

Appendix A – Core logs with the interpretation of lithofacies and facies associations

For the sedimentary symbol see Figure 5. Vertical red lines indicate interpreted thief zones from core observation and “T” is the plug data at which K>1000mD.

Well 6507/7-4

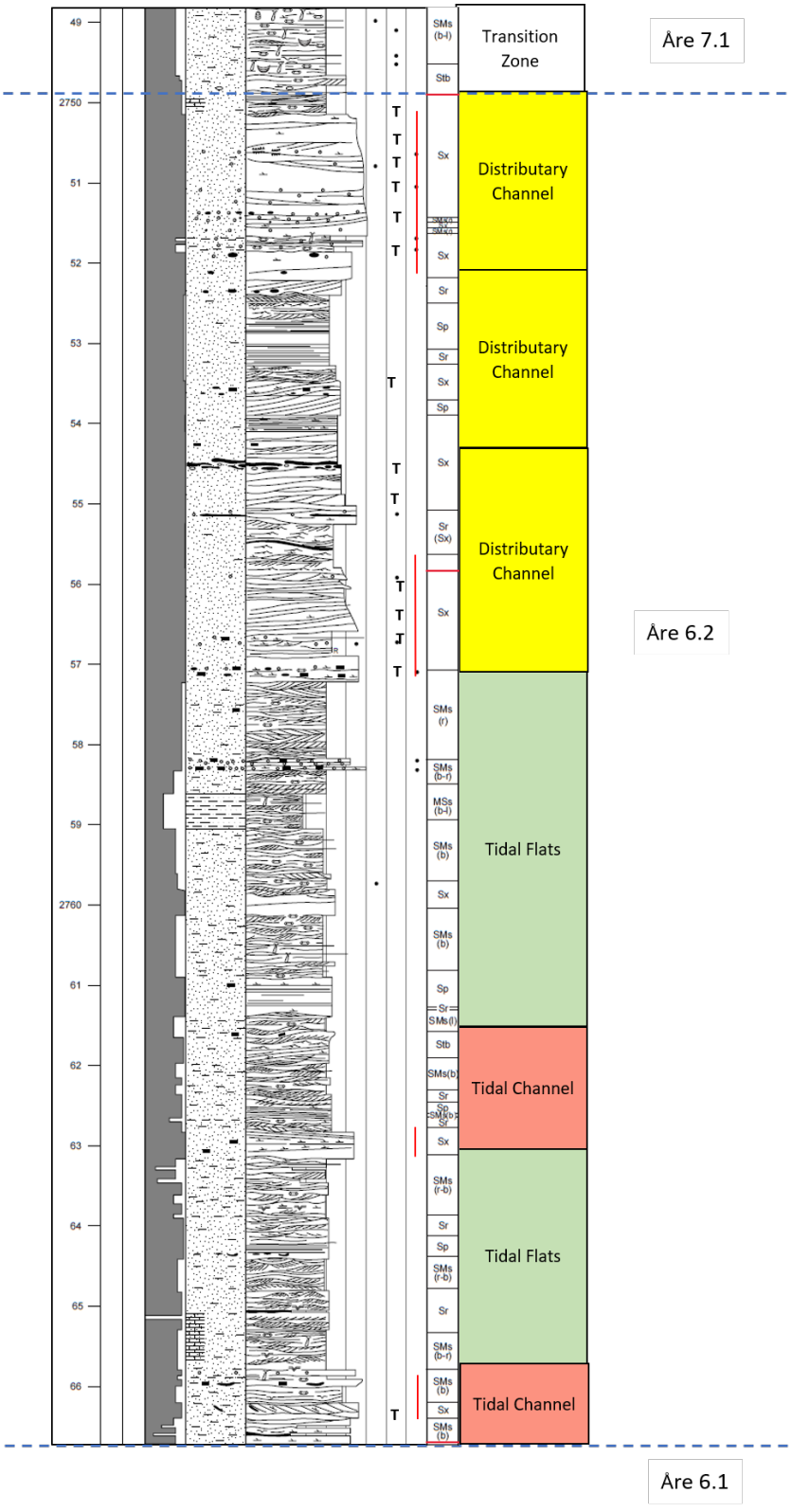

Well 6507/7-A-22

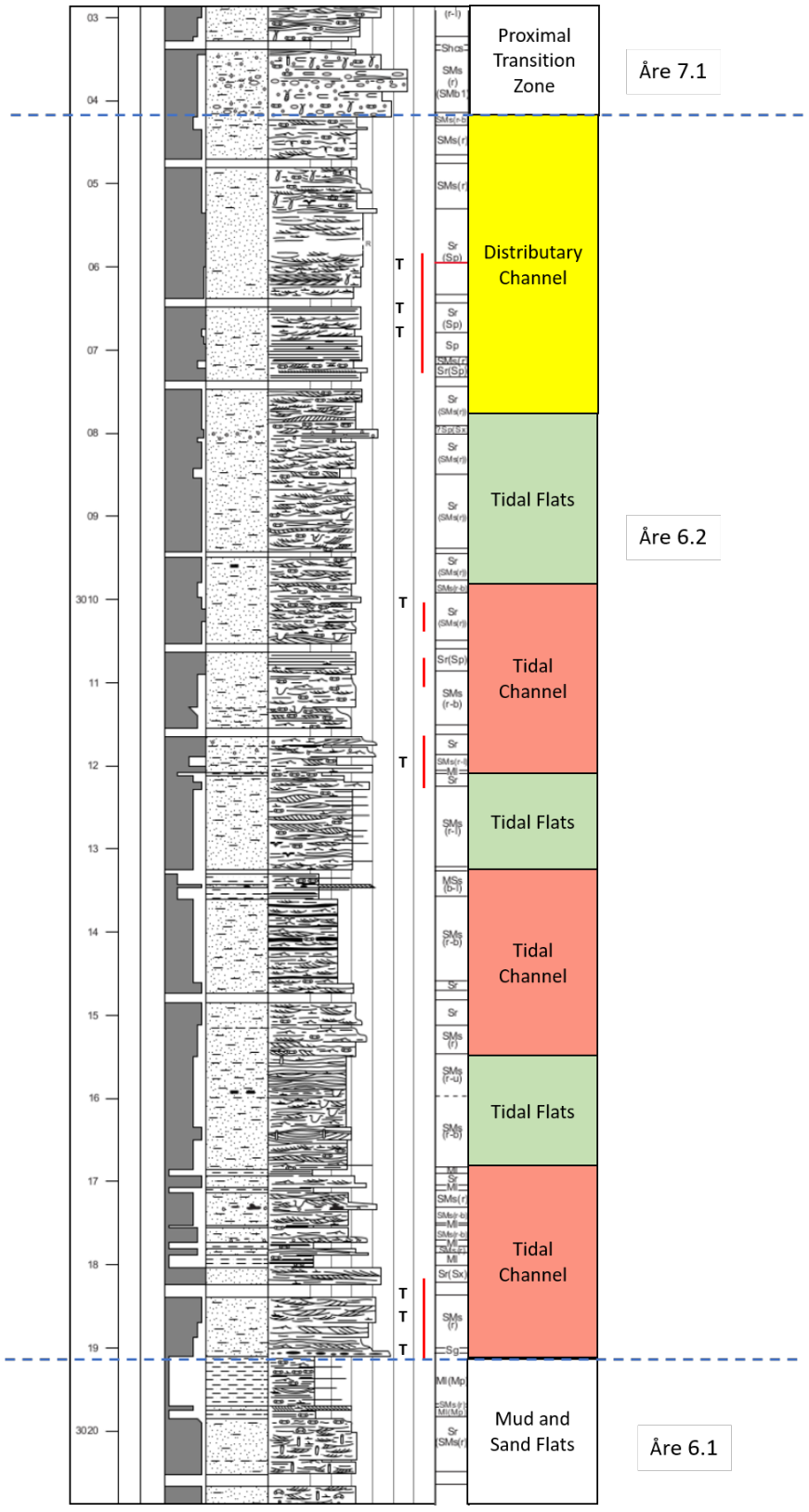

Well 6507/7-2

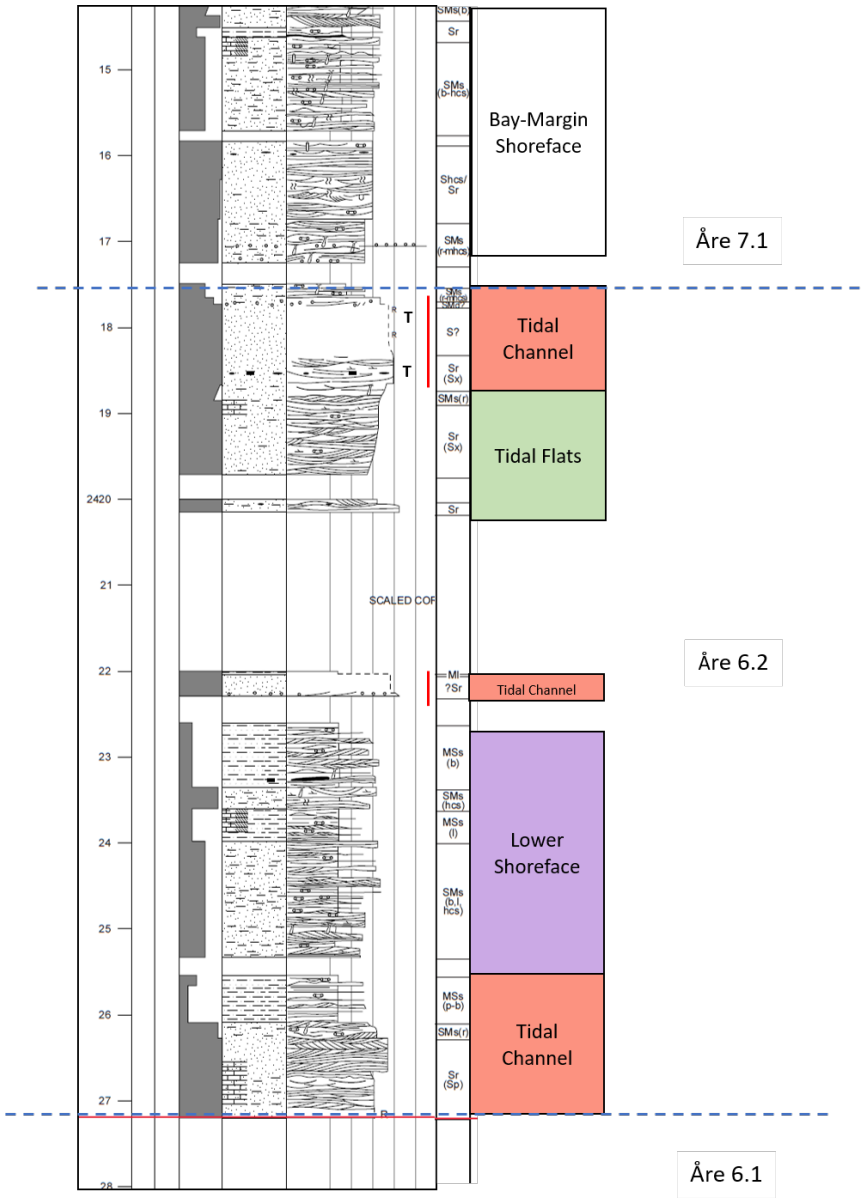
Bay-Margin Shoreface
Åre 7.1
Tidal Channel
Tidal Flats
Åre 6.2
Tidal Channel
Lower Shoreface
Tidal Channel
Åre 6.1
T
T
SCALED COR

Well 6507/7-A-40

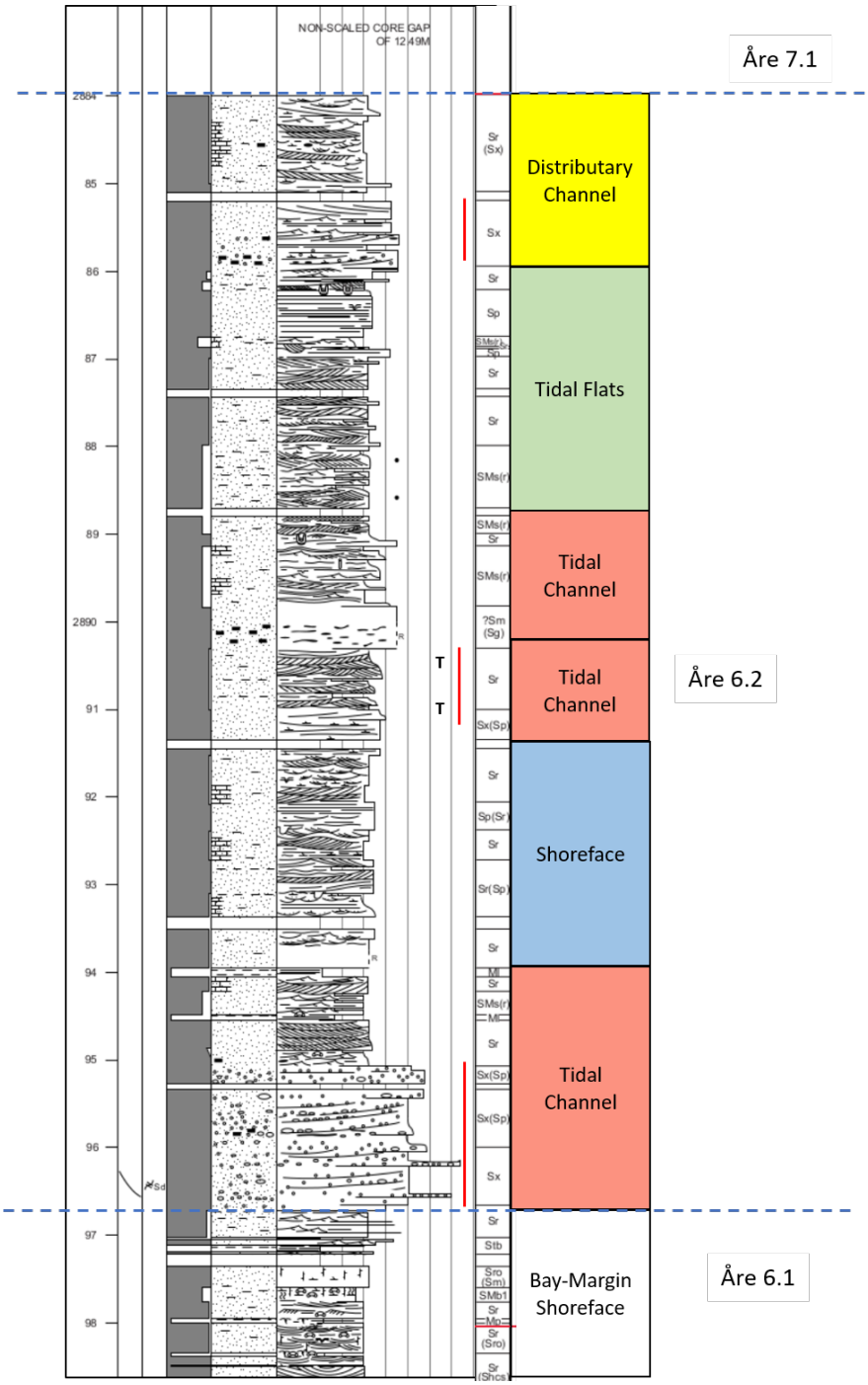

Well 6507/7-A-46

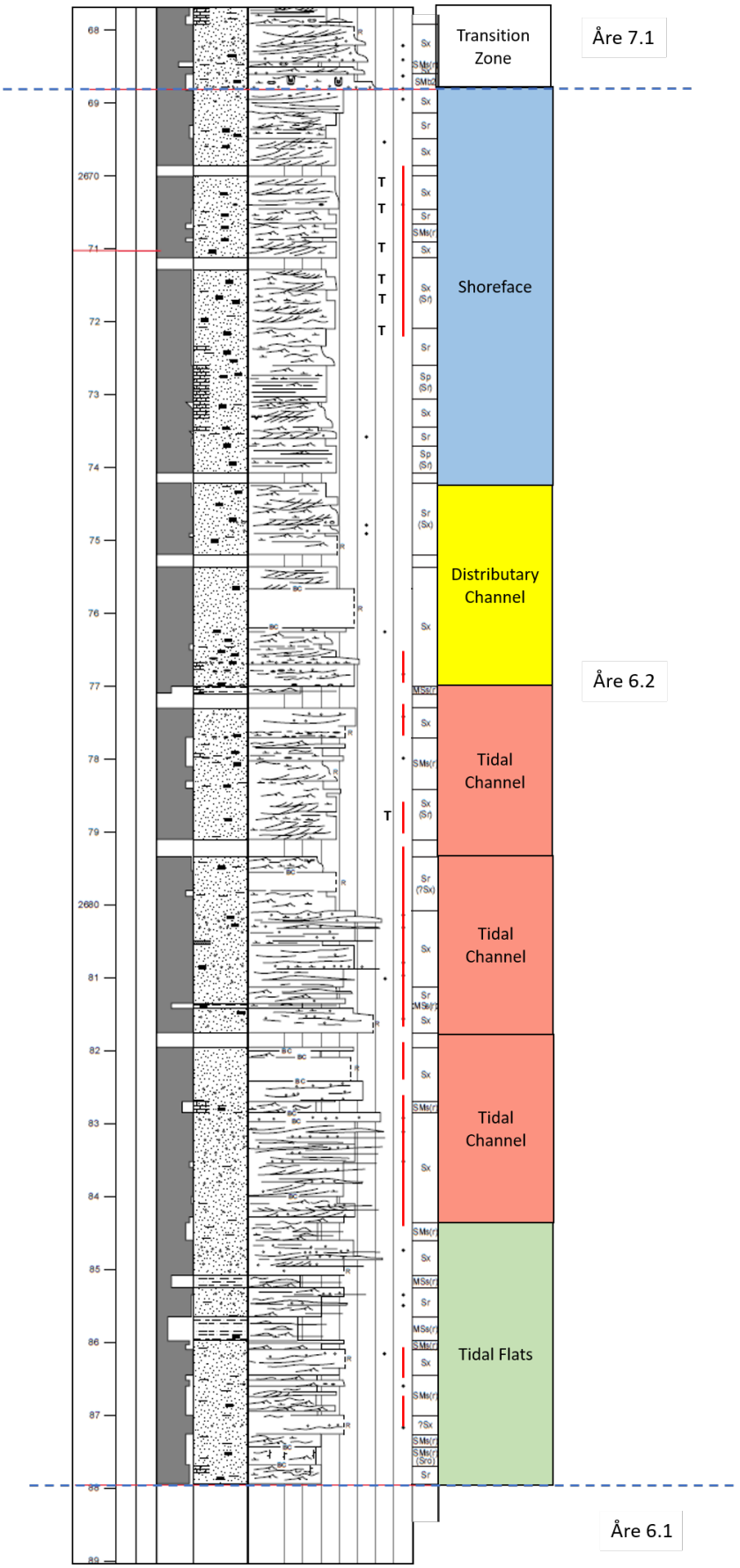

Well 6507/7-5

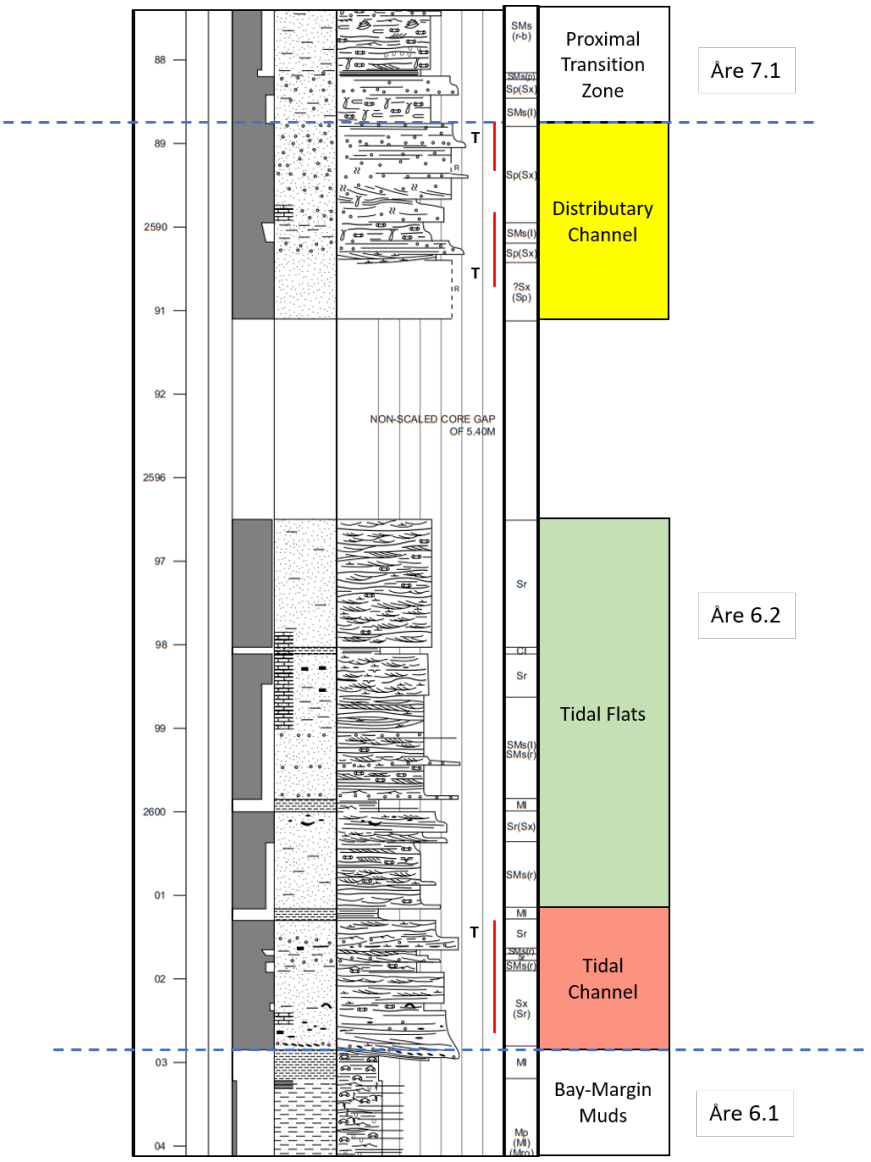
Proximal Transition Zone
Åre 7.1
Distributary Channel
Tidal Flats
Åre 6.2
Tidal Channel
Bay-Margin Muds
Åre 6.1
NON-SCALED CORE GAP OF 5.40M
T
T
T

Well 6507/7-3

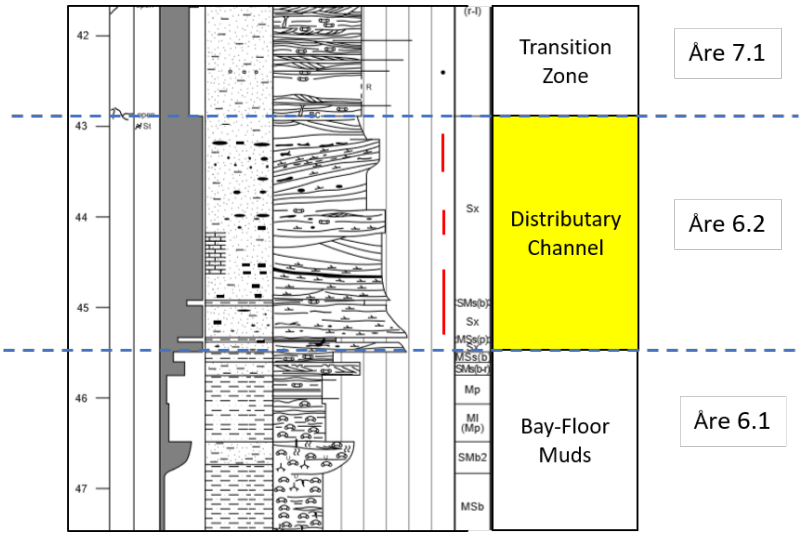
42
43
44
45
46
47
Sx
SMs(b)
Sx
MSs(p)
MSs(b)
SMs(b-t
Mp
MI
(Mp)
SMb2
MSb
Transition Zone
Distributary Channel
Bay-Floor Muds
Åre 7.1
Åre 6.2
Åre 6.1

Appendix B – Rock Physics Function

- Relative permeability as a function of water saturation (Sw), where Krw is relative permeability for water and Kro is for oil.

Sw	Krw	Kro
0.07961	0	1
0.09288	9.21E-05	0.94319
0.10216	0.000157	0.90346
0.11453	0.000242	0.8505
0.12812	0.000337	0.79233
0.14762	0.000472	0.70882
0.15165	0.0005	0.69159
0.16127	0.000967	0.6604
0.17945	0.001851	0.60143
0.20556	0.003119	0.51675
0.22369	0.004	0.45795
0.24815	0.007226	0.39989
0.29573	0.0135	0.28697
0.34009	0.024894	0.21328
0.36777	0.032	0.16731
0.4398	0.0625	0.088388
0.46315	0.077243	0.072864
0.51184	0.108	0.040477
0.58388	0.1715	0.014789
0.65592	0.256	0.003578
0.69191	0.31021	0.001948
0.72796	0.3645	0.000316
0.7999	0.49979	3.15E-14

- Capilary pressure (Cp) as a function of water saturation.

Sw	Cp (bar)
0.07961	3.9179
0.09288	2.9384
0.10216	2.4487
0.11453	1.9589
0.12812	1.5672
0.14762	1.1754
0.15165	1.1176
0.16127	0.97947
0.17945	0.78358
0.20556	0.58768
0.22369	0.50429
0.24815	0.39179
0.29573	0.29042
0.34009	0.19589
0.36777	0.17387
0.4398	0.11653
0.46315	0.097947
0.51184	0.085437
0.58388	0.066931
0.65592	0.048424
0.69191	0.039179
0.72796	0.036262
0.7999	0.030441
0.934	0.019589
1	0